Molecular Characteristics, Sources, and Formation Pathways ~~–~~of Organosulfur Compounds in Ambient Aerosol ~~-~~ in Guangzhou, South China~~: Heterogeneous Secondary Reactions Drivers the Molecular Distribution~~

Hongxing Jiang[1,2,3,6], Jun Li[1,3], Jiao Tang[1,3], Min Cui[4], Shizhen Zhao[1,3], Yangzhi, Mo[1,3], Chongguo Tian[5], Xiangyun Zhang[1,3], Bin Jiang[1,3], Yuhong Liao[1,3], Yinjun Chen[2], Gan Zhang[1,3]

[1]State Key Laboratory of Organic Geochemistry ~~and ,~~ Guangdong province Key Laboratory of Environmental Protection and Resources Utilization, and Guangdong-Hong Kong-Macao Joint Laboratory for Environmental Pollution and Control, Guangzhou Institute of Geochemistry, Chinese Academy of Sciences, Guangzhou, 510640, China
[2]Shanghai Key Laboratory of Atmospheric Particle Pollution and Prevention (LAP3), Department of Environmental Science and Engineering, Fudan University, Shanghai 200433, China
[3]CAS Center for Excellence in Deep Earth Science, Guangzhou, 510640, China
[4]College of Environmental Science and Engineering, Yangzhou university, 225009, Yangzhou, China
[5]Key Laboratory of Coastal Environmental Processes and Ecological Remediation, Yantai Institute of Coastal Zone Research, Chinese Academy of Sciences, Yantai, 264003, China
[6]University of Chinese Academy of Sciences, Beijing, 100049, China

Correspondence to: Jun Li (junli@gig.ac.cn)

Abstract. Organosulfur compounds (OrgSs), especially organosulfates, have been widely reported to be present at large quantities in particulate organic matter found in various atmospheric environments. Despite ~~various kinds~~hundreds of organosulfates and their formation mechanisms being previously identified, a large fraction of OrgSs remain unexplained at the molecular level, and a better understanding of their~~impeding further knowledge on additional~~ formation pathways and critical environmental parameters ~~that~~ is required~~help~~ to explain the~~ir~~ variations in their concentrations. In this study~~work~~, the abundance and molecular composition of OrgSs in fine particulate samples collected in Guangzhou was reported. ~~Our~~ The results revealed ~~that~~that the ratio of the annual average mass of organic sulfur ~~can averagely contribute~~ to ~~30% of~~ total particulate sulfur was 33±12%, and organic sulfur had~~showed~~ positive~~ly~~ correlations with ~~the~~ SO_2 (r=0.37, p<0.05) and oxidant~~s~~ (NO_x+O_3, r=0.40, p<0.01). A Fourier transform ion cyclotron resonance mass spectrometry (FT-ICR MS) analysis revealed ~~results presented~~ that more than 80% formular ~~by~~ number of the OrgSs detected ~~OrgSs~~ in ~~our~~ the samples had~~ve~~ the elemental composition of O/(4S+3N) ≥1, indicating that they were largely in the form of oxidized organosulfates ~~and/~~or nitrooxy organosulfates ~~–~~. Many OrgSs~~, which are~~ that were previously tentatively ~~attributed to previously~~ identified as having biogenic ~~and~~ or anthropogenic origins~~, ,~~ were also present in freshly emitted aerosols derived from ~~freshly emitted~~ combustion sources. The results indicated~~Results~~ that the formation of OrgSs through an epoxide intermediate pathway could account for up to 46% number of OrgSs from an upper bound estimation~~show that the formation of OrgSs through an epoxide intermediate pathway could be as much as 46%~~, and the oxidant~~s~~ levels could explain 20% of the variation in the

带格式的: 左侧: 1.65 厘米, 右侧: 1.65 厘米, 顶端: 1 厘米, 底端: 2.36 厘米, 宽度: 21 厘米, 高度: 24 厘米, 页眉到边缘距离: 0 厘米, 页脚到边缘距离: 1.3 厘米, 距正文: 2.27 字符

设置了格式: 下标

mass of organic sulfur ~~mass~~. The analysis ~~from~~ of our large dataset of FT-ICR MS ~~dataset~~ results suggested~~suggests~~ that relative humidity, oxidation of biogenic volatile organic compounds via ozonolysis, and NO_x-related nitrooxy organosulfate formation~~s~~ were the major reasons for the molecular variation of OrgSs, possibly highlighting the importance of the acid-catalyzed ring-opening of epoxides, oxidation processes, and heterogeneous reactions involving either the uptake of SO_2 or the heterogeneous oxidation~~s~~ of particulate organosulfates into additional unrecognized OrgSs.

1 Introduction

Organosulfur compounds (OrgSs) have been widely identified in atmospheric media including fog, rainwater, and ambient aerosols, and account for a substantial fraction of ambient ~~OM~~ organic matter mass, with percentage~~ratios~~ as large as 50% (Surratt et al., 2007; Altieri et al., 2009; Mazzoleni et al., 2010; Luk´Acs et al., 2009; Tolocka and Turpin, 2012; Surratt et al., 2008), ~~with~~ which potentially have adverse effects on the global climate system and toxicity to human health (Jimenez et al., 2009; Noziere et al., 2015; Nozière et al., 2010; Nguyen et al., 2012; Bates et al., 2019; Daellenbach et al., 2020). OrgSs ~~are~~is a class of relatively stable and long-lived organic compounds (Olson et al., 2011; Bruggemann et al., 2020), including not only organosulfates (OSs), but also sulfoxides, sulfonates, and sulfones, with OSs identified as the most abundant class (Olson et al., 2011; Chen et al., 2020; Tolocka and Turpin, 2012). A series of studies have reported the hygroscopicity (Peng et al., 2021), light absorption properties (Nguyen et al., 2012; Fleming et al., 2019), and possibly potential ~~toxicity~~ (Lin et al., 2016) of OSs, further highlighting the importance of studying the sources and formation mechanisms of OrgSs.

Various mechanistic studies have revealed the possible reaction pathways by which OSs form. The acid-catalyzed ring opening of epoxides in the presence of sulfuric acid seeds has been widely adopted to explain the formation of OSs from isoprene and other volatile organic compounds (VOCs) (Eddingsaas et al., 2010; Iinuma et al., 2007a; Lin et al., 2013; Bruggemann et al., 2020; Surratt et al., 2010; Lin et al., 2012b). Furthermore, heterogeneous reactions between SO_2 and unsaturated compounds or aerosol-phase organic peroxides were also identified to generate OSs both by simulation experiments and field observations (Shang et al., 2016; Passananti et al., 2016; Ye et al., 2018; Zhu et al., 2019). Other mechanisms such as nucleophilic substitution of organic nitrates by sulfate (Surratt et al., 2007; Iinuma et al., 2007b; Surratt et al., 2008), sulfate esterification of alcohols/epoxides (He et al., 2014), and sulfoxy radical-initiated oxidation of unsaturated compounds (Nozière et al., 2010; Huang et al., 2019; Wach et al., 2019; Huang et al., 2020) have also been proposed in many studies. ~~Nighttime~~Night-time NO_3-initiated oxidation of VOCs is considered as an important formation mechanism of nitrooxy-organosulfates (NOSs) (Iinuma et al., 2007b; Bruggemann et al., 2020). ~~It seems that t~~The presently proposed formation pathways presumably explain the large variety and ubiquity of OSs; and the above mechanisms suggest that OSs distributions can depend on both precursors of VOCs and inorganic gas (e.g., SO_2, NO_x, NH_3) concentrations, as well as environmental conditions, such as relative humidity (RH), aerosol acidity and oxidant concentrations. However, the OrgSs composition in the actual atmosphere is complex, and ~~most of the~~many present studies ~~only~~ focused on the existing known ~~Oss~~ OSs because they were abundant in particles(Ye et al., 2020; Hettiyadura et al., 2019; Hettiyadura et al., 2017;

设置了格式: 下标
设置了格式: 字体: Times New Roman
设置了格式: 下标
设置了格式: 字体: Times New Roman
设置了格式: 下标
设置了格式: 下标
设置了格式: 下标

Wang et al., 2018b). (Ye et al., 2020; Hettiyadura et al., 2019; Hettiyadura et al., 2017; Wang et al., 2018b). with A recent study showed that there is a large fraction of OrgSs (67–79%) remaining unexplained at the molecular level other than the OSs with known precursors (Chen et al., 2021). Additionally, recent analysis of high-resolution mass spectrometry data showed that OrgSs detected in freshly emitted sources samples, particularly coal combustion aerosols (Song et al., 2018; Cui et al., 2019; Tang et al., 2020), have a similar molecular composition to classical OSs, complicating the source apportionment and discrimination of reaction mechanisms of OrgSs in the real atmosphere. The above works suggest that there is insufficient understanding of the comprehensive sources, formation mechanisms and influencing factors of OrgSs overall for ambient samples (Bruggemann et al., 2020), which makes it an urgent need to fully understand their molecular composition.

Guangzhou is a megacity in South China where featured high temperature, RH and oxidation levels throughout the year, and it is heavily influenced by biogenic−anthropogenic interactions. Studies have shown that Guangzhou often suffers haze events influenced by biomass burning and fossil fuel combustion (mainly vehicle emissions), and organic aerosols can account for large fractions of the total $PM_{2.5}$ in haze (Jiang et al., 2021b; Dai et al., 2015; Liu et al., 2014). Additionally, the high emissions of anthropogenic pollutants (e.g., NO_x and SO_2) and high concentrations of particle-phase nitrates and sulfates are present in the particle phase, which makes the particles very acidic (He et al., 2014). Although several studies have reported the concentrations and possible formation mechanisms of biogenic VOCs (BVOCs) derived OSs in the Pearl River Delta region (PRD) (Bryant et al., 2021; He et al., 2014), these OSs only represented a small fraction of organic aerosol mass. Therefore, a better understanding of the chemical composition, source and influencing factors of OrgSs in Guangzhou will be important to know the particulate pollution and decrease the SOA concentration of secondary organic aerosol (SOA). It will also have importantreferential significance for areas where show high temperature, humidity and oxidation levels levels, which promote the and frequent occurrence of secondary processes.

In this study, the molecular composition of atmospheric OrgSs over an urban site in Guangzhou, was characterized by negative electrospray ionization Fourier transform ion cyclotron resonance mass spectrometry (ESI-FT-ICR MS) analysis through accurate mass measurements. The applications of high-resolution Fourier transform ion cyclotron resonance mass spectrometry (FT-ICR MS) or Orbitrap mass spectrometry coupled with electrospray ionization (ESI) in studying atmospheric OrgSs haves qualitatively provided more new molecular information on OrgSs composition (Ye et al., 2020; Kuang et al., 2016; Lin et al., 2012b; Gao and Zhu, 2021). Moreover, the FT-ICR MS results combined with chemical tracers and meteorological data were used to evaluate the possible formation pathways and driving factors of OrgSs. We showed that acid-catalysed ring-open of epoxides, heterogeneous reactions of the SO_2 uptake pathway and different oxidation processes, were potentially important formation pathways of OrgSs in Guangzhou where usually has high RH, oxidation levels and acidity. We show that liquid-phase related reactions such as heterogeneous oxidation and acid-catalyzed ring-open of epoxides, were potentially important formation pathways of OgrSs in Guangzhou, due to the high RH, oxidation levels and acidity in this region. This is consistent with a recent field observation that gas-phase oxidation and heterogeneous/multiphase reactions play important roles in SOA formation in Guangzhou (Guo et al., 2020).

设置了格式: 非上标/ 下标

设置了格式: 下标

设置了格式: 下标

设置了格式: 下标

设置了格式: 字体: Times New Roman

设置了格式: 下标

2 Experimental methods

2.1 Collection of $PM_{2.5}$ samples and sulfur-containing species analysis.

A total of 55 atmospheric $PM_{2.5}$ samples (24h) which were collected at an urban site in Guangzhou from July, 2017 to June, 2018, were used for organosulfur analysis**.** Detailed information about the samples and the measurement of organic tracers, water-soluble inorganic ions, and meteorological parameters (including trace gases, temperature, and ~~relative humidity~~RH), ~~was~~ were described in our recent studies (Jiang et al., 2021b; Jiang et al., 2021a) and in the Supplementary text. (Dai et al., 2015; Liu et al., 2014). Our previous source apportionment using the ^{14}C-based positive matrix factorization analysis have shown that the primary sources of fossil-fuel combustion and biomass burning averagely contributed half of organic matters at Guangzhou in total, and the rest of organic matters were associated with secondary processes. It should be noted that the mixed secondary factor of isoprene-derived SOA and organic sulfates formations accounted for 44% of the secondary sources, and showed lower concentrations in winter than in summer (Supplementary text) (Jiang et al., 2021b).

Here, the total fine particulate sulfur (TS) was measured by elemental analyser (Elemental, Germany) and directly compared to inorganic sulfate measured by ion chromatography (IC), and the TS to sulfate-sulfur ratios were calculated (Chen et al., 2021; Shakya and Peltier, 2013; Tolocka and Turpin, 2012). Detailed descriptions of the analysis procedures are presented in the Supplementary text ~~Supporting information (SI)~~. As assumed, if particulate sulfur was present only as SO_4^{2-} ~~SO_4^{2-}~~, the calculated ratio often shifts from 1 to the small range of 0.9 ~~–~~ 1.1 using an error propagation method (Shakya and Peltier, 2015, 2013). And the~~In this study, the~~ TS to sulfate-sulfur ratios of samples greater than 2 or less than 0.5~~, which~~ were considered as a measure of gross measurement error (Shakya and Peltier, 2015)~~,~~. In this study, the samples' data met to this criterion were ~~also~~ excluded from further ~~analysis~~discussion ~~(Shakya and Peltier, 2015)~~. Moreover, according to Chen et al. (2021), a calculated ratio of organic sulfur to TS (Org-S/TS) greater than their uncertainty ($\delta_{OrgS/TS}$) is considered significant (detailed calculations can be found in the Supplementary text). The content of organic sulfur (Org-S) was estimated as the amount of sulfate-sulfur subtracted from TS (two negative Org-S values were set as zero). By using this criterion, we exclude the unreasonable data caused by analytical uncertainties associated with measurements. Finally, the concentration data of sulfur-containing species of 40 samples were reserved and used for further discussion~~40 samples were reserved, the content of organic sulfur (Org-S) was estimated as the amount of sulfate-sulfur subtracted from TS, and two negative Org-S values were set as zero~~.

2.2 FT-ICR MS analysis on organosulfur compounds

The feasibility of the method is based on its high mass resolution in identifying mass peaks in conjunction with the assignment of formulas using narrow mass tolerance (< 1ppm absolute mass error for FT-ICR MS results). Previous studies have indicated that the OSs are readily ionized in negative ESI mode, and most of them were observed only in negative mode (Lin et al., 2012b; Kuang et al., 2016). ~~A total of~~All the total 55 $PM_{2.5}$ samples were used for negative ESI-FT-ICR MS analysis and each sample was ultrasonic extracted with methanol in a cold-water bath (Jiang et al., 2021a), because

设置了格式: 下标
设置了格式: 字体: (默认) Times New Roman
设置了格式: 上标
设置了格式: 字体: 10 磅, 字体颜色: 自动设置
设置了格式: 字体: 10 磅, 字体颜色: 自动设置
设置了格式: 字体: 10 磅, 字体颜色: 自动设置
设置了格式: 字体: 10 磅, 字体颜色: 自动设置
设置了格式: 字体: (默认) Times New Roman
设置了格式: 字体: 10 磅, 字体颜色: 自动设置
设置了格式: 字体: (默认) Times New Roman, 10 磅, 字体颜色: 自动设置
设置了格式: 字体: 10 磅, 字体颜色: 自动设置
设置了格式: 字体: 10 磅, 字体颜色: 自动设置, 下标
设置了格式: 字体: 10 磅, 字体颜色: 自动设置, 下标
设置了格式: 字体: 10 磅, 字体颜色: 自动设置
设置了格式: 字体: 10 磅, 字体颜色: 自动设置
设置了格式: 字体: 10 磅, 字体颜色: 自动设置
设置了格式: 字体: 10 磅, 字体颜色: 自动设置
设置了格式: 字体: 小四, 字体颜色: 自定义颜色(RGB(0,0,204))
带格式的: 段落间距段后: 0.5 行

previous studies have suggested that methanol could extracted more than 90% of organic matter, both for filed samples and fresh biomass burning samples (Chen and Bond, 2010; Cheng et al., 2017; Huang et al., 2018b). The methanol extracts were filtered with PTFE membranes~~members~~, concentrated, and directly injected into a 9.4T solariX XR FT-ICR mass spectrometer (Bruker Daltonik GmbH, Bremen, Germany) in negative ESI modes at a flow rate of 180 μL h^{-1} ~~mL h^{-1}~~ (Jiang et al., 2021a; Jiang et al., 2020). Detailed operating conditions are presented in the Supplementary text~~SI~~. The mass range was set as150–800 Da, and a total of 128 continuous 4M data FT-ICR transients were co-added to enhance the signal-to-noise ratio and dynamic range. Field blank filters were processed and analysed following the same procedures to detect possible contaminations, and all the contaminations in field blanks were subtracted from samples. It should be noted that~~,~~ the general molecular characteristics of ~~the~~ samples and their molecular linkages to light absorption properties were reported in our previous study ~~(Jiang et al., 2021a),~~ (Jiang et al., 2021a). ~~here~~Here, we focused on the detailed composition of OrgSs and their influencing factors and potential formation mechanisms.

2.3 Data processing and statistical analysis

A custom software was used to calculate all mathematically possible formulas for all ions with a signal-to-noise ratio above 4 using a mass tolerance of ±1 ppm. The compounds assigned as $C_cH_hO_oN_nS_s$ with s = 1, 2 will be collectively referred to as organosulfur compounds ~~(OSs)~~ including CHOS (n = 0) and CHONS (n = 1,2). The identified formulas containing isotopomers (i.e., ^{13}C, ^{18}O or ^{34}S) were not discussed. The double bond equivalent (DBE) is calculated using the equation: DBE = (2*c*+2-*h*+*n*)/2. Additionally, the modified index of aromaticity equivalent (Xc) was also calculated to estimate the degree of aromaticity, with the ~~calculations~~ detailed data processing is presented in the Supplementary text~~SI~~ (Yassine et al., 2014; Ye et al., 2020).

We assume that the different OSs may have similar ionization efficiency (Bateman et al., 2012), because the sulfate functional group on the OSs molecules are readily ionized during the ESI process and the ionization of OSs often takes place on the sulfate functional group (Lin et al., 2012b). Based on this assumption and the fact that all the samples with similar carbon concentration were analysed in the same condition in this study (Jiang et al., 2021a)), the peak intensities of OSs ions could be compared to provide information on relative abundances among different samples by assuming that matrix effects were relatively constant in all samples (Lin et al., 2012b; Kuang et al., 2016). However, the ionization efficiencies may vary among different OSs ~~compounds~~ and lead to inconsistency between the ratios of peak intensities and the ratios of concentrations for other reasons, such as surface activity on ESI droplets (Kuang et al., 2016). ~~Although all of the spectra were acquired under the same conditions,~~ , but the sum-normalized peak intensities of the organosulfur compounds provide information on the relative abundances among different samples. To evaluate the associations between environmental variables and OrgSs compounds, we conducted non-metric multidimensional scaling (NMDS) analysis based on Bray−Curtis distances in R using the vegan package (Jiang et al., 2021a). From the NMDS analysis, the OrgSs compounds were

设置了格式: 字体: 10 磅, 字体颜色: 自动设置
设置了格式: 字体: 10 磅, 字体颜色: 自动设置
设置了格式: 字体: 10 磅, 字体颜色: 自动设置
带格式的: 缩进: 首行缩进: 0 字符
设置了格式: 字体: (中文) Times New Roman
设置了格式: 字体: (中文) Times New Roman, 小四, 字体颜色: 自定义颜色(RGB(0,0,204))
带格式的: 缩进: 首行缩进: 2 字符, 段落间距段后: 0.5 行

dimensionally reduced to three components (NMDS1, NMDS2 and NMDS3)~~Three-dimensional ordination is calculated~~ with stress values 0.09. The selected environmental parameters (Table S12) that have relationships or influences with/on the OrgSs composition were also fitted on the bitplots to evaluate the relationships between the distributions of OrgSs and environmental conditions, with *p*-values calculated over 999 permutations. The significant correlated factors were reserved and could be considered as the possible drivers that associated with molecular distribution. Score and loading plots were constructed according to NMDS variables from each OrgSs compound (gray dots and triangles). The potential drivers that associated with molecular distribution of OrgSs were indicated by arrows. Direction and included angle of arrow show the relationship between the driver and each dimension. Spearman correlation between the sum-normalized intensities of individual molecules and some important environmental variables/chemical tracers was performed in R, and then VK diagrams were plotted for each variable based on the Spearman correlation coefficients (Kellerman et al., 2014). Molecules found in at least 4 samples were adopted for correlation analysis. A false discovery rate-adjusted *p*-value was applied to avoid errors arising from using a large dataset.

设置了格式: 字体: (中文) 等线

3 Results and discussion

3.1 Abundance of sulfur-containing species

The annual average ~~concentrations of~~ TS, inorganic sulfate-S and Org-S concentrations were 1.94±0.72~~1.94 μg/m³~~, 1.31±0.60~~1.31 μg/m³~~, and 0.62±0.26~~0.62~~ μg/m^3, respectively (Table 1, n=40). The Org-S concentrations ~~of Org-S~~ over Guangzhou were higher than those observed in a regional European site located in Hungary (0.02−0.33 μg/m^3) (Surratt et al., 2008; Luk´Acs et al., 2009), and close to the upper-bound measured in the U.S. (0.50 μg/m^3)~~, while the percentage of Org-S to fine particles (1.4%) was in the range of 0.75−2.0% estimated in U.S.A~~ (Table S1). These results suggest that the higher Org-S concentration ~~Org-S~~ in Guangzhou might be related to the high concentration of particulate matter and anthropogenic emissions. Furthermore, the high percentage Org-S content in fine particles (1.4±0.6%) was in the middle of the range estimated in the U.S. (0.75−2.0%), suggesting that Org-S might play~~s~~ a large~~r relative~~ role in the atmosphere and is probably an essential factor in~~to~~ the high particle pollution in Guangzhou compared to other sites. Our measurement of the annual Org-S to TS ratio~~s~~ ~~is~~ was 0.33, which ~~is~~ was significantly higher than that of ambient aerosols previously reported in~~at four sites of~~ Asia (0.01− 0.08) (Stone et al., 2012), the Arctic region (0.~~08~~06) (Frossard et al., 2011), Hungary (0.06−0.20) (Luk´Acs et al., 2009; Surratt et al., 2008), and the U.S. (up to 0.22) (Chen et al., 2021). A study conducted in Germany estimated that up to 40% of the TS mass fraction can be contributed by organic molecules (Vogel et al., 2016), which is consistent with our ~~work~~results. There may be many reasons for the ~~The~~ higher ratios ~~at~~ in our measurements than at other sites~~, may arise from many reasons~~ such as the high anthropogenic emissions, high relative humidity, or aerosol acidity levels, which were beneficial to the formation of organosulfur compounds (Bruggemann et al., 2020). Methanesulfonic acid (MSA) may account for a significant amount of the OrgSs mass in Guangzhou because it is a coastal city in southern China. The ratio of MSA-sulfur to Org-S was calculated based on the upper limit of the MSA-sulfur concentration (0.023 μg/m^3)

设置了格式: 字体颜色: 自动设置

设置了格式: 字体颜色: 自动设置

设置了格式: 字体颜色: 自动设置

设置了格式: 字体颜色: 自动设置

设置了格式: 字体颜色: 自动设置

measured in Hong Kong (a megacity near Guangzhou) during marine air mass influenced days (Huang et al., 2015). The estimated average ratio of MSA-sulfur to Org-S was 5.8±8.0, indicating that marine aerosols are probably also a non-ignorable source leading to the high Org-S values.

Table 1: Concentration (μg·m^{-3}) of sulfur-containing species and their fractionation in the $PM_{2.5}$ aerosols from Guangzhou (the samples with TS/SO_4^{2-}-S>2 or < 0.5, and Org-S/TS< $\delta_{Org\text{-}S/TS}$ were excluded as described in section 2.1).

Species/ratios	Spring (n=7)	Summer (n=13)	Autumn (n=5)	Winter (n=15)	Average (n=40)
TS	1.922.03±0.638	1.57±0.68	1.97±0.97	2.25±0.64	1.94±0.72
Sulfate-sulfur	1.2637±0.351	1.03±0.48	1.50±0.92	1.52±0.55	1.31±0.60
Org-S	0.66±0.19	0.54±0.28	0.47±0.27	0.72±0.21	0.62±0.26
Sulfate-sulfur/TS	0.66±0.09	0.67±0.14	0.74±0.11	0.66±0.10	0.67±0.12
Org-S/TS	0.34±0.09	0.33±0.14	0.26±0.11	0.34±0.10	0.33±0.12
f_{OS}(%)	48.2±15.9	45.4±21,9	30.9±14.5	39.1±18.9	41.7±19.7
~~OrgSs/OM~~	~~16.1±5.3~~	~~15.1±7.3~~	~~10.3±4.8~~	~~13.0±6.6~~	~~13.9±6.6~~
Org-S/OM (%)	4.3±1.5	3.9±1.9	2.8±1.8	3.5±1.8	3.7±1.8
Org-S/$PM_{2.5}$ (%)	1.3±0.4	1.8±0.7	1.1±0.4	1.4±0.5	1.4±0.6

In this study, it ~~is~~ was possible to estimate the fraction of OrgSs to the organic mass because~~as~~ the necessary mass-weighted average molecular weight (MW) ~~(or rather C/S ratio)~~ of all OrgSs~~organosulfates~~ ~~can~~ could be obtained from the FT-ICR MS analysis (Luk´Acs et al., 2009). According to Tolocka and Turpin (2012), the fractional contribution of ~~organosulfates~~ OSs to the organic mass (f_{OS}) can be estimated using the following equation:

$$f_{OS} = MW_{OS} \cdot \text{Org-S} / (\text{~~MW}_{Sulfate}\text{~~ MW}_{Sulfur} \cdot \text{Organic Mass}) \quad (1)$$

where MW_{OS} and ~~$MW_{Sulfate}$~~ MW_{Sulfur} denote the molecular weight of ~~organosulfate~~ organosulfur compounds and ~~sulfate~~S atom, respectively. The organic mass was derived from 1.8 times of the OC concentration measured by the Sunset OC/EC analyzer according to Tolocka and Turpin (2012). In this study, the intensity-weighted average MW of OrgSs obtained from the FT-ICR MS analysis (see section 3.2) was used in the calculations. Our estimates of the OrgSs mass to organic ~~matter~~ mass ratio (41.7±19.7%) ~~are~~ were ~~in the range of 0-30%, which are~~ comparable to observations of the ~~30%~~ organic mass~~observed~~ in PM_{10} ~~organic mass~~ over Hungary (Surratt et al., 2008; Luk´Acs et al., 2009), and ~~in the range of 5-50%~~the estimation~~ed~~ ~~in~~ at several sites for fine particulates (Frossard et al., 2011; Tolocka and Turpin, 2012), in which only OSs were considered (Table S1). Although there can be~~Despite the method may cause~~ large uncertainties associated with this method, the ~~our estimate, the likely importance of these~~ estimates clearly showed that OrgSs may be responsible for a sizable fraction of the ambient OM and PM mass, and it is essential to perform ~~the~~ a detailed chemical characterization of OrgSs to improve ~~the~~ our understanding of their sources, formation pathways, and fates in the ambient environment.

设置了格式: 字体颜色: 自定义颜色(RGB(0,0,204))

设置了格式: 下标

设置了格式: 上标

设置了格式: 字体: Times New Roman, 10 磅

设置了格式: 下标

带格式的: 段落间距段后: 10 磅

3.2 FT-ICR MS analysis ~~on~~ of organosulfur compounds

In this study, a total of 15,998 organosulfur formulas were detected in the organic extracts of a yearlong sample set from the FT-ICR MS analysis, and the organosulfur formulas detected in each sample accounted for an average of 33±4% of the total number of assigned molecules ~~on average~~ and 24−62% of the total ~~abundance~~ MS intensity (mean: 44±8%). These compounds ~~are~~were distributed over a wide mass range. Based on the numbers of S and N atoms that appeared in each formula, these OrgSs ~~can~~ could be grouped as $CHOS_1$, $CHOS_2$, $CHON_1S$ and $CHON_2S$. The fractions of the four subgroups are listed in Table S2, with approximately 90% of the molecular number and 96% of the total MS intensity ~~abundance~~ of OrgSs~~OSs~~ attributed to $CHOS_1$ and $CHON_1S$. ~~Since~~ Because a sulfate group ($-OSO_3H$) carries four oxygen atoms and nitrooxy ($-ONO_2$) carries three ~~oxygen~~ O atoms, and they are all readily deprotonated in ESI, OrgSs with excess ~~oxygen~~ O atoms ($o/(4s+3n)\geq 1$) are the likely organosulfates ~~(OSs)~~ or nitrooxy-organosulfates (NOSs). However, other OrgSs ~~such as~~(e.g., sulfonates), may also exist, but ~~have not~~ were not~~been~~ further ~~detected~~considered. As many as 82−92% of the OrgSs detected ~~OrgSs~~ in samples ~~have~~ had $o/(4s+3n)\geq 1$, suggesting that these compounds are potential OSs or NOSs, which is consistent with previous studies (Lin et al., 2012b; Tao et al., 2014; Wang et al., 2019).

3.2.1 CHOS compounds

Table S2 summarizes the average~~d~~ characteristics (molecular weight, elemental ratios, and DBE) of the assigned CHOS and CHONS compounds. The majority (87−95%) of the CHOS formulas in the 55 samples contained enough ~~oxygen~~ O atoms to allow for the assignment of $-OSO_3H$ ($o/4s \geq 1$) in their formulas. The average intensity-weighted H/C, O/C, O/S and DBE values for the CHOS compounds were 1.77±0.03, 0.52±0.07, 6.7±0.4 and 2.77±0.20, respectively. The average H/C ratios of the CHOS compounds in this study ~~are~~ were close to or higher than those previously reported in ambient aerosols (O'brien et al., 2014; Willoughby et al., 2014; Jiang et al., 2016; Jiang et al., 2020), clouds (Zhao et al., 2013; Bianco et al., 2018), and rainwater (Altieri et al., 2009) collected in ~~the~~ different locations worldwide and analyzed~~places of the world measured~~ by negative ESI-FT-ICR MS, indicating that the ~~the~~ OrgSs in Guangzhou are enriched with saturated structures (Table S3). However, the average O/C ratios of the ~~OrgSs~~ CHOS compounds identified~~presented~~ in this study were~~work are~~ slightly higher than those of cloud water (Bianco et al., 2018; Zhao et al., 2013), and comparable to the values measured in east-central~~middle~~ Chinese cities ~~,~~(Wang et al., 2016; Wang et al., 2017a), ~~while~~ but ~~are remarkably~~were much ~~less-oxidized~~lower than ~~samples~~ those of CHOS compounds in polluted organic aerosols ~~measured~~ collected in Mainz and Chinese cities measured using high-resolution Orbitrap~~obtrip~~ MS ~~on pollution days~~ (Wang et al., 2019; Wang et al., 2021b)~~.~~. This implies that CHOS in Guangzhou might arise due to emissions from different sources and then be subjected to complex atmospheric oxidation processes. The differences identified from the comparisons also suggested that the CHOS compounds in Guangzhou might have a clear distinctive molecular composition compared to other locations due to the spatiotemporal heterogeneity, which suggests a need for further investigations of the sources and molecular distribution of OrgSs. ~~Note that t~~The average DBE value of $CHOS_2$ compounds ~~is~~ was approximately ~~3~~ three times that of $CHOS_1$ compounds, indicating

that $CHOS_2$ probably contains numerous aromatic OSs, but $CHOS_1$ compounds are dominated by OSs with long aliphatic carbon chains and low degrees of oxidation and unsaturation.

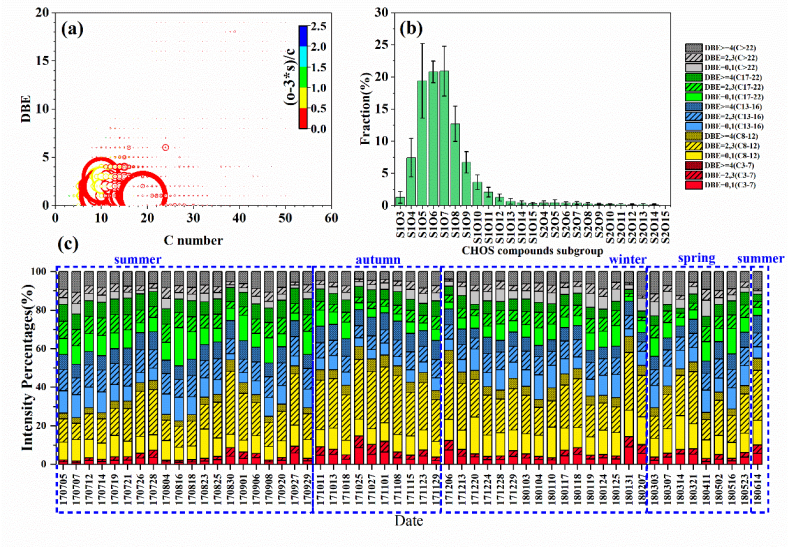
(a)
DBE
C number
(o-3*s)/c
(b)
Fraction(%)
CHOS compounds subgroup
(c)
summer
autumn
winter
spring
summer
Intensity Percentages(%)
Date

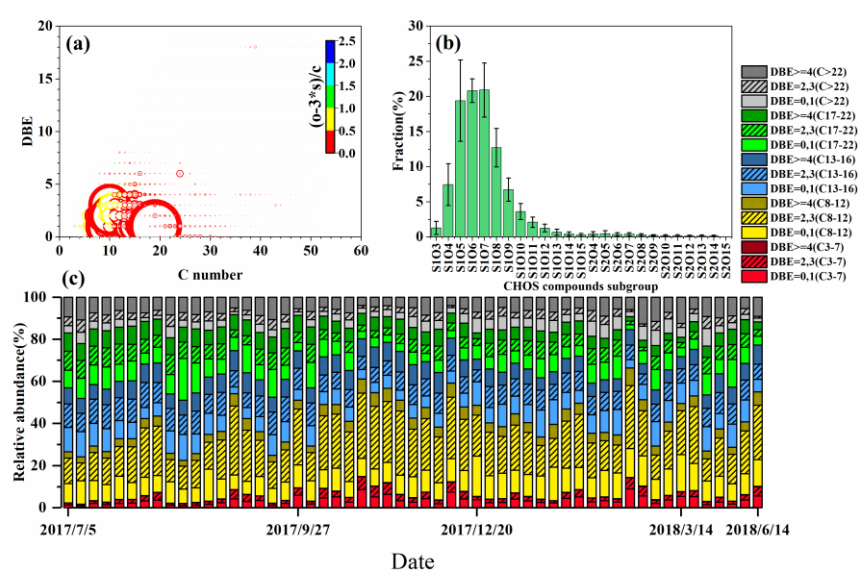

Figure 1: Molecular distribution of CHOS compounds detected by FT-ICR MS for the sample set collected in Guangzhou. (a) Double bond equivalent (DBE) vs C number for all the CHOS compounds of all samples. Each circle denotes a molecule, and t~~T~~he colour bar and marker size denote the number of oxidation state and the average sum-normalized relative peak intensities of the compounds, respectively. Several most intense CHOS species list in descending order by their average intensities in Figure 1a are $C_{19}H_{37}O_7S^-$, $C_{10}H_{19}O_5S^-$, $C_{10}H_{15}O_7S^-$, $C_{10}H_{17}O_7S^-$, $C_9H_{15}O_7S^-$, $C_{14}H_{27}O_5S^-$, $C_{15}H_{29}O_5S^-$; (b) Classification of CHOS species into different subgroups according to the numbers of S and O atoms in their molecules; (c) ~~Relative abundance~~Percentages of signal intensity of each subgroup which divided based on the DBE value and the length of carbon skeleton in the formulas (all 55 samples were presented, yymmdd).

Figure 1&S1 show~~s~~ the DBE, and C, and O atomic distributions in the CHOS compounds. The most abundant CHOS species class identified in all our samples, had 5−7 O atoms and ~~1~~ one S atom. The high number of O atoms in CHOS compounds probably suggested the existence of additional oxidized groups (e.g., hydroxyl and carbonyl). The CHOS compounds with a medium DBE value (=2, 3) accounted for the highest average percentages ~~contribution~~ (40±5%) of ~~the~~ the total MS intensity for the assigned CHOS compounds (Figure 1c). The additional double bonds (or olefinic structures) ~~make~~ made them ~~be~~ potential candidates ~~for~~ for BVOC~~s~~-derived ~~Oss~~ OSs (Jiang et al., 2016; Lin et al., 2012b). ~~Aliphatic (DBE ≤ 1) and aromatic~~ The CHOS compounds ~~(~~with DBE≤1 and DBE ~~≥~~ 4, which were tentatively assigned as ~~)~~ saturated aliphatic-like and aromatic species, took up 34±6% and 26±2% of the total CHOS intensity, respectively. Note that the DBE-based criteria

设置了格式: 字体: 小五, 字体颜色: 自动设置

设置了格式: 字体: 小五, 字体颜色: 自动设置

provided upper bound estimations of the relative abundance of aromatic OrgSs, which was about two times higher than that obtained using the aromaticity equivalent (Xc). The latter was considered a better index to describe potential monocyclic and polycyclic aromatic compounds with S atoms (Ye et al., 2020; Yassine et al., 2014). The aromatic OrgSs were dominated by phenyl OrgSs with Xc values between 2.500 and 2.7143, accounting for 76±9% of the total aromatic OrgSs peak intensity, possibly indicating important influences from anthropogenic primary emissions (Figure S1) (Song et al., 2018; Cui et al., 2019). ~~It should be mentioned that t~~The ~~signal intensity~~relative abundance of high-ring OSs (Xc≥2.7143) increased in winter and spring, suggesting the possibility of more combustion source emissions during these seasons.

Meanwhile, the low and medium DBE CHOS compounds (DBE<4) were further grouped based on the length of the ~~carbon~~ C skeleton in the formulas ~~and for studying~~to enable the distribution of BVOC-derived CHOS compounds to be studied. The relatively low DBE (< 4) CHOS compounds with 3 ~~to~~ 7 carbons (C_{3-7}) ~~are~~ were smaller compounds, which ~~could~~ were probably ~~be~~ the fragments produced by atmospheric oxidation processes or ~~the~~ isoprene-derivatives (Nozière et al., 2010; Riva et al., 2016c; Rudzi´Nski et al., 2009). ~~.~~ Larger compounds with $C_{>22}$ were also detected, but the average percentage of MS intensity~~contribution~~ to the total ~~OrgSs~~ CHOS intensity was as small as ~~those~~ that for C_{3-7} compounds. T~~C$_{8-22}$ compounds were t~~he major fraction in low and medium DBE CHOS compounds (DBE≤3) was C_{8-22} compounds~~with DBE≤3~~, with ~~the~~ C_{8-12}, C_{13-16} and C_{17-22} compounds accounting for 30±7%, 17±3% and 14±5% of the total OrgSs ~~abundance~~intensity, respectively (Figure 1c). The C_{8-22} compounds ~~were thought to~~ likely ha~~d~~ve associations with biogenic sources related to monoterpenoids/sesquiterpenoids~~monoterpened/sesquiterpened~~ and their dimeric oxidation products (Kristensen et al., 2016; Daellenbach et al., 2019). As highlighted by Kourtchev et al. (2016), the higher percentages of MS intensity for dimeric and trimeric BVOC oxidation products in both filed samples and laboratory-generated SOA could be related to the higher precursor and SOA mass. They suggested that a higher temperature could lead to an enhancement of oligomers because it affects not only the biogenic emissions, but also the partitioning of dimeric and monomeric compounds in the gas and particle phases. In this study, the average temperature during the sampling period was 24 ℃. According to Kourtchev et al. (2016), the average maximum temperature of 24±6 ℃ could have an oligomer fraction of 0.3 among the total intensity of all peaks in the mass spectrum. This higher percentage of MS intensity suggested the importance of dimeric oxidation products to the aerosols. However, it should be noted that C_{8-22} CHOS compounds ~~this group of OrgSs~~ ha~~ve~~s also been reported in previous studies and are proposed to be mainly derived from the photooxidation of long-chain alkanes from vehicle emissions (Tao et al., 2014; Riva et al., 2016b), and the reactions of SO_2 and unsaturated acids in ambient particle samples (Shang et al., 2016; Zhu et al., 2019). For example, compounds such as $C_6H_{11}O_6S^-$, $C_7H_{13}O_6S^-$, $C_8H_{17}O_6S^-$, and $C_{10}H_{19}O_6S^-$ were ~~both~~ observed in both the formation processes via monoterpene ozonolysis intermediates (Ye et al., 2018) and uptake of SO_2 by olefinic acid (the possible olefinic acid precursors were all detected in the FT-ICR MS analysis) (Zhu et al., 2019). Therefore, due to our limited data, the origins of CHOS with a low DBE remains large ~~uncertainty~~ uncertainties and needs to be confirmed by further studies.

设置了格式: 字体: 10 磅, 字体颜色: 自动设置
设置了格式: 字体: 10 磅, 字体颜色: 自动设置
设置了格式: 字体: 10 磅, 字体颜色: 自动设置
设置了格式: 字体: 10 磅, 字体颜色: 自动设置
设置了格式: 字体: 10 磅, 字体颜色: 自动设置
设置了格式: 字体: 10 磅, 字体颜色: 自动设置
设置了格式: 字体: 10 磅, 字体颜色: 自动设置
设置了格式: 字体: 10 磅, 字体颜色: 自动设置
设置了格式: 字体: 10 磅, 字体颜色: 自动设置
设置了格式: 字体: 10 磅, 字体颜色: 自动设置
设置了格式: 字体: 10 磅, 字体颜色: 自动设置
设置了格式: 字体: 10 磅, 字体颜色: 自动设置
设置了格式: 字体: Times New Roman
设置了格式: 字体: 10 磅, 字体颜色: 自动设置
设置了格式: 字体: 10 磅, 字体颜色: 自动设置
设置了格式: 字体: Times New Roman

3.2.2 CHONS compounds

As shown in Table S2, the assigned CHONS formulas in each sample accounted for 27–42% and 16–41% of the OrgSs compounds in terms of the formular number of formulas and MS intensityabundance, respectively. These compounds have had a higher average MW, O/C, O/S, and DBE values than the CHOS compounds, which was probably due to the presence of additional nitrate groups. The results of the comparison between the average H/C and O/C ratios of the CHONS compounds and those reported previously were consistent with the results for the CHOS compounds (Table S4). Despite CHONS compounds containing two N atoms were also being identified, their relatively low MS intensityabundance makes them not asless important as than those containing one N atom. In this study, 70-89% (in number) of the CHONS compounds have had $o/(4s+3n) \geq 1$, implying that these CHONS compounds arey were candidates for NOSs. NOSs It have has been demonstrated that NOSs canto form via the photooxidation of biogenic BVOCs in smog chamber experiments conducted under high NO_x conditions (Surratt et al., 2008; Iinuma et al., 2007b). However, recent combustion experiments have found that freshly emitted organic aerosols also contain a significant fraction of CHONS compounds, especially in coal combustion aerosols (Song et al., 2018; Blair et al., 2017; Tang et al., 2020; Cui et al., 2019).

For tThe CHONS species observed in this study, the CHONS compounds observed were $O_4N_1S_1$–$O_{15}N_1S_1$ and $O_7N_2S_1$–$O_{14}N_2S_1$ class species, of which the $O_7N_1S_1$ class species is was the most abundant family. The most abundant chemical formula in most of the samples was $C_{10}H_{16}NO_7S^-$ with DBE=3 and m/z = 294.0653, which was is usually considered to be generated from the oxidation of α-pinene in the atmosphere (Figure S2a) (Surratt et al., 2008). However, it was also identified in coal combustion-emitted aerosols in a recent study, indicating that this compound probably has had multiple sources (Song et al., 2018). The distribution of the CHONS compounds across DBE and carbon C numbers are was quite similar to that of the CHOS compounds (Figure S2a). Note that fFrom the equation of the DBE calculation, each nitrooxy group in the CHONS compounds also contains contained one double bond and therefore contributes contributeed to a DBE value of 1. Therefore, the DBE values minus the number of N atoms (DBE−N) is a better criterion to determine the aromatic structure or whether this is not possible (Lin et al., 2012b). The CHONS compounds were dominated by olefinics ((DBE−N)=2, 3), followed by saturated aliphatic ((DBE-N)≤1) and aromatic ((DBE−N)≥4) CHONS (Figure S2c&d). Furthermore, the most abundant classes in the saturated aliphatic and olefinic CHONS were C_8-C_{12} compounds with O numbers higher than 7 (Figure S2 b&c&de&f). Likewise, as described above, they were most likely formed from the reactions of anthropogenically and biogenically emitted VOCs, respectively.

3.3 Comparison and Potential potential precursor apportionmentappointment of OrgSs with previous knowledge.

A substantial overlap of OrgSs were observed in this work with source samples, including BBOA, coal combustion organic aerosols (CCOA) and vehicle emissions, non-road excavator and ship emissions, and tunnel aerosol samples (Table S5) (Tang et al., 2020; Cui et al., 2019). Figure S2a shows the a comparison of the molecular characteristics of OrgSsorganosulfur compounds for our field observation samples and source samples. The intense OrgSs in Guangzhou were

设置了格式: 下标

mainly composed of unsaturated aliphatic molecules, which ~~is~~ was similar to the tunnel aerosol sample that may have undergone atmospheric aging processes. However, the OrgSs in fresh vehicle emissions were abundant in aromatics~~abundant by aromatics~~, with 69% of identified OrgSs having Xc≥2.500 (Table S5). Despite the diesel fuel combustion-emitted aerosols also containing unsaturated aliphatic molecules with a high intensity, their oxidation levels were ~~clearly~~ lower than those of our field samples. Both BBOA and CCOA were abundant with aromatic and highly unsaturated organosulfur molecules, which ~~show~~ had distinctive molecular characteristics compared to our field samples. Although 50±5% (in number) of the OrgSs identified in Guangzhou~~GZ~~ could be attributed to aromatic OrgSs, most of them ~~have~~ had a low intensity. Although~~These results probably show that although~~ combustion sources can emit large numbers of OrgSs, the ~~low abundance of~~ primary low-oxidative and aromatic OrgSs abundant in source samples had a low MS intensity in our ambient samples. This ~~but abundant in source samples~~ probably suggested that the OrgSs in Guangzhou ~~suffered~~ were ~~little~~ less or indirectly affected by~~influence from~~ primary emissions (e.g., secondary formation via ~~the~~ combustion-emitted precursors). Additionally, we apportioned~~appointed~~ the detected OrgSs into five groups based on their potential precursors, including BVOC~~s~~-derived OSs ~~such as~~ (e.g., isoprene-derived OSs, monoterpene-derived OSs, and other BVOC~~s~~-derived OSs from the precursors of green leaf volatiles)~~.~~, ~~Moreover, the relative abundances of~~ anthropogenic VOCs-derived OSs from the precursors of aromatics and anthropogenically emitted alkane precursors~~s~~, and multiple-source-derived OSs from ~~the precursors of several~~ carbonyl compounds, unsaturated acid~~s~~ and alkanes~~, were also summarized and calculated~~. Details of these OSs formulas with the determined precursors are listed in Table S6-10. ~~It should be mentioned that~~ T~~t~~he OSs ~~that~~ that were identical to the published OSs (their precursors previously have been ~~clearly~~ verified) were temporarily considered to have the same precursors as the published OSs in the ~~present~~ this study. This method has been widely used~~, as the~~ because its feasibility ~~of this method~~ is based on the high mass resolution of HR-MS ~~in~~ for the ~~identifying~~ identification of mass peaks in conjunction, with the assignment of formulas using a narrow mass tolerance (Lin et al., 2012b; Kuang et al., 2016; Ye et al., 2020).

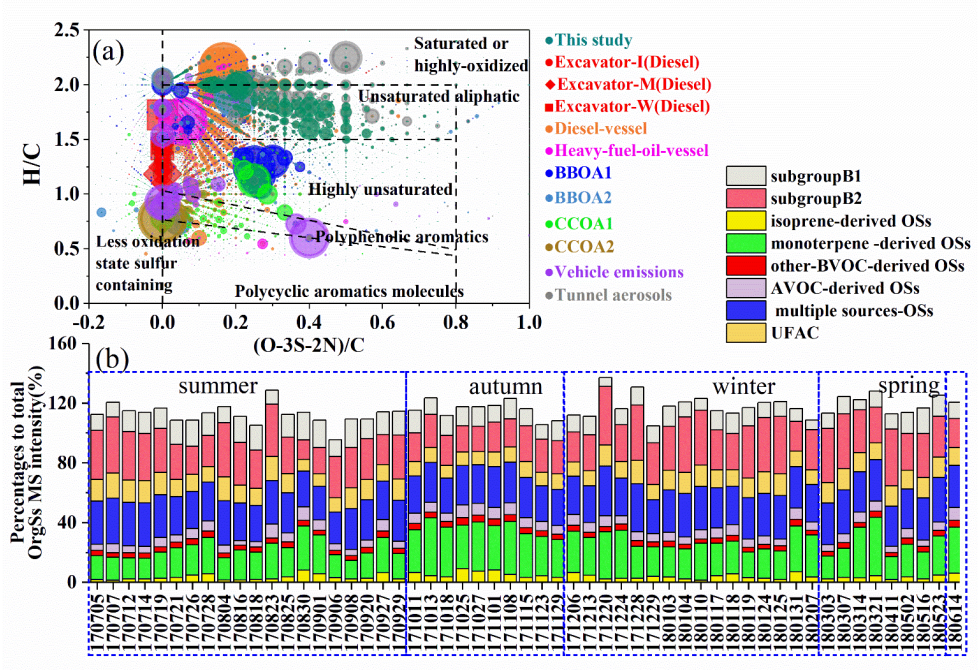
(a)
Saturated or highly-oxidized
Unsaturated aliphatic
Highly unsaturated
Polyphenolic aromatics
Less oxidation state sulfur containing
Polycyclic aromatics moleculs
H/C
(O-3S-2N)/C
This study
Excavator-I(Diesel)
Excavator-M(Diesel)
Excavator-W(Diesel)
Diesel-vessel
Heavy-fuel-oil-vessel
BBOA1
BBOA2
CCOA1
CCOA2
Vehicle emissions
Tunnel aerosols
subgroupB1
subgroupB2
isoprene-derived OSs
monoterpene -derived OSs
other-BVOC-derived OSs
AVOC-derived OSs
multiple sources-OSs
UFAC
(b)
summer
autumn
winter
spring
Percentages to total OrgSs MS intensity(%)

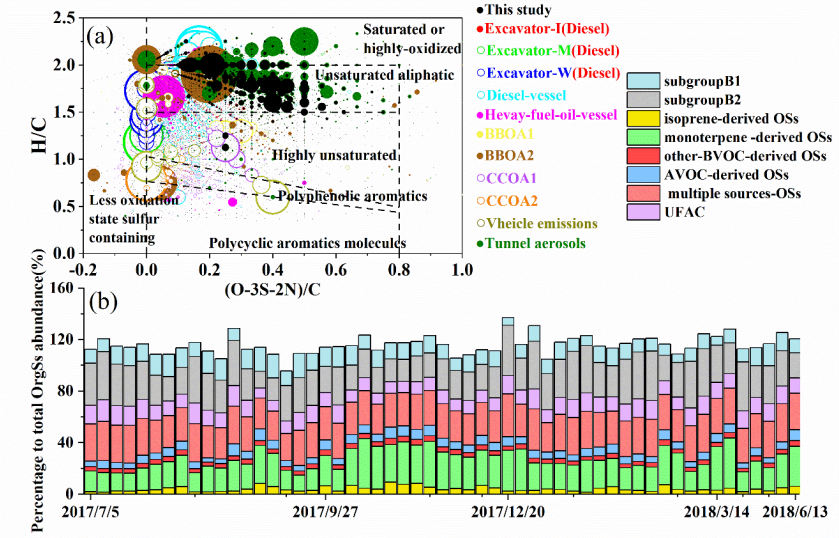

Figure 2: (a) Van Krevelen diagrams of the ~~filed~~ field samples collected in Guangzhou and source samples obtained from Cui et al. (2019) and Tang et al. (2020), including biomass burning organic aerosols (BBOA), coal combustion organic aerosols (CCOA), vehicle emissions, tunnel aerosols, and off-road engine emissions (excavator and vessel). Excavator-I, -M and -W denotes the operation modes of idling, moving, and working, respectively. The marker size denotes the percentages of MS intensity~~relative abundance~~ to the total identified organosulfur compounds. (b) Annual variations of potential precursor of detected OSs to the total identified organosulfur compounds MS intensity ~~abundance~~; subgroupB1 denotes OSs having C>8, DBE<3 and 3<O<7 (for CHOS)/ 6<O<10 (for CHONS), while subgroupB2 denotes OSs having C>8, DBE<3 and O≥7 (for CHOS)/ O≥10 (for CHONS).

设置了格式: 字体: 加粗

设置了格式: 字体: 加粗

Figure 2b shows the annual variations of the ~~sum~~ total MS intensity~~relative abundance~~ of the ~~above~~ five OSs groups ~~to~~ as a percentage of the total OrgSs ~~-~~MS intensity~~abundance~~, with annual average proportions of 3.8±1.9%, 23±6.7%, 3.6±0.5%, 6.1±1.4% and 27±2.3% for isoprene-derived OSs, monoterpene-derived OSs, other BVOC~~s~~-derived OSs, anthropogenic VOC~~s~~-derived OSs and multiple-source-derived OSs, respectively. The high percentages of MS intensity ~~contribution~~for ~~of~~ known terpene-derived OSs to the total OrgSs intensity in this study~~GZ is~~ was consistent with previous observations of the dominance of terpene-derived OSs in Guangzhou~~GZ~~ (Wang et al., 2017b; He et al., 2014; Bryant et al., 2021). Several highly abundant formulas of terpene-derived OSs, $C_{10}H_{16}O_7NS^-$ (m/z 294); $C_{10}H_{19}O_5S^-$ (m/z 251), $C_{10}H_{15}O_7S^-$ (m/z 279), $C_{10}H_{17}O_7S^-$ (m/z 281) and $C_9H_{15}O_7S^-$ (m/z 267), ~~were~~ have been widely reported ~~in previous studies~~ as ~~all~~ being predominantly formed by the acid-catalyzed chemistry of BVOC~~s~~-derived oxidation products (Hettiyadura et al., 2019;

Bruggemann et al., 2020). Notably, ~~the intense specie~~ $C_9H_{15}O_7S^-$ was also observed ~~in the~~ as a secondary product ~~formed~~ by isoprene (Meade et al., 2016), which was partially supported here by the positive correlation between their sum-normalized intensity and the concentration of ~~C5 alkenetriols~~MTLs (SOA tracers of isoprene, the sum of 2-methylthreitol and 2-methylerythritol) (r=0.~~71~~73, p<0.01) (Li et al., 2013). ~~Considering that the i~~Isomers ~~integrating~~ acting as both anthropogenic and biogenic precursors cannot be distinguished ~~due to the application of direct infusion of~~by an FT-ICR MS analysis, because compounds with specific m/z values ~~only~~ are manifested as a single signal in the FT-ICR mass spectra, and our reported ratios may therefore be subjected to~~have~~ uncertainty~~ies~~. Furthermore, due to the limitation of detection techniques and trace concentrations, the incomplete OSs list in the SI for the different SOA precursor groups may ~~, which due to the limitation of detection techniques and trace concentrations,~~ also leads to uncertainty in our classification.

Polycyclic aromatic hydrocarbons have been recognized as ~~important~~ precursors of aromatic OSs from laboratory evidence (Riva et al., 2015). Aromatic OSs with benzyl and polycyclic aromatic ~~carbon~~ C backbones, such as $C_6H_5SO_4^-$, $C_7H_5SO_4^-$, $C_7H_7SO_4^-$, $C_8H_7SO_4^-$, and $C_9H_{11}SO_4^-$ and several OSs from the photooxidation of naphthalene and 2-methylnaphthalene, ~~were~~ have been widely observed in urban and semirural fine particles worldwide (Le Breton et al., 2018; Huang et al., 2018a; Wang et al., 2018b; Hettiyadura et al., 2015; Bruggemann et al., 2020) and were also detected in our samples. However, ~~there are~~ presently only a~~oo~~ few ~~classified~~ species of aromatic OSs with a relatively low MS intensity have been classified~~abundance~~. ~~In overall, the a~~Aromatic OrgSs with Xc≥2.5 accounted for 9~~–~~-20% of the total OrgSs peak intensity in this study, emphasizing the significant contribution of anthropogenic emissions ~~to~~ in Guangzhou.

Among the classified OrgSs with their precursors from multiple sources, a high intensity fraction ~~was contributed by those OrgSs~~ that was likely derived from~~from~~ unsaturated fatty acids (USFA) was identified, ~~with~~and contributed 8%−17% (average: 12%) of the total OrgSs potentially assigned, despite the limitations imposed by the large numbers of different OrgSs variants. We observed a positive correlation between ~~unsaturated fatty acid (~~USFA~~)~~-derived OSs and RH (r^2=0.19, p<0.01), which partly~~probably~~ ~~supporting~~ supported the mechanism of USFA-derived OSs formation by direct SO_2 uptake. This ~~is~~ was consistent with a recent study showing that USFA-derived OSs accounted for a high fraction of the total OSs intensity (5%−7% sulfur of all the OrgSs) and were positively correlated with RH in the PRD (Zhu et al., 2019). The authors tentatively attributed the formation of these OSs to the direct reaction of SO_2 with unsaturated acids in ambient particle samples in the presence of gas-phase oxidants such as OH radicals or ~~O_3~~ O_3, because several laboratory studies (Shang et al., 2016; Passananti et al., 2016) have observed ~~the~~ a dependency of USFA-derived OSs formation~~s~~ on RH. It has been ~~and~~ suggested that RH is an important influencing factor, ~~in which~~ and increasing humidity would accelerate SO_2 uptake and thereby OSs formation.

We noted that the subgroup of OSs with unidentified precursors and ~~having~~ C>8, DBE<3, and 3<O<7 (for CHOS)/ 6<O<10 (for CHONS)~~, took up~~ accounted for 27±7% of the MS intensity~~abundance~~ of the total identified OrgSs. This subgroup of ~~Oss~~OSs (subgroupB1) is characterized by a high molecular weight, alkyl chains and a low degree of oxidation, and was first reported by Tao et al. (2014) who speculated that the precursors of this subgroup of OSs could be long-chain alkanes from traffic emissions. The long-chain alkanes were photooxidized by a mixture of oxidants under typical urban conditions and

formed hydroxylated or carbonylated products, which were further esterified to form alkyl OSs. Riva et al. (2016a) conducted an experiment on the photooxidation of alkanes in an outdoor smog chamber and proposed that gaseous epoxide precursors with subsequent acid-catalyzed reactive uptake onto sulfate aerosols and/or heterogeneous reactions of hydroperoxides can also be used to explain the formation of alkane-derived OSs. Furthermore, the formation of OSs via heterogeneous reactions of SO_2 with ~~unsaturated fatty acids~~USFA was also important for these highly saturated OSs (Zhu et al., 2019). The~~The positive correlations between the~~ total relative intensity of ~~this~~ subgroup ~~of OSs~~B1 was positively correlated ~~and~~with RH and ~~the~~ the concentrations of chemical tracers associated with fossil fuel combustion (Cl^-, steranes and hopanes: ~~(~~ΣSH) ~~and RH~~ (Figure S3), support the ~~above~~ influences of heterogeneous reactions and photooxidation of traffic-emitted long-chain alkanes on subgroupB1 ~~formation mechanisms~~, but more detailed source information ~~remains equivocal~~ is required to confirm this.

3.4 Possible formation pathways of OrgSs and the influencing factors

As shown in the ~~the~~ previous section, ~~the current result suggests that~~ OrgSs in the atmosphere ~~on~~ in Guangzhou~~GZ~~ were significantly influenced by different sources, including both primary emissions and secondary formation~~s~~. However, although a variety of reaction pathways have been proposed for the secondary formation of OSs, the formation mechanisms of OSs in the atmosphere are not fully understood. ~~Recently,~~ Bruggemann et al. (2020) reviewed and summarized the OSs formation pathways that have been identified thus far and outlined their potential atmospheric relevance. ~~Overall,~~ It has been shown to be kinetically feasible for acid-catalyzed reactions of the epoxides formed by the oxidation of VOCs~~OS product distributions are expected to depend on precursor concentrations (including organic compounds and anthropogenic pollutants of NOx, SO_2, …), acidity, RH and oxidant concentrations. Acid-catalyzed reactions of epoxides oxidized from VOCs were shown to be kinetically feasible~~ to produce Oss, and this mechanism ~~are~~ has been widely adopted to explain ~~the formation of Oss~~OSs formation (Surratt et al., 2007; Iinuma et al., 2007b; Surratt et al., 2008; Surratt et al., 2010; Lin et al., 2013). The distribution of OS products is~~OS product distributions are~~ expected to depend on precursor concentrations (including organic compounds and anthropogenic pollutants, e.g., ~~of~~ NO_x and ~~,~~ SO_2, …), acidity, RH, and oxidant concentrations. ~~Acid-catalyzed reactions of epoxides oxidized from VOCs~~A recent study conducted in South China also ~~showed~~ revealed that high levels of isoprene-derived OSs were derived from the acid ~~ring~~ ring-opening reactions of ~~-~~isoprene-derived epoxydiols (He et al., 2018). In view of the products' molecular structure, the acid-catalyzed ring-opening of epoxides by the addition of inorganic sulfate ions~~HSO_4^-~~ usually leads to the formation of β-hydroxyl OSs (Figure 3, Scheme 1) (Lin et al., 2012b). Thus, the OSs and ~~nitrooxy~~ NOSs generated from the epoxide pathway usually have O>4 for CHOS compounds and O>7 for CHONS compounds, respectively. Lin et al. (2012b) removed $-SO_3$ from the OrgSs to obtain the corresponding alcohols and examined their presence by comparing them with the non-S-containing formulas in the samples collected at the P~~earl River Delta~~RD. They found that 65~~–~~–75% of the CHOS compounds could be formed from the epoxide intermediate pathway. In our samples, an upper bound estimation for the fraction of OrgSs formed via the epoxide intermediate pathway could reach half number of the detected OrgSs because ~~of~~ 46±12% (both in number and MS intensity) of OrgSs satisfied the

设置了格式: 下标

设置了格式: 下标

~~abovedabove~~ criterion (Table S11). The percentage of MS intensity for these OrgSs had a decreasing trend from summer to winter, and then increased in spring. It presented positive correlations with the fraction of SO_4^{2-} in secondary ion aerosols (SIA) (r=0.54, p<0.01), temperature (r=0.63, p<0.01) and biogenic SOA tracer (r=0.34, p<0.05), which was consistent with a recent study (Bryant et al., 2021) and suggested that the temperature and available particulate SO_4^{2-} are important influencing factors in the formation of OrgSs via the acid-catalyzed ring-opening of epoxides.~~Other formation pathways are also important and could contributed large fraction of OrgSs.~~

设置了格式: 字体: Times New Roman
设置了格式: 字体: Times New Roman
设置了格式: 字体: Times New Roman
设置了格式: 下标
设置了格式: 上标
设置了格式: 字体: 倾斜
设置了格式: 字体: 倾斜

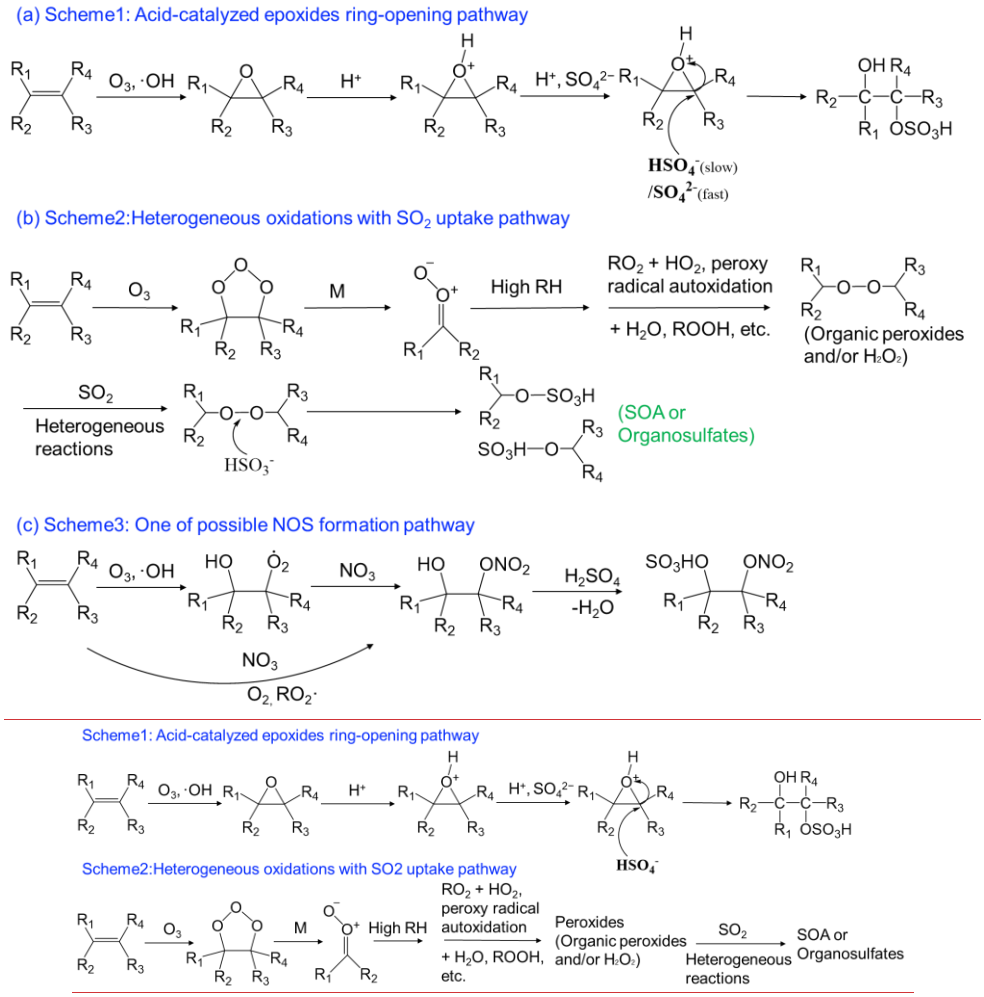

Figure 3: The two potentially important OSs formation mechanisms in Guangzhou (Duporte et al., 2020; Ye et al., 2018; Bruggemann et al., 2020; Aoki et al., 2020; Lind et al., 1987). (a) Proposed OSs formation mechanism of acid-catalyzed ring-opening of epoxides; (b) Proposed OSs formation mechanism for heterogeneous reactions of SO_2 and

设置了格式: 下标

the secondary products from ozonolysis unsaturated hydrocarbon at high relative humidity; (c) one of possible NOSs formation pathway.

From the Org-S mass data, as shown in Table 1, the Org-S, ~~species~~ along with TS and sulfate-sulfur levels exhibited a clear seasonal variation, with all ~~show~~ having higher values in autumn and winter than in spring and summer (ANOVA, p<0.01). The higher levels of sulfur-containing species in cold seasons ~~values~~ may be due to the higher anthropogenic emissions ~~in cold seasons~~. However, both the Org-S/$PM_{2.5}$ ~~to particulate mass ratio~~ and ~~the OrgSs to organic mass ratio~~f_{OS} exhibited different seasonal variation~~s compared to its concentration~~, with higher ratios observed in summer than in the ~~warm~~ cold seasons. This different seasonal characteristic may have been influenced by several factors, including precursor emissions of ~~biogenic~~ B~~VOCs~~ VOCs, and high RH levels, which might increase the SO_2 uptake and formation of OrgSs during warm seasons (Bruggemann et al., 2020; Zhu et al., 2019). Additionally, gas-phase oxidation initiated by O_3 or OH radicals, which promote the generation of oxidation products, hydroxyl, and carbonyl (Riva et al., 2016b), also contributed to the formation of OrgSs. This~~ese~~ was~~ere~~ supported by the finding that the Org-S concentration ~~of Org-S~~ was positively correlated with oxidant levels (indicated by NO_x+O_3, r=0.40, p<0.01) and SO_2 (r=0.37, p<0.05) (Figure S4). Furthermore, we observed that the Org-S concentration ~~of Org-S~~ was positively correlated with ~~the fraction of~~ NO_3^- ~~in secondary ion aerosols (~~SIA~~)~~ (r=0.41, p<0.01), but negatively correlated with the SO_4^{2-}/SIA ratio~~s~~ (r= −0.40, p<0.01), probably suggesting the presence of competition between SO_4^{2-} and OrgS~~s~~ in their formation (Figure S4) ~~(Figure S4)~~. This wa~~s~~ is inconsistent with a previous observation that ~~the~~ OSs increased with SO_4^{2-}/SIA, which showed a linear relationship~~regression~~ with particulate acid (Guo et al., 2016; Wang et al., 2018b). Several studies have also reported that some isoprene-derived OSs, which were produced through the reactive uptake of isoprene-epoxydiol (IEPOX) onto acidic particles, exhibited no correlation with aerosol acidity (He et al., 2014; Lin et al., 2013; Worton et al., 2013). In this study, the pH of all samples was below 5 and we did not observe a significant correlation between pH values (or H^+) and the Org-S concentration, but a molecular-level assessment showed that a ~~hundreds~~ small number of individual organosulfur species were ~~positively~~ significantly correlated with the H^+ concentration~~pH~~, probably indicating that the variation~~s~~ in particulate acid have minor associations with ~~the~~ OrgSs formation in overall. Additionally, ~~it is worth mentioning that~~ we found that ~~that~~ the Org-S concentration ~~of Org-S~~ ha~~s~~d a ~~insignificant~~ non-significant correlation with ~~the concentration of~~ levoglucosan and ΣSH concentration, ~~indicateing~~indicating that primary ~~combustion sourc~~biomass burning and fossil fuel combustion~~es~~ probably ~~have~~ had little or no direct impact on the variation of Org-S~~organosulfur~~, which ~~is~~ was consistent with the compar~~ativeison~~ analysis reported in ~~the~~ section 3.3.

~~Also, o~~Our findings ~~may~~ also provide support for the heterogeneous reactions of ~~the~~ ~~the~~ SO_2 uptake pathway, which ~~is~~ was expected because, as discussed above, the Org-S concentration was positively correlated with O_3, NO_2, and SO_2, and RH was negatively correlated with SO_2 (Ye et al., 2018; Bruggemann et al., 2020). Both laboratory studies and field observations have suggested that SO_2 uptake by unsaturated compounds and naphthalene, and the formation of OSs were shown to increase with higher RH levels (Zhu et al., 2019; Shang et al., 2016; Riva et al., 2015). Blair et al. (2017) also reported an

带格式的: 段落间距段后: 0.5 行
设置了格式: 字体: 倾斜
设置了格式: 下标
设置了格式: 下标
设置了格式: 上标
设置了格式: 字体: 小四
设置了格式: 非上标/ 下标

increase in ~~their~~ concentration~~s~~ with increasing RH for some specific aromatic OSs in biodiesel and diesel fuel SOA. Ye et al. (2018) found that SO_2 uptake and OSs formation ~~were shown to~~ increas~~ede~~ with higher RH levels for the monoterpene ozonolysis intermediate, which was likely ~~owing~~ due to reactions between SO_2 and organic peroxides. Given the high RH levels during the sampling campaign (average=~~71~~70±14%) and the above results, it ~~is~~was reasonable to speculate that SO_2 was preferentially partitioned into the aqueous phase and formed HSO_3^-, with the formation of OSs through ~~the~~ reactions between HSO_3^- and the organic precursor ozonolysis intermediate, organic (hydro-)peroxides (Figure 3, Scheme 2) (Ye et al., 2018; Bruggemann et al., 2020).

设置了格式: 字体: Times New Roman

设置了格式: 下标

设置了格式: 下标

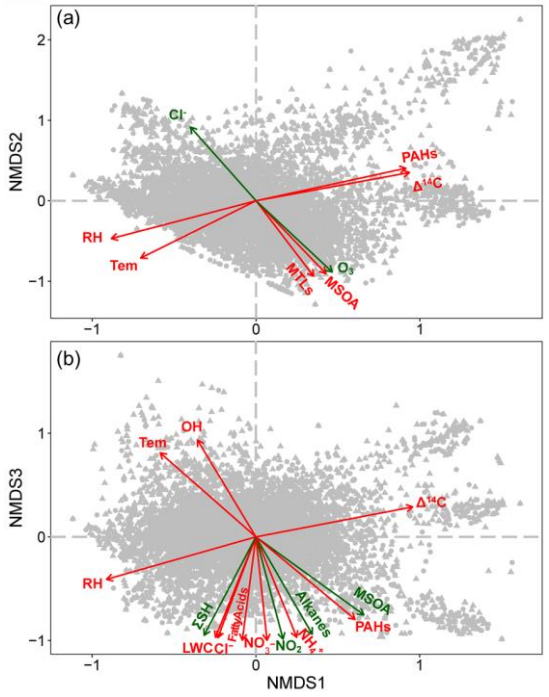
(a)
NMDS2
Cl-
PAHs
Δ14C
RH
Tem
MTLs
O3
MSOA
(b)
NMDS3
OH
Tem
Δ14C
RH
ΣSH
FattyAcids
Alkanes
MSOA
PAHs
LWCCl
NO3-
NO2-
NH4+
NMDS1

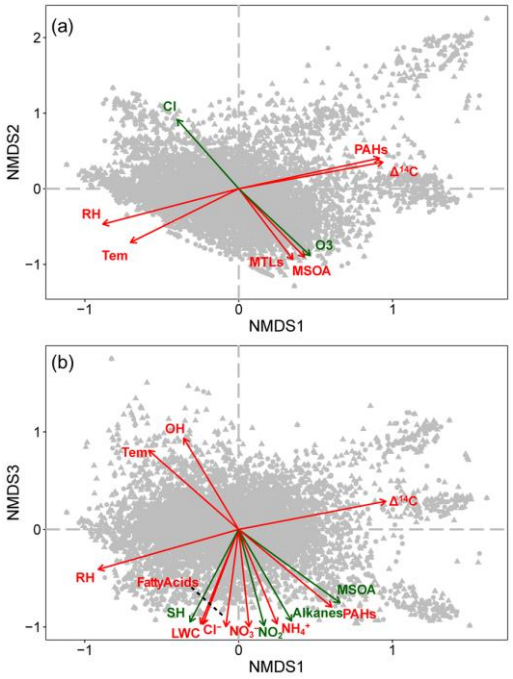

Figure 4: Nonmetric multidimensional scaling analysis of the influences from environmental parameters on organosulfur compounds. The three-dimensional ordination Ordinations are based on Bray−Curtis (stress = 0.09, non-liner r^2=0.99), which utilizes sum-normalized relative compound intensity. Environmental parameters listed in Table ~~S6~~ S12 were fit to the ordination. Gray-shaded dots and triangles~~circles~~ are ~~organosulfur~~ CHOS and CHONS compounds, respectively. Variables with significance levels of <0.05 (green) and <0.01 (red) are shown, and nonsignificant correlations are not shown.

To ~~better~~ support our speculation and discern the possible environmental drivers of the molecular distribution of OrgSs, NMDS analysis of OrgSs was ~~used~~ conducted (Figure~~.~~ 4 and Table S12). Among the significant drivers, ~~We~~ it was noted that RH wa~~i~~s ~~an~~ important and ~~driver~~ associated with the seasonal distribution of the OrgSs composition, with~~as~~ RH and temperature ~~are~~ clustered at the negative end of the first dimension, while $\Delta^{14}C$ was positively correlated with the first dimension. Notably, ~~the~~ an "older" ^{14}C age of organic carbon ~~is~~ was generally accompanied by a high RH, and the results a from recent compound-specific dual-carbon isotopic ($\delta^{13}C$ and $\Delta^{14}C$) analysis of dicarboxylic acids (SOA tracers) indicated that large fractions of the organic mass were substantially ~~contributed~~ supplied by the aqueous-phase transformation of

fossil-fuel precursors (Xu et al., 2021a). These results ~~may suggest~~indicate the importance of the aqueous-phase formation of OrgSs via fossil-fuel precursors ~~other than~~in addition to the direct emissions from combustion sources (Wang et al., 2021a). Additionally, we found that the BVOC~~s~~-derived SOA tracers and O_3 were distributed at the negative end of the second dimension, while the anthropogenic species (e.g., NO_3^-, NH_4^+, NO_2, fatty acids, and ΣSH~~...~~) and aerosol liquid water content (LWC) were negatively correlated with the third dimension, ~~which was inversely~~with the opposite pattern for temperature and OH radical (Figure 4). This probably suggested that there were the different oxidation processes involved in the formation of OrgSs between the warm and cold seasons, ~~as~~ with cold seasons often ~~featured~~ experiencing high anthropogenic emissions, while ~~and~~ high biogenic emissions ~~are often happen~~occur in warm seasons (see Supplementary text). The cluster of BVOC~~s~~-derived SOA tracers and O_3 probably suggested that SOA products produced by the reactions of BVOCs with O_3 ~~are~~ were important precursors of the OrgSs in this study, which was supported by recent studies showing that ~~the~~ daytime/~~nighttime~~night-time O_3-related oxidation in the presence of SO_2 also potentially contributed to the ~~organosulfates~~ OSs formation (Xu et al., 2021b; Chen et al., 2020). However, the cluster of anthropogenic organic compounds, together with reactive nitrogen species and LWC, probably also suggested the influence ~~s~~ of aqueous-phase reactions of fatty acids and other fossil-fuel precursors on OrgSs formation, particularly the inorganic nitrogen ~~species~~ species-related formation of NOSs (Bryant et al., 2021). This ~~is~~ was expected because aerosol LWC provides a ~~media~~ medium for ~~aqueous~~ aqueous-phase reactions (Guo et al., 2016; Liu et al., 2017; Wang et al., 2018b), and positive correlations were observed between LWC and secondary inorganic aerosols (r=0.69, p<0.01), particularly the inorganic nitrogen species. Moreover, a direct~~ly~~ assessment of the~~ing~~ relationships between individual compounds and LWC, NO_3^-, and NH_4^+ suggested that an~~the~~ increase ~~of~~ in their concentrations would promote the formation of CHONS species~~,~~. It was found that ~~as~~ 100%, 64%, and 74%~~72%, 65% and 75%~~ of the OrgSs that ~~have~~ had positive correlations (~~*p*~~ *p*-adjusted with "fdr") with the LWC, NO_3^-, and NH_4^+, respectively, ~~are~~ were CHONS species (Table S13~~),).~~ ~~respectively.~~This further ~~supports~~ indicated that~~the~~ OrgSs formation via aqueous-phase chemistry in Guangzhou was influenced by LWC, such as the NO_3-initiated oxidation~~,~~ and acid-~~catalyzed~~catalysed epoxide pathways (Wang et al., 2020; Xu et al., 2021b). Recently, Bryant et al. (2021) reported that oxidants and temperature are important factors that affect OSs formation in Guangzhou, and high-NO_x pathways became more important in the winter when ~~usually suffering high~~ anthropogenic emissions usually high, ~~while~~ whereas low-NO_x formation pathways were dominant in ~~the~~ summer. The observed opposite influence of OH radicals and inorganic species on OrgSs distributions also suggested ~~the existence of~~ OrgSs formation occurred through~~from~~ heterogeneous OH radical oxidation when ~~there was less~~ anthropogenic emissions were low (Chen et al., 2020; Lam et al., 2019). These results suggested the importance of atmospheric oxidation on the molecular composition of OrgSs, but there may be distinct effects for different oxidation processes (i.e., gas-phase O_3 oxidation, liquid-phase NO_3-initiated oxidation and heterogeneous OH radical oxidation).

设置了格式: 下标

设置了格式: 下标

设置了格式: 下标

4 Conclusions

This study ~~reports~~ investigated the abundance and molecular characteristics of the ~~the~~ atmospheric organic sulfur fraction in Guangzhou, South China, with yearly $PM_{2.5}$ samples ~~were~~ collected and ~~analyzed~~analyzed. ~~Our estimation~~The results showed that organosulfur can ~~contribute~~ accounted for up to ~~25~~42% of the total organic mass on average, ~~which~~ and is particularly important ~~to~~ in fine particulate pollution. A ~~Molecular~~ molecular composition analysis performed ~~by~~ using negative ESI-FT-ICR MS suggested ~~the~~ a complex chemical composition and ~~their~~ multiple sources. The substantial overlap of the organosulfur species observed in this study with those identified in previous chamber and field studies ~~suggests~~ suggested that ~~these~~ alternative mechanisms of organosulfur formation could be important in the atmosphere ~~in~~ over Guangzhou. ~~Furthermore, w~~We also compared the organosulfur species composition with several source samples and found clear differences ~~were found~~ among different source samples. ~~It should be noted that m~~Many organosulfur species in our data that were previously classified as having biogenic, anthropogenic, or unidentified sources were also found among the collected source samples. Despite most of time the~~y~~ aromatic organosulfur compounds ~~show~~ had a relatively low MS intensity~~abidance than aromatic organosulfur compounds~~, the high fraction of formular number to the total assigned OrgSs suggesting that ~~the~~ extensive~~large~~ human activities~~,~~ and high level of anthropogenic emissions (e.g., vehicle emissions, coal combustion and biomass burning) made an ~~possibly imply their~~ important contributions~~ ototo~~ the~~se~~ OrgSs composition~~commonly detected species and they require additional scrutiny~~.

~~As~~ Because the formation pathways and influencing factors of OrgSs were hardly recognized, we employed an NMDS analysis based on the large amounts of data obtained~~huge data~~ from the FT-ICR MS analysis and chemical tracers. Both the mass concentration and chemical composition data ~~provide~~ indicated the potential OrgSs formation ~~of~~ from acid-catalyzed aqueous-phase reactions, and RH and oxidant levels~~s~~ (NO_x+O_3) ~~are~~ were important environmental drivers that influenced the OrgSs distributions and heterogeneous reactions of SO_2 uptake in OrgSs formation~~s~~. This wa~~i~~s consistent with most previous observations of higher yields of organosulfur species at elevated RH during laboratory experiments. The oxidation of BVOCs with O_3~~,~~ and oxidation of anthropogenic VOCs in the presence of ~~anthropogenic VOCs with~~ NO_{2x} were two potentially important pathways for the formation of OrgSs ~~formation~~ or their precursors ~~of OrgSs~~. From our results, we stress~~ed~~ that although RH ~~is~~ was an immutable parameter, reducing ~~the~~ SO_2 emissions ~~is not~~alone was insufficient ~~enough~~ to decrease the OrgSs fraction ~~of OrgSs~~ in ~~the~~ atmospheric particulates, and it was ~~but~~ also ne~~cessaryeds~~ to reduce NO_2 and other anthropogenic emissions.

设置了格式: 下标

Data availability

Data are available upon request, by the corresponding authors.

Author contributions

HJ and JL designed the experiment. HJ, JT, BJ and YL carried out the measurements. HJ, JT and YM analysed the data. HJ, JL and GZ organized and supported the samplings. JL and GZ supervised the study and worked for funding acquisition. MC

and JT provide the original data about the source samples. HJ wrote the paper. JL, GZ, MC, YM, SZ, XZ, and GZ reviewed and commented on the paper.

Competing interests

The authors declare that they have no conflict of interest.

Acknowledgements

This study was supported by the Natural Science Foundation of China (42030715, 41773120, 42192514, and 41977177), National Key R&D Program of China (2018YFC1802801), the, Guangdong Foundation for Program of Science and Technology Research (Grant No. 2019B121205006 and 2020B1212060053).

References

Altieri, K. E., Turpin, B. J., and and Seitzinger, S. P.: Oligomers, organosulfates, and nitrooxy organosulfates in rainwater identified by ultra-high resolution electrospray ionization FT-ICR mass spectrometry, Atmos. Chem. Phys., 2533-2542, doi:10.5194/acp-9-2533-2009, 2009.

Aoki, E., Sarrimanolis, J. N., Lyon, S. A., and Elrod, M. J.: Determining the Relative Reactivity of Sulfate, Bisulfate, and Organosulfates with Epoxides on Secondary Organic Aerosol, ACS Earth and Space Chemistry, 4, 1793-1801, doi:10.1021/acsearthspacechem.0c00178, 2020.

Bateman, A. P., Laskin, J., Laskin, A., and Nizkorodov, S. A.: Applications of high-resolution electrospray ionization mass spectrometry to measurements of average oxygen to carbon ratios in secondary organic aerosols, Environ. Sci. Technol., 46, 8315-8324, doi:10.1021/es3017254, 2012.

Bates, J. T., Fang, T., Verma, V., Zeng, L., Weber, R. J., Tolbert, P. E., Abrams, J. Y., Sarnat, S. E., Klein, M., Mulholland, J. A., and Russell, A. G.: Review of Acellular Assays of Ambient Particulate Matter Oxidative Potential: Methods and Relationships with Composition, Sources, and Health Effects, Environ. Sci. Technol., 53, 4003-4019, doi:10.1021/acs.est.8b03430, 2019.

Bianco, A., Deguillaume, L., Vaitilingom, M., Nicol, E., Baray, J. L., Chaumerliac, N., and Bridoux, M.: Molecular Characterization of Cloud Water Samples Collected at the Puy de Dome (France) by Fourier Transform Ion Cyclotron Resonance Mass Spectrometry, Environ. Sci. Technol., 52, 10275-10285, doi:10.1021/acs.est.8b01964, 2018.

Blair, S. L., MacMillan, A. C., Drozd, G. T., Goldstein, A. H., Chu, R. K., Pasa-Tolic, L., Shaw, J. B., Tolic, N., Lin, P., Laskin, J., Laskin, A., and Nizkorodov, S. A.: Molecular Characterization of Organosulfur Compounds in Biodiesel and Diesel Fuel Secondary Organic Aerosol, Environ. Sci. Technol., 51, 119-127, doi:10.1021/acs.est.6b03304, 2017.

Bruggemann, M., Xu, R., Tilgner, A., Kwong, K. C., Mutzel, A., Poon, H. Y., Otto, T., Schaefer, T., Poulain, L., Chan, M. N., and Herrmann, H.: Organosulfates in Ambient Aerosol: State of Knowledge and Future Research Directions on Formation, Abundance, Fate, and Importance, Environ. Sci. Technol., 54, 3767-3782, doi:10.1021/acs.est.9b06751, 2020.

Bryant, D. J., Elzein, A., Newland, M., White, E., Swift, S., Watkins, A., Deng, W., Song, W., Wang, S., Zhang, Y., Wang, X., Rickard, A. R., and Hamilton, J. F.: Importance of Oxidants and Temperature in the Formation of Biogenic Organosulfates and Nitrooxy Organosulfates, ACS Earth Space Chem., 5, 2291-2306, doi:10.1021/acsearthspacechem.1c00204, 2021.

Chen, Y. and Bond, T. C.: Light absorption by organic carbon from wood combustion, Atmospheric Chemistry and Physics, 10, 1773-1787, 2010.

Chen, Y., Dombek, T., Hand, J., Zhang, Z., Gold, A., Ault, A. P., Levine, K. E., and Surratt, J. D.: Seasonal Contribution of Isoprene-Derived Organosulfates to Total Water-Soluble Fine Particulate Organic Sulfur in the United States, ACS Earth Space Chem., 5, 2419-2432, doi:10.1021/acsearthspacechem.1c00102, 2021.

Chen, Y., Zhang, Y., Lambe, A. T., Xu, R., Lei, Z., Olson, N. E., Zhang, Z., Szalkowski, T., Cui, T., Vizuete, W., Gold, A., Turpin, B. J., Ault, A. P., Chan, M. N., and Surratt, J. D.: Heterogeneous Hydroxyl Radical Oxidation of Isoprene-Epoxydiol-Derived Methyltetrol Sulfates: Plausible Formation Mechanisms of Previously Unexplained Organosulfates in Ambient Fine Aerosols, Environ. Sci. Technol. Lett., doi:10.1021/acs.estlett.0c00276, 2020.

Cheng, Y., He, K. B., Engling, G., Weber, R., Liu, J. M., Du, Z. Y., and Dong, S. P.: Brown and black carbon in Beijing aerosol: Implications for the effects of brown coating on light absorption by black carbon, Science of the Total Environment, 599-600, 1047-1055, doi:10.1016/j.scitotenv.2017.05.061, 2017.

Cui, M., Li, C., Chen, Y., Zhang, F., Li, J., Jiang, B., Mo, Y., Li, J., Yan, C., Zheng, M., Xie, Z., Zhang, G., and Zheng, J.: Molecular characterization of polar organic aerosol constituents in off-road engine emissions using Fourier transform ion cyclotron resonance mass spectrometry (FT-ICR MS): implications for source apportionment, Atmos. Chem. Phys., 19, 13945-13956, doi:10.5194/acp-19-13945-2019, 2019.

Daellenbach, K. R., Kourtchev, I., Vogel, A. L., Bruns, E. A., Jiang, J., Petäjä, T., Jaffrezo, J.-L., Aksoyoglu, S., Kalberer, M., Baltensperger, U., El Haddad, I., and Prévôt, A. S. H.: Impact of anthropogenic and biogenic sources on the seasonal variation in the molecular composition of urban organic aerosols: a field and laboratory study using ultra-high-resolution mass spectrometry, Atmos. Chem. Phys., 19, 5973-5991, doi:10.5194/acp-19-5973-2019, 2019.

Daellenbach, K. R., Uzu, G., Jiang, J., Cassagnes, L. E., Leni, Z., Vlachou, A., Stefenelli, G., Canonaco, F., Weber, S., Segers, A., Kuenen, J. J. P., Schaap, M., Favez, O., Albinet, A., Aksoyoglu, S., Dommen, J., Baltensperger, U., Geiser, M., El Haddad, I., Jaffrezo, J. L., and Prevot, A. S. H.: Sources of particulate-matter air pollution and its oxidative potential in Europe, Nature, 587, 414-419, doi:10.1038/s41586-020-2902-8, 2020.

Dai, S., Bi, X., Chan, L. Y., He, J., Wang, B., Wang, X., Peng, P., Sheng, G., and Fu, J.: Chemical and stable carbon isotopic composition of PM2.5 from on-road vehicle emissions in the PRD region and implications for vehicle emission control policy, Atmos. Chem. Phys., 15, 3097-3108, doi:10.5194/acp-15-3097-2015, 2015.

Duporte, G., Flaud, P. M., Kammer, J., Geneste, E., Augagneur, S., Pangui, E., Lamkaddam, H., Gratien, A., Doussin, J. F., Budzinski, H., Villenave, E., and Perraudin, E.: Experimental Study of the Formation of Organosulfates from alpha-Pinene Oxidation. 2. Time Evolution and Effect of Particle Acidity, J. Phys. Chem. A, 124, 409-421, doi:10.1021/acs.jpca.9b07156, 2020.

Eddingsaas, N. C., VanderVelde, D. G., and Wennberg, P. O.: Kinetics and Products of the Acid-Catalyzed Ring-Opening of Atmospherically Relevant Butyl Epoxy Alcohols, J. Phys. Chem. A, 114, 8106–8113, doi:10.1021/jp103907c, 2010.

Fleming, L. T., Ali, N. N., Blair, S. L., Roveretto, M., George, C., and Nizkorodov, S. A.: Formation of Light-Absorbing Organosulfates during Evaporation of Secondary Organic Material Extracts in the Presence of Sulfuric Acid, ACS Earth Space Chem., 3, 947-957, doi:10.1021/acsearthspacechem.9b00036, 2019.

Frossard, A. A., Shaw, P. M., Russell, L. M., Kroll, J. H., Canagaratna, M. R., Worsnop, D. R., Quinn, P. K., and Bates, T. S.: Springtime Arctic haze contributions of submicron organic particles from European and Asian combustion sources, Journal of Geophysical Research, 116, doi:10.1029/2010jd015178, 2011.

Gao, K. and Zhu, T.: Analytical methods for organosulfate detection in aerosol particles: Current status and future perspectives, Sci. Total Environ., 784, 147244, doi:10.1016/j.scitotenv.2021.147244, 2021.

Guo, H., Sullivan, A. P., Campuzano-Jost, P., Schroder, J. C., Lopez-Hilfiker, F. D., Dibb, J. E., Jimenez, J. L., Thornton, J. A., Brown, S. S., Nenes, A., and Weber, R. J.: Fine particle pH and the partitioning of nitric acid during winter in the northeastern United States, J. Geophys. Res. Atmos., 121, doi:10.1002/2016jd025311, 2016.

Guo, J., Zhou, S., Cai, M., Zhao, J., Song, W., Zhao, W., Hu, W., Sun, Y., He, Y., Yang, C., Xu, X., Zhang, Z., Cheng, P., Fan, Q., Hang, J., Fan, S., Wang, X., and Wang, X.: Characterization of submicron particles by time-of-flight aerosol chemical speciation monitor (ToF-ACSM) during wintertime: aerosol composition, sources, and chemical processes in Guangzhou, China, Atmos. Chem. Phys., 20, 7595-7615, doi:10.5194/acp-20-7595-2020, 2020.

He, Q.-F., Ding, X., Tang, M.-J., Wang, X.-M., Fu, X.-X., Zhang, Y.-Q., Wang, J.-Q., Liu, Y.-X., and Rudich, Y.: Secondary Organic Aerosol Formation From Isoprene Epoxides in the Pearl River Delta, South China: IEPOX- and HMML-Derived Tracers, J. Geophys. Res. Atmos., 123, 6999–7012, doi:10.1029/2017JD028242, 2018.

He, Q. F., Ding, X., Wang, X. M., Yu, J. Z., Fu, X. X., Liu, T. Y., Zhang, Z., Xue, J., Chen, D. H., Zhong, L. J., and Donahue, N. M.: Organosulfates from pinene and isoprene over the Pearl River Delta, South China: seasonal variation and implication in formation mechanisms, Environ. Sci. Technol., 48, 9236-9245, doi:10.1021/es501299v, 2014.

Hettiyadura, A. P. S., Al-Naiema, I. M., Hughes, D. D., Fang, T., and Stone, E. A.: Organosulfates in Atlanta, Georgia: anthropogenic influences on biogenic secondary organic aerosol formation, Atmos. Chem. Phys., 19, 3191-3206, doi:10.5194/acp-19-3191-2019, 2019.

Hettiyadura, A. P. S., Stone, E. A., Kundu, S., Baker, Z., Geddes, E., Richards, K., and Humphry, T.: Determination of atmospheric organosulfates using HILIC chromatography with MS detection, Atmos. Meas. Tech., 8, 2347-2358, doi:10.5194/amt-8-2347-2015, 2015.

Hettiyadura, A. P. S., Jayarathne, T., Baumann, K., Goldstein, A. H., de Gouw, J. A., Koss, A., Keutsch, F. N., Skog, K., and Stone, E. A.: Qualitative and quantitative analysis of atmospheric organosulfates in Centreville, Alabama, Atmos. Chem. Phys., 17, 1343-1359, doi:10.5194/acp-17-1343-2017, 2017.

Huang, D. D., Li, Y. J., Lee, B. P., and Chan, C. K.: Analysis of organic sulfur compounds in atmospheric aerosols at the HKUST supersite in Hong Kong using HR-ToF-AMS, Environ Sci Technol, 49, 3672-3679, doi:10.1021/es5056269, 2015.

Huang, L., Coddens, E. M., and Grassian, V. H.: Formation of Organosulfur Compounds from Aqueous Phase Reactions of S(IV) with Methacrolein and Methyl Vinyl Ketone in the Presence of Transition Metal Ions, ACS Earth Space Chem., 3, 1749-1755, doi:10.1021/acsearthspacechem.9b00173, 2019.

Huang, L., Liu, T., and Grassian, V. H.: Radical-Initiated Formation of Aromatic Organosulfates and Sulfonates in the Aqueous Phase, Environ. Sci. Technol., 54, 11857-11864, doi:10.1021/acs.est.0c05644, 2020.
Huang, R.-J., Cao, J., Chen, Y., Yang, L., Shen, J., You, Q., Wang, K., Lin, C., Xu, W., Gao, B., Li, Y., Chen, Q., Hoffmann, T., amp, apos, Dowd, C. D., Bilde, M., and Glasius, M.: Organosulfates in atmospheric aerosol: synthesis and quantitative analysis of PM2.5 from Xi'an, northwestern China, Atmos. Meas. Tech., 11, 3447-3456, doi:10.5194/amt-11-3447-2018, 2018a.
Huang, R. J., Yang, L., Cao, J. J., Chen, Y., Chen, Q., Li, Y., Duan, J., Zhu, C., Dai, W., Wang, K., Lin, C., Ni, H., Corbin, J. C., Wu, Y., Zhang, R., Tie, X., Hoffmann, T., O'Dowd, C., and Dusek, U.: Brown Carbon Aerosol in Urban Xi'an, Northwest China: The Composition and Light Absorption Properties, Environmental Science & Technology, 52, 6825-6833, doi:10.1021/acs.est.8b02386, 2018b.
Iinuma, Y., Müller, C., Böge, O., Gnauk, T., and Herrmann, H.: The formation of organic sulfate esters in the limonene ozonolysis secondary organic aerosol (SOA) under acidic conditions, Atmos. Environ., 41, 5571-5583, doi:10.1016/j.atmosenv.2007.03.007, 2007a.
Iinuma, Y., Mu¨ Ller, C., Berndt, T., Bo¨ Ge, O., Claeys, M., and Herrmann, H.: Evidence for the Existence of Organosulfates from β-Pinene Ozonolysis in Ambient Secondary Organic Aerosol, Environ. Sci. Technol., 6678-6683, doi:10.1021/es070938t, 2007b.
Jiang, B., Kuang, B. Y., Liang, Y., Zhang, J., Huang, X. H. H., Xu, C., Yu, J. Z., and Shi, Q.: Molecular composition of urban organic aerosols on clear and hazy days in Beijing: a comparative study using FT-ICR MS, Environ. Chem., 13, 888-901, doi:10.1071/en15230, 2016.
Jiang, H., Li, J., Sun, R., Tian, C., Tang, J., Jiang, B., Liao, Y., Chen, C. E., and Zhang, G.: Molecular Dynamics and Light Absorption Properties of Atmospheric Dissolved Organic Matter, Environ. Sci. Technol., 55, 10268-10279, doi:10.1021/acs.est.1c01770, 2021a.
Jiang, H., Li, J., Chen, D., Tang, J., Cheng, Z., Mo, Y., Su, T., Tian, C., Jiang, B., Liao, Y., and Zhang, G.: Biomass burning organic aerosols significantly influence the light absorption properties of polarity-dependent organic compounds in the Pearl River Delta Region, China, Environ. Int., 144, 106079, doi:10.1016/j.envint.2020.106079, 2020.
Jiang, H., Li, J., Sun, R., Liu, G., Tian, C., Tang, J., Cheng, Z., Zhu, S., Zhong, G., Ding, X., and Zhang, G.: Determining the Sources and Transport of Brown Carbon Using Radionuclide Tracers and Modeling, J. Geophys. Res. Atmos., 126, e2021JD034616, doi:10.1029/2021jd034616, 2021b.
Jimenez, J. L., Canagaratna, M. R., Donahue, N. M., Prevot, A. S. H., Zhang, Q., Kroll, J. H., DeCarlo, P. F., Allan, J. D., Coe, H., Ng, N. L., Aiken, A. C., Docherty, K. S., Ulbrich, I. M., Grieshop, A. P., Robinson, A. L., Duplissy, J., Smith, J. D., Wilson, K. R., Lanz, V. A., Hueglin, C., Sun, Y. L., Tian, J., Laaksonen, A., Raatikainen, T., Rautiainen, J., Vaattovaara, P., Ehn, M., Kulmala, M., Tomlinson, J. M., Collins, D. R., Cubison, M. J., Dunlea, J., Huffman, J. A., Onasch, T. B., Alfarra, M. R., Williams, P. I., Bower, K., Kondo, Y., Schneider, J., Drewnick, F., Borrmann, S., Weimer, S., Demerjian, K., Salcedo, D., Cottrell, L., Griffin, R., Takami, A., Miyoshi, T., Hatakeyama, S., Shimono, A., Sun, J. Y., Zhang, Y. M., Dzepina, K., Kimmel, J. R., Sueper, D., Jayne, J. T., Herndon, S. C., Trimborn, A. M., Williams, L. R., Wood, E. C., Middlebrook, A. M., Kolb, C. E., Baltensperger, U., and Worsnop, D. R.: Evolution of Organic Aerosols in the Atmosphere, Science, 326, 1525, doi:10.1126/science.1180353, 2009.
Kellerman, A. M., Dittmar, T., Kothawala, D. N., and Tranvik, L. J.: Chemodiversity of dissolved organic matter in lakes driven by climate and hydrology, Nat. Commun., 5, 3804, doi:10.1038/ncomms4804, 2014.
Kourtchev, I., Giorio, C., Manninen, A., Wilson, E., Mahon, B., Aalto, J., Kajos, M., Venables, D., Ruuskanen, T., Levula, J., Loponen, M., Connors, S., Harris, N., Zhao, D., Kiendler-Scharr, A., Mentel, T., Rudich, Y., Hallquist, M., Doussin, J. F., Maenhaut, W., Back, J., Petaja, T., Wenger, J., Kulmala, M., and Kalberer, M.: Enhanced Volatile Organic Compounds emissions and organic aerosol mass increase the oligomer content of atmospheric aerosols, Sci Rep, 6, 35038, doi:10.1038/srep35038, 2016.
Kristensen, K., Bilde, M., Aalto, P. P., Petäjä, T., and Glasius, M.: Denuder/filter sampling of organic acids and organosulfates at urban and boreal forest sites: Gas/particle distribution and possible sampling artifacts, Atmos. Environ., 130, 36-53, doi:10.1016/j.atmosenv.2015.10.046, 2016.
Kuang, B. Y., Lin, P., Hu, M., and Yu, J. Z.: Aerosol size distribution characteristics of organosulfates in the Pearl River Delta region, China, Atmos. Environ., 130, 23-35, doi:10.1016/j.atmosenv.2015.09.024, 2016.
Lam, H. K., Kwong, K. C., Poon, H. Y., Davies, J. F., Zhang, Z., Gold, A., Surratt, J. D., and Chan, M. N.: Heterogeneous OH oxidation of isoprene-epoxydiol-derived organosulfates: kinetics, chemistry and formation of inorganic sulfate, Atmos. Chem. Phys., 19, 2433-2440, doi:10.5194/acp-19-2433-2019, 2019.
Le Breton, M., Wang, Y., Hallquist, Å. M., Pathak, R. K., Zheng, J., Yang, Y., Shang, D., Glasius, M., Bannan, T. J., Liu, Q., Chan, C. K., Percival, C. J., Zhu, W., Lou, S., Topping, D., Wang, Y., Yu, J., Lu, K., Guo, S., Hu, M., and Hallquist, M.: Online gas- and particle-phase measurements of organosulfates, organosulfonates and nitrooxy organosulfates in Beijing utilizing a FIGAERO ToF-CIMS, Atmos. Chem. Phys., 18, 10355-10371, doi:10.5194/acp-18-10355-2018, 2018.
Li, J. J., Wang, G. H., Cao, J. J., Wang, X. M., and Zhang, R. J.: Observation of biogenic secondary organic aerosols in the atmosphere of a mountain site in central China: temperature and relative humidity effects, Atmospheric Chemistry and Physics, 13, 11535-11549, doi:10.5194/acp-13-11535-2013, 2013.
Lin, P., Yu, J. Z., Engling, G., and Kalberer, M.: Organosulfates in Humic-like Substance Fraction Isolated from Aerosols at Seven Locations in East Asia: A Study by Ultra-High-Resolution Mass Spectrometry, Environ. Sci. Technol., 46, 13118-13127, doi:10.1021/es303570v, 2012.

Lin, Y.-H., Knipping, E. M., Edgerton, E. S., Shaw, S. L., and Surratt, J. D.: Investigating the influences of SO2 and NH3 levels on isoprene-derived secondary organic aerosol formation using conditional sampling approaches, Atmos. Chem. Phys., 13, 8457–8470, doi:10.5194/acp-13-8457-2013, 2013.

Lin, Y.-H., Arashiro, M., Martin, E., Chen, Y., Zhang, Z., Sexton, K. G., Gold, A., Jaspers, I., Fry, R. C., and Surratt, J. D.: Isoprene-Derived Secondary Organic Aerosol Induces the Expression of Oxidative Stress Response Genes in Human Lung Cells, Environ. Sci. Technol. Lett., 3, 250-254, doi:10.1021/acs.estlett.6b00151, 2016.

Lind, J. A., Lazrus, A. L., and Kok, G. L.: Aqueous phase oxidation of sulfur(IV) by hydrogen peroxide, methylhydroperoxide, and peroxyacetic acid, Journal of Geophysical Research: Atmospheres, 92, 4171-4177, doi:https://doi.org/10.1029/JD092iD04p04171, 1987.

Liu, J., Li, J., Zhang, Y., Liu, D., Ding, P., Shen, C., Shen, K., He, Q., Ding, X., Wang, X., Chen, D., Szidat, S., and Zhang, G.: Source apportionment using radiocarbon and organic tracers for PM2.5 carbonaceous aerosols in Guangzhou, South China: contrasting local- and regional-scale haze events, Environ. Sci. Technol., 48, 12002-12011, doi:10.1021/es503102w, 2014.

Liu, M., Song, Y., Zhou, T., Xu, Z., Yan, C., Zheng, M., Wu, Z., Hu, M., Wu, Y., and Zhu, T.: Fine particle pH during severe haze episodes in northern China, Geophys. Res. Lett., 44, 5213-5221, doi:10.1002/2017gl073210, 2017.

Luk´acs, H., Gelencs´er, A., Hoffer, A., Kiss, G., Horv´ath, K., and Harty´ani, Z.: Quantitative assessment of organosulfates in size-segregated rural fine aerosol, Atmos. Chem. Phys., 9, 231–238, doi:10.5194/acp-9-231-2009, 2009.

Mazzoleni, L. R., Ehrmann, B. M., Shen, X., Marshall, A. G., and Collett, J. L.: Water-Soluble Atmospheric Organic Matter in Fog: Exact Masses and Chemical Formula Identification by Ultrahigh-Resolution Fourier Transform Ion Cyclotron Resonance Mass Spectrometry, Environ. Sci. Technol., 44, 3690-3697, doi:10.1021/es903409k, 2010.

Meade, L. E., Riva, M., Blomberg, M. Z., Brock, A. K., Qualters, E. M., Siejack, R. A., Ramakrishnan, K., Surratt, J. D., and Kautzman, K. E.: Seasonal variations of fine particulate organosulfates derived from biogenic and anthropogenic hydrocarbons in the mid-Atlantic United States, Atmos. Environ., 145, 405-414, doi:10.1016/j.atmosenv.2016.09.028, 2016.

Nguyen, T. B., Lee, P. B., Updyke, K. M., Bones, D. L., Laskin, J., Laskin, A., and Nizkorodov, S. A.: Formation of nitrogen- and sulfur-containing light-absorbing compounds accelerated by evaporation of water from secondary organic aerosols, J. Geophys. Res. Atmos., 117, D01207, doi:10.1029/2011jd016944, 2012.

Noziere, B., Kalberer, M., Claeys, M., Allan, J., D'Anna, B., Decesari, S., Finessi, E., Glasius, M., Grgic, I., Hamilton, J. F., Hoffmann, T., Iinuma, Y., Jaoui, M., Kahnt, A., Kampf, C. J., Kourtchev, I., Maenhaut, W., Marsden, N., Saarikoski, S., Schnelle-Kreis, J., Surratt, J. D., Szidat, S., Szmigielski, R., and Wisthaler, A.: The molecular identification of organic compounds in the atmosphere: state of the art and challenges, Chem. Rev., 115, 3919-3983, doi:10.1021/cr5003485, 2015.

Nozière, B., Ekström, S., Alsberg, T., and Holmström, S.: Radical-initiated formation of organosulfates and surfactants in atmospheric aerosols, Geophys. Res. Lett., 37, n/a-n/a, doi:10.1029/2009gl041683, 2010.

O'Brien, R. E., Laskin, A., Laskin, J., Rubitschun, C. L., Surratt, J. D., and Goldstein, A. H.: Molecular characterization of S- and N-containing organic constituents in ambient aerosols by negative ion mode high-resolution Nanospray Desorption Electrospray Ionization Mass Spectrometry: CalNex 2010 field study, J. Geophys. Res. Atmos., 119, 12706-12720, doi:10.1002/2014jd021955, 2014.

Olson, C. N., Galloway, M. M., Yu, G., Hedman, C. J., Lockett, M. R., Yoon, T., Stone, E. A., Smith, L. M., and Keutsch, F. N.: Hydroxycarboxylic acid-derived organosulfates: synthesis, stability, and quantification in ambient aerosol, Environ. Sci. Technol., 45, 6468-6474, doi:10.1021/es201039p, 2011.

Passananti, M., Kong, L., Shang, J., Dupart, Y., Perrier, S., Chen, J., Donaldson, D. J., and George, C.: Organosulfate Formation through the Heterogeneous Reaction of Sulfur Dioxide with Unsaturated Fatty Acids and Long-Chain Alkenes, Angew. Chem. Int. Ed., 55, 10336-10339, doi:10.1002/anie.201605266, 2016.

Peng, C., Razafindrambinina, P. N., Malek, K. A., Chen, L., Wang, W., Huang, R.-J., Zhang, Y., Ding, X., Ge, M., Wang, X., Asa-Awuku, A. A., and Tang, M.: Interactions of organosulfates with water vapor under sub- and supersaturated conditions, Atmos. Chem. Phys., 21, 7135-7148, doi:10.5194/acp-21-7135-2021, 2021.

Riva, M., Barbosa, T. D. S., Lin, Y.-H., Stone, E. A., Gold, A., and Surratt, J. D.: Chemical characterization of organosulfates in secondary organic aerosol derived from the photooxidation of alkanes, Atmos. Chem. Phys., 16, , 2016, 16, 11001-11018, doi:10.5194/acp-16-11001-2016, 2016a.

Riva, M., Da Silva Barbosa, T., Lin, Y.-H., Stone, E. A., Gold, A., and Surratt, J. D.: Chemical characterization of organosulfates in secondary organic aerosol
derived from the photooxidation of alkanes, Atmos. Chem. Phys., 16, 11001-11018, doi:10.5194/acp-16-11001-2016, 2016b.

Riva, M., Tomaz, S., Cui, T., Lin, Y. H., Perraudin, E., Gold, A., Stone, E. A., Villenave, E., and Surratt, J. D.: Evidence for an unrecognized secondary anthropogenic source of organosulfates and sulfonates: gas-phase oxidation of polycyclic aromatic hydrocarbons in the presence of sulfate aerosol, Environ. Sci. Technol., 49, 6654-6664, doi:10.1021/acs.est.5b00836, 2015.

Riva, M., Budisulistiorini, S. H., Chen, Y., Zhang, Z., D'Ambro, E. L., Zhang, X., Gold, A., Turpin, B. J., Thornton, J. A., Canagaratna, M. R., and Surratt, J. D.: Chemical Characterization of Secondary Organic Aerosol from Oxidation of Isoprene Hydroxyhydroperoxides, Environ Sci Technol, 50, 9889-9899, doi:10.1021/acs.est.6b02511, 2016c.

Rudzi´nski, K. J., Gmachowski, L., and Kuznietsova, I.: Reactions of isoprene and sulphoxy radical-anions – a possible source of atmospheric organosulphites and organosulphates, Atmospheric Chemistry and Physics, 9, 2129–2140, 2009.

Shakya, K. M. and Peltier, R. E.: Investigating missing sources of sulfur at Fairbanks, Alaska, Environ. Sci. Technol., 47, 9332-9338, doi:10.1021/es402020b, 2013.
Shakya, K. M. and Peltier, R. E.: Non-sulfate sulfur in fine aerosols across the United States: Insight for organosulfate prevalence, Atmos. Environ., 100, 159-166, doi:10.1016/j.atmosenv.2014.10.058, 2015.
Shang, J., Passananti, M., Dupart, Y., Ciuraru, R., Tinel, L., Rossignol, S., Perrier, S., Zhu, T., and George, C.: SO2 Uptake on Oleic Acid: A New Formation Pathway of Organosulfur Compounds in the Atmosphere, Environ. Sci. Technol. Lett., 3, 67-72, doi:10.1021/acs.estlett.6b00006, 2016.
Song, J., Li, M., Jiang, B., Wei, S., Fan, X., and Peng, P. a.: Molecular Characterization of Water-Soluble Humic like Substances in Smoke Particles Emitted from Combustion of Biomass Materials and Coal Using Ultrahigh-Resolution Electrospray Ionization Fourier Transform Ion Cyclotron Resonance Mass Spectrometry, Environ. Sci. Technol., 52, 2575-2585, doi:10.1021/acs.est.7b06126, 2018.
Stone, E. A., Yang, L., Yu, L. E., and Rupakheti, M.: Characterization of organosulfates in atmospheric aerosols at Four Asian locations, Atmos. Environ., 47, 323-329, doi:10.1016/j.atmosenv.2011.10.058, 2012.
Surratt, J. D., Chan, A. W., Eddingsaas, N. C., Chan, M., Loza, C. L., Kwan, A. J., Hersey, S. P., Flagan, R. C., Wennberg, P. O., and Seinfeld, J. H.: Reactive intermediates revealed in secondary organic aerosol formation from isoprene, Proceedings of the National Academy of Sciences of the United States of America, 107, 6640-6645, doi:10.1073/pnas.0911114107, 2010.
Surratt, J. D., Kroll, J. H., Kleindienst, X. T. E., Edney, E. O., Claeys, M., Sorooshian, A., Ng, N. L., Offenberg, J. H., Lewandowski, M., Jaoui, M., Flagan, R. C., and Seinfeld, J. H.: Evidence for Organosulfates in Secondary Organic Aerosol, Environ. Sci. Technol., 41, 517-527, doi:10.1021/es062081q, 2007.
Surratt, J. D., Gómez-González, Y., Chan, A. W. H., Vermeylen, R., Shahgholi, M., Kleindienst, T. E., Edney, E. O., Offenberg, J. H., Lewandowski, M., Jaoui, M., Maenhaut, W., Claeys, M., Flagan, R. C., and Seinfeld, J. H.: Organosulfate Formation in Biogenic Secondary Organic Aerosol, J. Phys. Chem. A, 112, 8345-8378, doi:10.1021/jp802310p, 2008.
Tang, J., Li, J., Su, T., Han, Y., Mo, Y., Jiang, H., Cui, M., Jiang, B., Chen, Y., Tang, J., Song, J., Peng, P. a., and Zhang, G.: Molecular compositions and optical properties of dissolved brown carbon in biomass burning, coal combustion, and vehicle emission aerosols illuminated by excitation–emission matrix spectroscopy and Fourier transform ion cyclotron resonance mass spectrometry analysis, Atmos. Chem. Phys., 20, 2513-2532, doi:10.5194/acp-20-2513-2020, 2020.
Tao, S., Lu, X., Levac, N., Bateman, A. P., Nguyen, T. B., Bones, D. L., Nizkorodov, S. A., Laskin, J., Laskin, A., and Yang, X.: Molecular characterization of organosulfates in organic aerosols from Shanghai and Los Angeles urban areas by nanospray-desorption electrospray ionization high-resolution mass spectrometry, Environ. Sci. Technol., 48, 10993-11001, doi:10.1021/es5024674, 2014.
Tolocka, M. P. and Turpin, B.: Contribution of organosulfur compounds to organic aerosol mass, Environ. Sci. Technol., 46, 7978-7983, doi:10.1021/es300651v, 2012.
Vogel, A. L., Schneider, J., Muller-Tautges, C., Phillips, G. J., Pohlker, M. L., Rose, D., Zuth, C., Makkonen, U., Hakola, H., Crowley, J. N., Andreae, M. O., Poschl, U., and Hoffmann, T.: Aerosol Chemistry Resolved by Mass Spectrometry: Linking Field Measurements of Cloud Condensation Nuclei Activity to Organic Aerosol Composition, Environ Sci Technol, 50, 10823-10832, doi:10.1021/acs.est.6b01675, 2016.
Wach, P., Spolnik, G., Rudzinski, K. J., Skotak, K., Claeys, M., Danikiewicz, W., and Szmigielski, R.: Radical oxidation of methyl vinyl ketone and methacrolein in aqueous droplets: Characterization of organosulfates and atmospheric implications, Chemosphere, 214, 1-9, doi:10.1016/j.chemosphere.2018.09.026, 2019.
Wang, J., Ye, J., Zhang, Q., Zhao, J., Wu, Y., Li, J., Liu, D., Li, W., Zhang, Y., Wu, C., Xie, C., Qin, Y., Lei, Y., Huang, X., Guo, J., Liu, P., Fu, P., Li, Y., Lee, H. C., Choi, H., Zhang, J., Liao, H., Chen, M., Sun, Y., Ge, X., Martin, S. T., and Jacob, D. J.: Aqueous production of secondary organic aerosol from fossil-fuel emissions in winter Beijing haze, Proc. Natl. Acad. Sci. U. S. A., 118, doi:10.1073/pnas.2022179118, 2021a.
Wang, K., Zhang, Y., Huang, R. J., Wang, M., Ni, H., Kampf, C. J., Cheng, Y., Bilde, M., Glasius, M., and Hoffmann, T.: Molecular Characterization and Source Identification of Atmospheric Particulate Organosulfates Using Ultrahigh Resolution Mass Spectrometry, Environ. Sci. Technol., 53, 6192-6202, doi:10.1021/acs.est.9b02628, 2019.
Wang, K., Huang, R.-J., Brüggemann, M., Zhang, Y., Yang, L., Ni, H., Guo, J., Wang, M., Han, J., Bilde, M., Glasius, M., and Hoffmann, T.: Urban organic aerosol composition in eastern China differs from north to south: molecular insight from a liquid chromatography–mass spectrometry (Orbitrap) study, Atmos. Chem. Phys., 21, 9089-9104, doi:10.5194/acp-21-9089-2021, 2021b.
Wang, X., Hayeck, N., Brüggemann, M., Yao, L., Chen, H., Zhang, C., Emmelin, C., Chen, J., George, C., and Wang, L.: Chemical Characteristics of Organic Aerosols in Shanghai: A Study by Ultrahigh-Performance Liquid Chromatography Coupled With Orbitrap Mass Spectrometry, J. Geophys. Res. Atmos., 122, 11703-11722, doi:10.1002/2017jd026930, 2017a.
Wang, X. K., Rossignol, S., Ma, Y., Yao, L., Wang, M. Y., Chen, J. M., George, C., and Wang, L.: Molecular characterization of atmospheric particulate organosulfates in three megacities at the middle and lower reaches of the Yangtze River, Atmos. Chem. Phys., 16, 2285–2298, doi:10.5194/acp-16-2285-2016, 2016.
Wang, Y., Ren, J., Huang, X. H. H., Tong, R., and Yu, J. Z.: Synthesis of Four Monoterpene-Derived Organosulfates and Their Quantification in Atmospheric Aerosol Samples, Environ. Sci. Technol., 51, 6791-6801, doi:10.1021/acs.est.7b01179, 2017b.

Wang, Y., Hu, M., Wang, Y.-C., Li, X., Fang, X., Tang, R., Lu, S., Wu, Y., Guo, S., Wu, Z., Hallquist, M., and Yu, J. Z.: Comparative Study of Particulate Organosulfates in Contrasting Atmospheric Environments: Field Evidence for the Significant Influence of Anthropogenic Sulfate and NOx, Environ. Sci. Technol. Lett., 7, 787-794, doi:10.1021/acs.estlett.0c00550, 2020.

Wang, Y., Hu, M., Guo, S., Wang, Y., Zheng, J., Yang, Y., Zhu, W., Tang, R., Li, X., Liu, Y., Le Breton, M., Du, Z., Shang, D., Wu, Y., Wu, Z., Song, Y., Lou, S., Hallquist, M., and Yu, J.: The secondary formation of organosulfates under interactions between biogenic emissions and anthropogenic pollutants in summer in Beijing, Atmos. Chem. Phys., 18, 10693-10713, doi:10.5194/acp-18-10693-2018, 2018.

Willoughby, A. S., Wozniak, A. S., and Hatcher, P. G.: A molecular-level approach for characterizing water-insoluble components of ambient organic aerosol particulates using ultrahigh-resolution mass spectrometry, Atmos. Chem. Phys., 14, 10299-10314, doi:10.5194/acp-14-10299-2014, 2014.

Worton, D. R., Surratt, J. D., Lafranchi, B. W., Chan, A. W., Zhao, Y., Weber, R. J., Park, J. H., Gilman, J. B., de Gouw, J., Park, C., Schade, G., Beaver, M., Clair, J. M., Crounse, J., Wennberg, P., Wolfe, G. M., Harrold, S., Thornton, J. A., Farmer, D. K., Docherty, K. S., Cubison, M. J., Jimenez, J. L., Frossard, A. A., Russell, L. M., Kristensen, K., Glasius, M., Mao, J., Ren, X., Brune, W., Browne, E. C., Pusede, S. E., Cohen, R. C., Seinfeld, J. H., and Goldstein, A. H.: Observational insights into aerosol formation from isoprene, Environ. Sci. Technol., 47, 11403-11413, doi:10.1021/es4011064, 2013.

Xu, B., Zhang, G., Gustafsson, Ö., Kawamura, K., Li, J., Andersson, A., Bikkina, S., Kunwar, B., Pokhrel, A., Zhong, G., Zhao, S., Li, J., Huang, C., Cheng, Z., Zhu, S., Peng, P. a., and Sheng, G.: Large contribution of fossil anthropogenic source components to aqueous secondary organic aerosols, Submitted, doi:10.21203/rs.3.rs-1155038/v1, 2021a.

Xu, L., Yang, Z., Tsona, N. T., Wang, X., George, C., and Du, L.: Anthropogenic-Biogenic Interactions at Night: Enhanced Formation of Secondary Aerosols and Particulate Nitrogen- and Sulfur-Containing Organics from beta-Pinene Oxidation, Environ. Sci. Technol., 55, 7794-7807, doi:10.1021/acs.est.0c07879, 2021b.

Yassine, M. M., Harir, M., Dabek-Zlotorzynska, E., and Schmitt-Kopplin, P.: Structural characterization of organic aerosol using Fourier transform ion cyclotron resonance mass spectrometry: aromaticity equivalent approach, Rapid Commun. Mass Spectrom., 28, 2445-2454, doi:10.1002/rcm.7038, 2014.

Ye, J., Abbatt, J. P. D., and Chan, A. W. H.: Novel pathway of SO2 oxidation in the atmosphere: reactions with monoterpene ozonolysis intermediates and secondary organic aerosol, Atmos. Chem. Phys., 18, 5549-5565, doi:10.5194/acp-18-5549-2018, 2018.

Ye, Y., Zhan, H., Yu, X., Li, J., Wang, X., and Xie, Z.: Detection of organosulfates and nitrooxy-organosulfates in Arctic and Antarctic atmospheric aerosols, using ultra-high resolution FT-ICR mass spectrometry, Sci. Total Environ., 767, 144339, doi:10.1016/j.scitotenv.2020.144339, 2020.

Zhao, Y., Hallar, A. G., and Mazzoleni, L. R.: Atmospheric organic matter in clouds: exact masses and molecular formula identification using ultrahigh-resolution FT-ICR mass spectrometry, Atmos. Chem. Phys., 13, 12343-12362, doi:10.5194/acp-13-12343-2013, 2013.

Zhu, M., Jiang, B., Li, S., Yu, Q., Yu, X., Zhang, Y., Bi, X., Yu, J., George, C., Yu, Z., and Wang, X.: Organosulfur Compounds Formed from Heterogeneous Reaction between SO2 and Particulate-Bound Unsaturated Fatty Acids in Ambient Air, Environ. Sci. Technol. Lett., 6, 318-322, doi:10.1021/acs.estlett.9b00218, 2019.

Supplement of

"Molecular Characteristics, Sources and Formation Pathways of Organosulfur Compounds in Ambient Aerosol in Guangzhou, South China~~Molecular Characteristics of Organosulfur Compounds in Guangzhou, South China: Heterogeneous Secondary Reactions Drivers the Molecular Distribution~~"

Hongxing Jiang et al.,

Correspondence to: Jun Li (junli@gig.ac.cn)

Supplementary text

Measurements for $PM_{2.5}$ and Organics

A total of 55 $PM_{2.5}$ samples collected on prebaked quartz fiber filters once a week at Guangzhou from July, 2017 to June, 2018 (June–September: summer, October–November: fall; December–February: winter; March–May: spring) over a period of 24 h with a high-volume air sampler at a flow rate of 1 $m^3 \cdot min^{-1}$. Quartz fiber filters were preheated at 450°C for 6 h before used and weighed. After sampling, each filter was wrapped with prebaked aluminum foil, sealed. Before weighing again, the $PM_{2.5}$ samples were kept at constant temperature and humidity for 24 h. The difference between two weighing is the amount of collected $PM_{2.5}$. A punch of filter (1.5 cm^2) was used for carbon concentration measurement. The concentration of organic and elemental carbon were measured using an OC/EC analyzer (Sunset Laboratory,Inc.) following the NIOSH870 thermaleoptical transmittance (TOT) standard method. We converted OC to organic mass using a typical ratio of OM/OC of 1.8(Tolocka and Turpin, 2012). Detailed information about the analysis procedures of chemical tracers, and meteorological parameters have been described in previous studies(Jiang et al., 2021b; Jiang et al., 2021a) and are included in the Table S12. The organic tracers' analysis performed included levoglucosan, polycyclic aromatic hydrocarbons [PAHs], steranes, and hopenes, biogenic SOA tracers (isoprene-derived SOA, MTLs; monoterpene-derived SOA, MSOA), fatty acids, long-chain alkanes. Online data regarding temperature, RH, and NO_x were obtained from a local monitoring station. A gas filter correlation analyzer (Thermo Scientific, Model 48i) was used to observed the CO. SO_2 and O_3 was measured with the pulsed fluorescence analyzer (Thermo Scientific, Model 43iTLE) and the UV photometric analyzer (Thermo Scientific, Model 49i), respectively. NO and NO_2 were determined with a chemiluminescence instrument (Thermo Scientific, Model 42iTL). Meteorological parameters of temperature (T) and relative humidity (RH) were measured with a portable weather station (WXT520, Vaisala, Finland). The concentration of gas-phase OH radical was approximated from a nonlinear Pad• function, and the NO_x effects were considered.

Results from our previous work(Jiang et al., 2021b)**:** Seven-days backward trajectories were generated using the Hybrid Single Particle Lagrangian Integrated Trajectory (HYSPLIT) model. Trajectories were calculated for air masses starting from the sampling site at 500 m above ground level with 6-h intervals during the 24-h sampling period. All trajectories were classified into four clusters, including marine-origin air masses (summer monsoon period) from the Western Pacific and South East Asia regions, and continental-origin air masses (winter monsoon period) from Mongolia and Central Asia.

From the ^{14}C-based positive matrix factorization (PMF) analysis, we obtained 5 sources that contributed to the DOM: biomass burning (18%), fossil fuels combustion (32%), secondary inorganic nitrogen chemistry processes (20%), SOA formation associated with photochemical processes and waste combustion (7%), and SOA formation associated with isoprene-derived SOA and organic sulfates (22%). Fossil fuels combustion showed the highest average contribution to DOM but small changes in concentration across the year. Biomass burning explained 18% of the DOM and showed a marked

设置了格式: 下标
设置了格式: 字体颜色: 自动设置
设置了格式: 字体颜色: 自动设置, 下标
设置了格式: 字体颜色: 自动设置
带格式的: 缩进: 首行缩进: 0 字符
设置了格式: 字体颜色: 自动设置, 上标
设置了格式: 字体颜色: 自动设置
设置了格式: 字体颜色: 自动设置, 上标
设置了格式: 字体颜色: 自动设置
设置了格式: 字体颜色: 自动设置
设置了格式: 字体颜色: 自动设置, 下标
设置了格式: 字体颜色: 自动设置, 非上标/ 下标
设置了格式: 字体颜色: 自动设置
设置了格式: 字体颜色: 自动设置
设置了格式: 字体颜色: 自动设置
设置了格式: 字体颜色: 自动设置
域代码已更改
设置了格式: 下标
设置了格式: 下标
设置了格式: 下标
设置了格式: 字体: 加粗
设置了格式: 字体: 非加粗
设置了格式: 字体: 加粗
设置了格式: 字体: Times New Roman
设置了格式: 字体: Times New Roman
带格式的: 无
设置了格式: 字体: Times New Roman
设置了格式: 字体: Times New Roman
设置了格式: 字体: Times New Roman
设置了格式: 字体: Times New Roman
设置了格式: 字体: Times New Roman
设置了格式: 字体: Times New Roman

increasing trend from fall to winter. SOA factors were responsible for 50% of DOM mass, most of which was contributed by the factors that associated with secondary inorganic nitrogen chemistry processes, and isoprene-derived SOA and organic sulfates formations. DOM formed from secondary inorganic nitrogen chemistry processes showed higher concentrations in fall and winter, while DOM formed from secondary processes of isoprene and organic sulfates formations had lower concentrations in winter than in summer.

Measurements for particulate total sulfur and water-soluble sulfate

About 1~3 pieces of filters were cut using the steel punchers (1.5 cm^2) and then put it into clean tin boats directly. The sample were then crashed into a ball and further analyzed using elemental analyzer (Germany, elementar unicube) coupled with high sensitivity thermal conductivity detector in the CNS mode. The particle sulfur in $PM_{2.5}$ samples were calculated according to the calibration curve which were obtained by analyzing standard samples with different mass. The water-soluble sulfate or SO_4^{2-} was analyzed with ion-chromatography (761 Compact IC, Metrohm, Switzerland). A piece of filter (d=24 mm) was punched for each of collected field filter and dissolved into 12 mL distilled deionized water (≥18.2 Ω). Each sample was sonicated for 30 minutes allowing the solution reaching equilibrium. Then the filtrate was filtered through 0.22 μm PTFE membrane (Jinteng, China) and stored in a prewashed clean bottle at 4 ℃ until sample analysis. Detailed information about the analysis procedures were described in our previous studies (Jiang et al., 2020; Jiang et al., 2021b). Anions were separated on a Metrohm Metrosep A sup5-250 column with 3.2 mM Na_2CO_3 and 1.0 mM $NaHCO_3$ as the eluent and 35 mM H_2SO_4 for a suppressor. The injection loop volume for anion was 100 μL. The water-soluble sulfate-sulfur was calculated as 1/3 of the SO_4^{2-} concentration. The organic sulfur (Org-S) is calculated as the amount of sulfate-sulfur (SO_4^{2-}-S) subtracted from TS, and the ratio of organic sulfur to TS (Org-S/TS) can be calculated as:

$$\text{Org-S} = \text{TS} - \text{sulfate-sulfur} \quad \text{(S1)}$$

$$\text{Org-S/TS} = (\text{TS} - \text{sulfate-sulfur})/\text{TS} \quad \text{(S2)}$$

And the uncertainty of organosulfur fraction of total sulfur ($\delta_{OrgS/TS}$) for filter samples can be calculated using the following equation:

$$\delta_{OrgS/TS} = (RSD_{TS}^2 + RSD_{sulfate\text{-}sulfur}^2)^{1/2} * \text{sulfate-sulfur}/TS \quad \text{(S3)}$$

where RSD_{TS} and $RSD_{sulfate\text{-}sulfur}$ are the relative standard deviations determined for SO_4^{2-} and TS, respectively, both were 0.05 μg m^{-3} in this study.

Operating conditions for FT-ICR MS analysis

The ultrahigh-resolution FT-ICR-MS enables identification of complex atmospheric mixtures by giving accurate m/z value, and each peak was assigned to an ambiguous formula with <1ppm absolute mass error was achieved (Jiang et al.,

设置了格式: 字体: Times New Roman
设置了格式: 字体: Times New Roman
设置了格式: 字体: 非加粗, 字体颜色: 自动设置
设置了格式: 字体颜色: 自动设置
设置了格式: 字体颜色: 自动设置
设置了格式: 字体颜色: 自动设置
设置了格式: 字体颜色: 自动设置
设置了格式: 字体颜色: 自动设置
设置了格式: 字体颜色: 自动设置
设置了格式: 下标
设置了格式: 上标
带格式的: 居中
设置了格式: 字体: 10 磅
设置了格式: 字体: 10 磅
设置了格式: 非上标/ 下标
带格式的: 居中
带格式的: 左, 段落间距段后: 0.5 行
设置了格式: 非上标/ 下标
设置了格式: 上标
设置了格式: 字体颜色: 自动设置
设置了格式: 字体颜色: 自动设置

2021a). Previous study has indicated that the OSs are readily ionized in the negative ESI mode, and most of them were observed only in the negative mode (Lin et al., 2012b; Kuang et al., 2016). Therefore, the negative ESI FT-ICR-MS analysis could provide a comprehensive understanding about the chemical composition of organosulfur compounds (OSCs) in atmosphere, though the molecular structures such as potential isomers were generally hidden behind a given m/z value.

A total of 55 $PM_{2.5}$ samples were used for negative ESI-FT-ICR MS analysis and each sample were ultrasonic extracted with methanol in cold water bath (Jiang et al., 2021a). Though we did not calculate the extraction efficiency of OSs with methanol in a cold-water bath, many previous studies have suggested that methanol could extracted more than 90% of OC both for filed samples or fresh biomass burning samples(Chen and Bond, 2010; Cheng et al., 2017; Huang et al., 2018b). Considering OSs are polar compounds, and most of OSs can be dissolved in methanol(Ye et al., 2020). The potential artifacts resulted from extraction with methanol were not tested in this study. However, in a previous study, methanol was used as eluent to collected the humic-like substance for OSs characterization. Direct using methanol as extraction solvent to extract OSs was reported by Ye et al. (2020). All these studies have successfully characterized the OSs and made comparisons between ambient samples collected at different location. Therefore, we think that there might be small or no potential artifacts resulted from extraction with methanol. The methanol extracts were filtered with PTFE members and concentrated, and direct injected into a 9.4T solariX XR FT-ICR mass spectrometer (Bruker Daltonik GmbH, Bremen, Germany) in negative ESI modes at a flow rate of 180 ~~mL~~ μL h^{-1} (Jiang et al., 2021a; Jiang et al., 2020). Detailed operating conditions are set as: capillary voltage and capillary column end voltage for the negative ESI-FT-ICR MS analysis were set to 4.5 kV and –500 V, ions were accumulated in a hexapole for 0.65s, and the conditions of Octupole were set as 5 MHz and 350 V of peak to-peak (Vp-p) radio frequency (RF) amplitude. An argon-filled hexapole collision pool was operated at 2 MHz and RF amplitude of 1400 Vp-p, in which ions were accumulated for 0.02 s. The optimized mass for quadrupole (Q1) was 170 Da with the time of flight is 0.65ms. The mass range was set as150–800 Da, and a total of 128 continuous 4M data FT-ICR transients were co-added to enhance the signal-to-noise ratio and dynamic range. Field blank filters were processed and analyzed following the same procedure to detect possible contamination. ~~The~~ All mass spectra were calibrated externally with arginine clusters in negative ion mode using a linear calibration. The final spectrum was internally recalibrated with typical O_2 class species peaks using quadratic calibration in DataAnalysis 5.0 (Bruker Daltonics). A typical mass-resolving power (m/Δm50 %, in which Δm50% is the magnitude of the mass spectral peak full width at half-maximum peak height) >450 000 at m/z 319 with <0.3 ppm absolute mass error was achieved. In this study, three duplicate representative aerosol samples were analyzed at the beginning, middle, and end of the analysis to test the reproducibility of sample extraction, the peak detection of the method, and the molecular formula assignment procedures. Pearson's correlation analysis of the relative intensities of all molecules between duplicates confirmed the high level of reproducibility of the selected samples (r = 0.98) (Jiang et al., 2021a).

FT-ICR MS data processing

设置了格式: 字体颜色: 自动设置
设置了格式: 字体颜色: 自动设置
设置了格式: 字体颜色: 自动设置
设置了格式: 字体颜色: 自动设置
设置了格式: 字体颜色: 自动设置
设置了格式: 字体颜色: 自动设置
带格式的: 段落间距段后: 0.5 行
设置了格式: 字体颜色: 自动设置
设置了格式: 字体颜色: 自动设置
设置了格式: 字体颜色: 自动设置
设置了格式: 字体颜色: 自动设置
设置了格式: 字体颜色: 自动设置
设置了格式: 字体颜色: 自动设置
设置了格式: 字体颜色: 自动设置

A custom software was used to calculate all mathematically possible formulas for all ions with a signal-to-noise ratio above 4 using a mass tolerance of ±1ppm. The compounds assigned as $C_cH_hO_oN_nS_s$ with s = 1, 2 will be collectively referred to as organosulfur compounds (OSs) including CHOS (n = 0) and CHONS (n = 1,2). The identified formulas containing isotopomers (i.e., ^{13}C, ^{18}O or ^{34}S) was not discussed. The intensity-weighted elemental ratios such as O/C, H/C, O/S were calculated as described in previous study (Jiang et al., 2021a). The double bond equivalent (DBE) is calculated using the equation:

$$DBE = (2c+2-h+n)/2 \quad (S4)$$

Additionally, the modified index of aromaticity equivalent (Xc) which was considered as a better index to describe potential monocyclic and polycyclic aromatic compounds with S atoms, were also calculated using the flowing equation (Ye et al., 2020; Yassine et al., 2014):

$$X_c = \frac{3[DBE-(m\times o+n\times s)]-2}{DBE-(m\times o+n\times s)} \quad (S5)$$

Where m and n correspond to the fraction of oxygen and sulfur involved in the π-bond structure of the compound, respectively. If DBE ≤ (m×o+n×s), then Xc=0 is assumed. For chemical classes including alchohol, ether, sulfide, disulfide, sulfinic and sulfonic acids, m=n=0 should be used. And for chemical classes including carboxylic acid, ester and nitro, m=0.5 was adopted. Assuming the sulfur atom of organosulfur molecule exists in a sulfate group (R-OSO_3H) or a sulfonate group (R-SO_3H), the organosulfur molecule can be converted into a virtual organic carbon molecule by replacing -OSO_3H with -OH (or -SO_3H with -H). Considering negative ESI-FT-ICR MS analysis was performed, and the negative ESI mode is sensitive to compounds containing carboxylate, sulfonate and nitro groups. Thus, the calculation for Xc of organosulfur compounds can be simplified as (Ye et al., 2020):

$$X_c = \frac{3[DBE-0.5\times(o-4)]-2}{DBE-0.5\times(o-4)} \quad (S6)$$

We rounded 0.5×(*o*–4) down to the next lower integer if *o* is an odd number. A value of Xc≥2.5000 was supposed as the unambiguous minimum criterion for the presence of an aromatic structure. Xc≥2.7143, 2.8000, 2.8333, 2.9231 were considered as the thresholds for molecules containing cores of naphthalene, anthracene, pyrene and ovalene, respectively.

设置了格式: 字体颜色: 自动设置
设置了格式: 字体颜色: 自动设置
设置了格式: 字体颜色: 自动设置
设置了格式: 字体颜色: 自动设置
设置了格式: 字体颜色: 自动设置
设置了格式: 字体颜色: 自动设置
带格式的: 居中
设置了格式: 字体颜色: 自动设置
带格式的: 居中

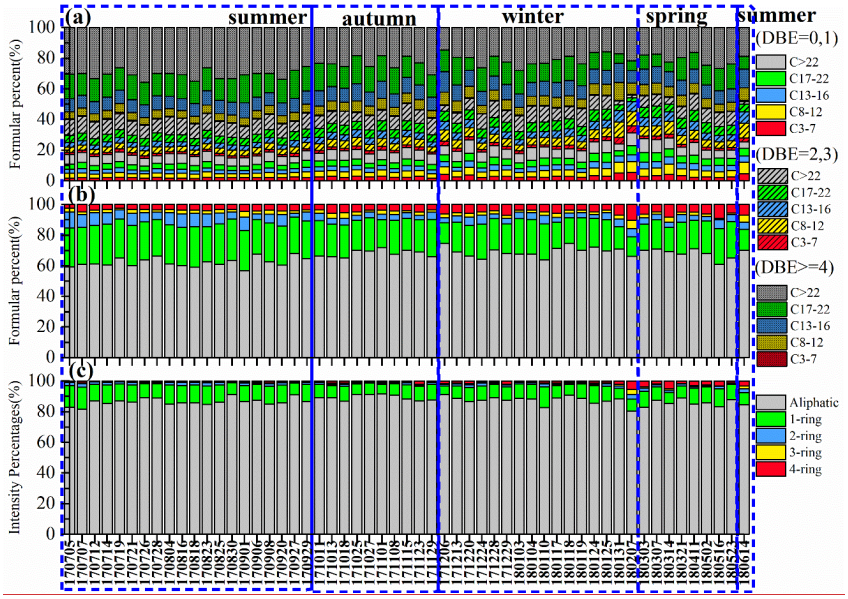
(a)
summer
autumn
winter
spring
summer
Formular percent(%)
(DBE=0,1)
C>22
C17-22
C13-16
C8-12
C3-7
(DBE=2,3)
C>22
C17-22
C13-16
C8-12
C3-7
(b)
Formular percent(%)
(DBE>=4)
C>22
C17-22
C13-16
C8-12
C3-7
(c)
Intensity Percentages(%)
Aliphatic
1-ring
2-ring
3-ring
4-ring

带格式的：居中

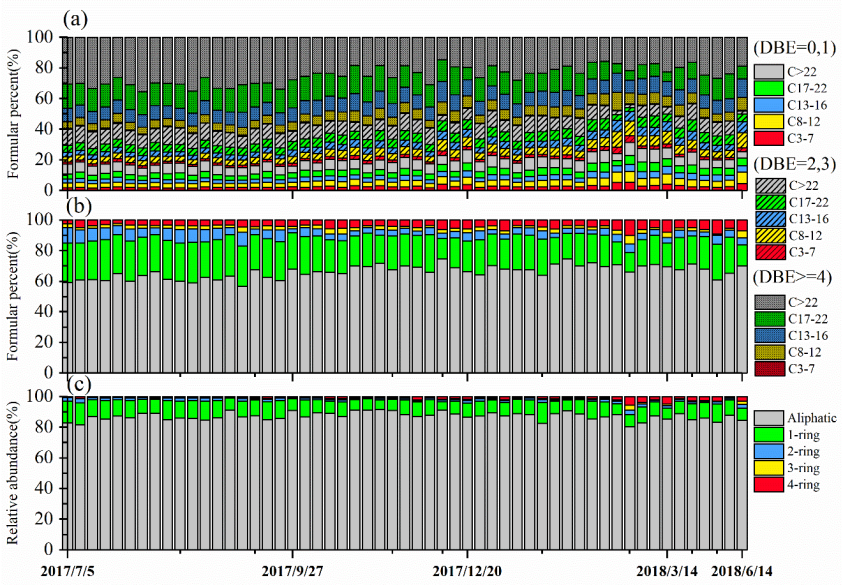

Figure S1. (a) Formular number percentages of each subgroup which divided based on the DBE value and the length of carbon skeleton in the CHOS formulas; (b) and (c) ~~Relative~~ Intensity percentages~~abundance~~ and formular number percentages of each subgroup which divided based on the Xc value of formulas.

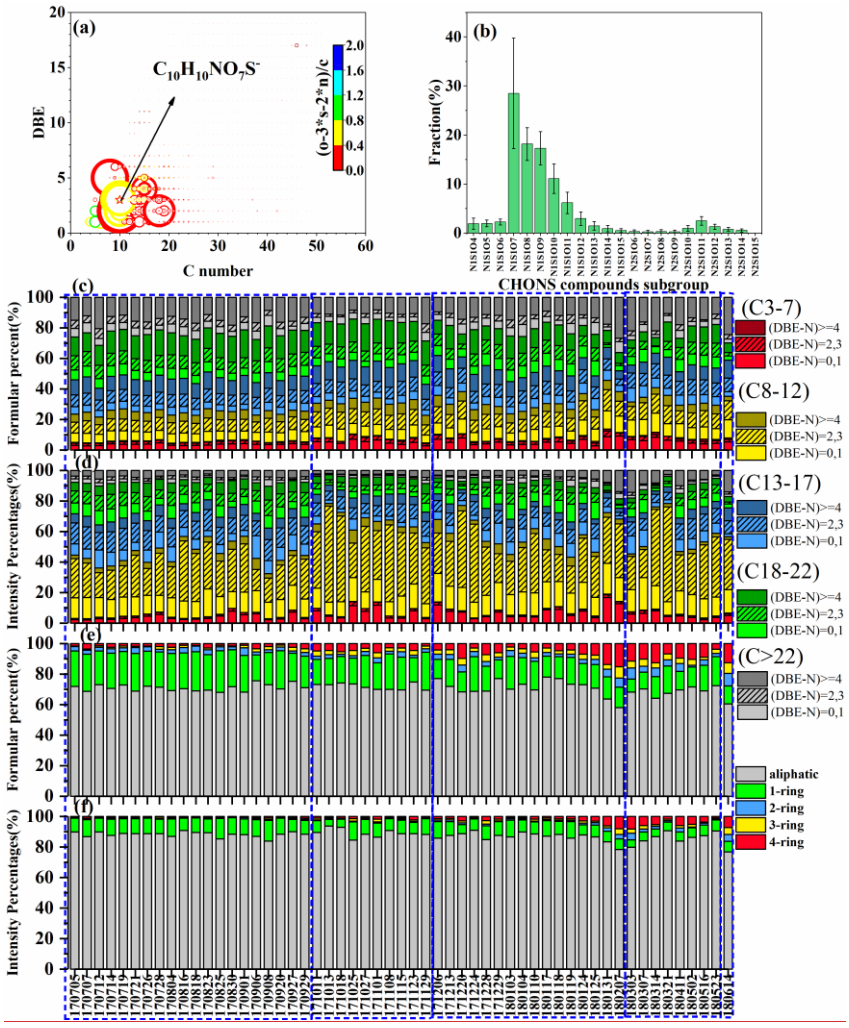
(a)
$C_{10}H_{10}NO_7S^-$
DBE
C number
(o-3*s-2*n)/c
(b)
Fraction(%)
CHONS compounds subgroup
(c)
Formular percent(%)
(C3-7)
(C8-12)
(C13-17)
(C18-22)
(C>22)
(DBE-N)>=4
(DBE-N)=2,3
(DBE-N)=0,1
(d)
Intensity Percentages(%)
(e)
Formular percent(%)
aliphatic
1-ring
2-ring
3-ring
4-ring
(f)
Intensity Percentages(%)

带格式的：居中

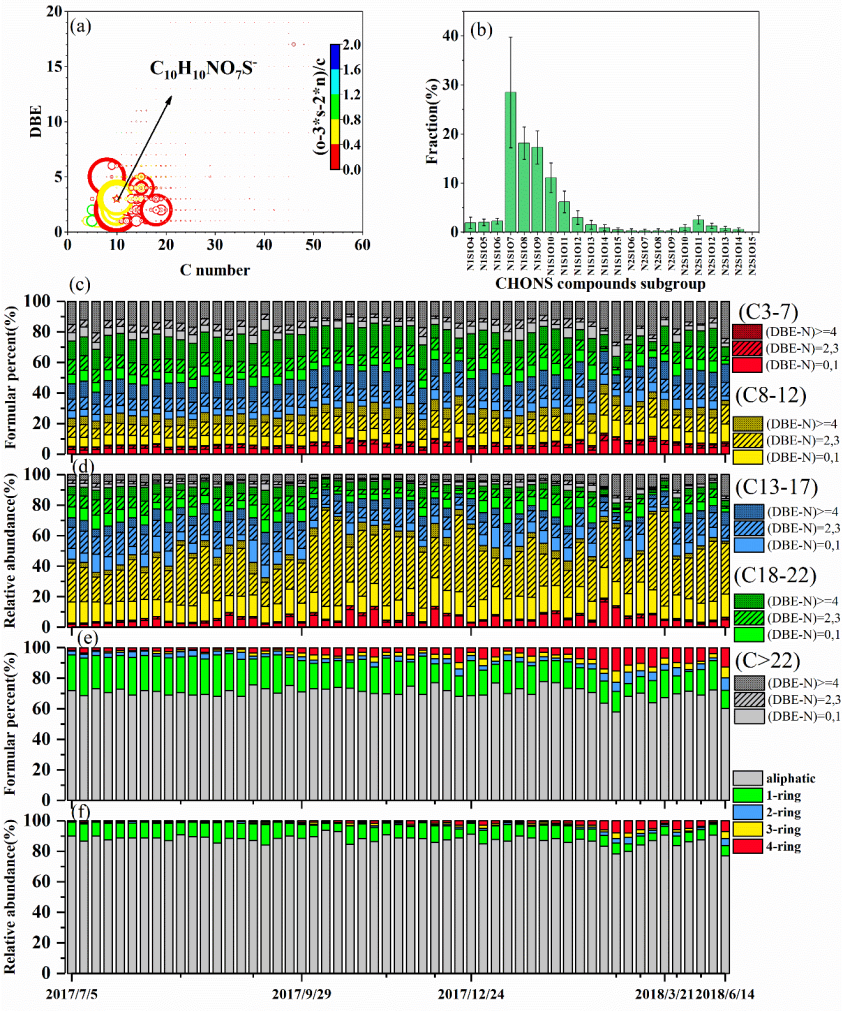

Figure S2. Molecular distribution of CHONS compounds detected by FT-ICR MS for the sample set collected in Guangzhou. (a) Double bond equivalent (DBE) vs C number for all the CHONS compounds of all samples. The color bar and marker size denote the number of oxidation state and the average sum-normalized relative peak intensities of the

compounds; (b) Classification of CHONS species into different subgroups according to the numbers of S and O atoms in their molecules; (c) and (d) Intensity percentages~~Relative abundance~~ and formular number percentages of each subgroup which divided based on the DBE value and the length of carbon skeleton in the formulas; (e) and (f) Intensity percentages~~Relative abundance~~ and formular number percentages of each subgroup which divided based on the Xc value of formulas.

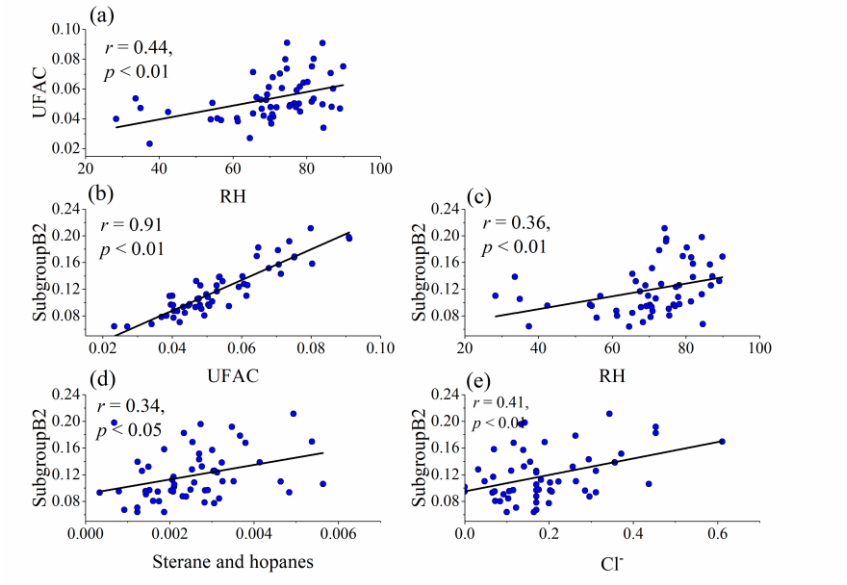

Figure S3. Significant correlations between (a) the sum-normalized intensity of OSs form potential unsaturated fatty acid compounds (UFAC) and RH, and the sum-normalized intensity of OSs classified into the subgroupB2 (with DBE≤2, C->-8, 3<O<7 for CHOS and DBE≤2, N=1, C->-8, 6<O<10 for CHONS compounds) and (b) UFAC, (c) RH, the concentrations of (d) sterane and hopanes, (e) Cl^-.

设置了格式: 上标

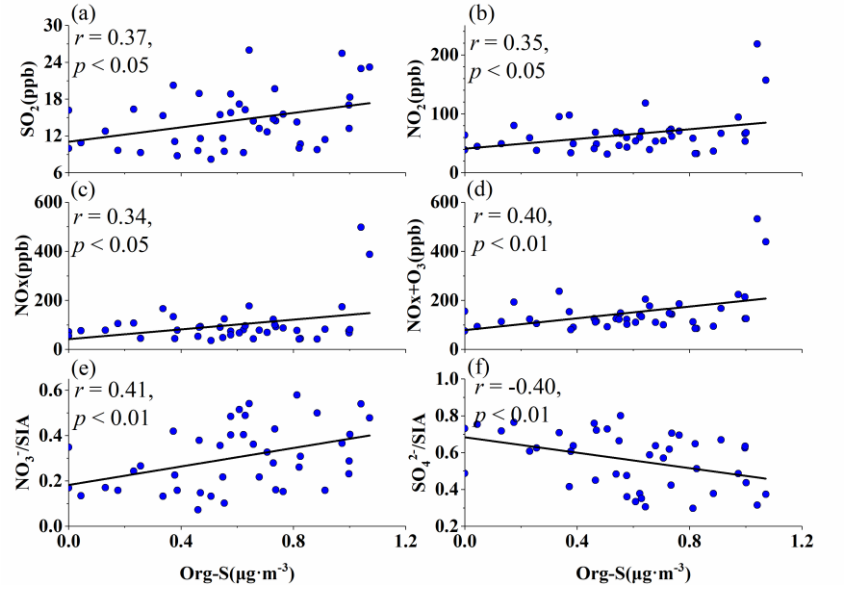

Figure S4. Significant correlations between the concentration of Org-S and (a) SO_2, (b) NO_2, (c) NO_x, (d) NO_x+O_3, (e) NO_3^-/SIA, (f) SO_4^{2-}/SIA.

设置了格式: 下标

设置了格式: 下标

设置了格式: 下标

Table S1. Summary of the concentration of organosulfur (Org-S) and fraction in total particulate sulfur (TS), organic carbon (OC), organic matter (OM), and $PM_{2.5}$ mass reported in recent studies (OS denotes organosulfates).

Sites		Org-S ($\mu g/m^3$)	Org-S/TS	Org-S /OC	OrgSs /OM	Org-S /PM	Ref.
Guangzhou		0.04–1.1 (0.6)	0.07–50% (33%)		3.511–3089% (1442%)	0–3% (1.4%)	This study
Four Asian sites	Maldives	0.3 (OS)	2.1%	4.4%		0.9%(OS)	(Stone et al., 2012)
	Gosan	0.1 (OS)	1.1%	3.5%		0.6% (OS)	
	Singapore	0.3 (OS)	2.5%			1.4% (OS)	
	Lahore	0.9–2 (OS)	5.9–7.7%	0.4–0.8%		0.7–0.9% (OS)	
Continental aerosol						4% (OS)	(Hawkins et al., 2010)
Whistler, British Columbia						< 1%(OS)	(Schwartz et al., 2010)
Polar region			6%		9–11%(OS)		(Frossard et al., 2011)
Kpuszta, Hungary		0.02–0.09	6–12%		8–50 %(OS)		(Luk´Acs et al., 2009)
		0.33	20%		30 %(OS)		(Surratt et al., 2008)
Fairbanks, Alaska				1.3%		0.8%	(Shakya and Peltier, 2013)
				0.7–2.1% (OS)		0.6–1.0% (OS)	
Eight sites in U.S.		up to 0.07		10–13%		1–3%	(Shakya and

					Peltier, 2015)
12 sites in U.S.	0.1–1.4		1–20% (OS)	5–10% (OS)	(Tolocka and Turpin, 2012)
Mt Kleiner Feldberg in central Germany		40%			(Vogel et al., 2016)
21 sites in U.S.	<0.0376 to 0.3				(Dombek et al., 2020)
U.S. (eastern and western, composite)	0.3±0.2 to 0.5±0.2	16±3 to 17±5			(Chen et al., 2021)

Table S2. Summary of the calculated molecular characteristics of organosulfur compounds groups detected in the yearlong sample set.

Group	Subgroup	For sample										For OrgSs formulas set[b]	
		Number of formulas	% of total OrgSs[a] formulas	% of total OrgSs Intensity ~~abundance~~	Number of formulas with $o/(4s+3n) \geq 1$	% of formulas with $o/(4s+3n) \geq 1$	MW	H/C	O/C	O/S	DBE	Number of formulas	% of formulas with $o/(4s+3n) \geq 1$
CHOS	$CHOS_1$	406-2199	57(50-67)	70(56-80)	389-2143	97(94-99)	349(305-378)	1.78(1.72-1.84)	0.52(0.40-0.67)	6.7(5.8-7.7)	2.64(2.22-2.90)	5664	5256(93%)
	$CHOS_2$	82-291	6(4-12)	2(1-6)	35-149	46(31-63)	583(519-649)	1.50(1.30-1.66)	0.33(0.21-0.50)	3.8(3-4.3)	7.80(5.78-9.38)	3722	2017(54%)
	Total	**498-2383**	**64(58-73)**	**72(59-84)**	**432-2262**	**92(87-95)**	**355(315-389)**	**1.77(1.72-1.83)**	**0.52(0.40-0.68)**	**6.7(5.7-7.7)**	**2.77(2.39-3.50)**	**9386**	**7273(77%)**
CHONS	$CHON_1S$	190-1344	31(22-35)	26(15-37)	159-1177	83(75-89)	366(325-399)	1.72(1.65-1.77)	0.71(0.63-0.84)	8.4(7.5-9.5)	3.46(3.10-4.45)	4397	3253(74%)
	$CHON_2S$	40-247	5(2-10)	2(1-6)	25-227	78(48-94)	455(390-553)	1.69(1.42-1.80)	0.90(0.61-1.35)	11.0(9.7-11.9)	4.85(3.49-8.06)	2215	1357(61%)
	Total	**269-1591**	**36(27-42)**	**28(16-41)**	**202-1389**	**82(70-89)**	**373(331-405)**	**1.72(1.62-1.76)**	**0.72(0.63-0.85)**	**8.6(7.7-9.7)**	**3.56(3.15-4.89)**	**6612**	**4610(70%)**

a OrgSs: Organosulfur Compounds

b OrgSs formulas set denotes the all organosulfur compounds detected in all samples.

带格式的: 无, 段落间距段后: 0 磅

Table S3. Comparison of O/C and H/C ratios of CHOS compounds in this study and other studies.

Sample/type	Site/type		Extraction solution	O/C	H/C	Instrument	Ref.
$PM_{2.5}$	CHOS		Methanol	0.52±0.07	1.77±0.03	FT-ICR MS	This study
Rainwater	Northeastern United States		Water	1.3±0.8	1.9±0.5	FT-ICR MS	(Altieri et al., 2009)
$PM_{2.5}$	Pearl River Delta		Water	0.55 ± 0.17	1.67±0.31	Orbitrap MS	(Lin et al., 2012a)
$PM_{2.5}$	Cambridge	winter	Water and acetonitrile	0.47	1.47	Orbitrap MS	(Rincón et al., 2012)
		summer		0.66	1.50		
Cloud	Colorado		Water	0.43±0.09	1.41±0.27	FT-ICR MS	(Zhao et al., 2013)
				0.42±0.05	1.41±0.17		
PM (0.18-1.8 μm)	California	after midnight		0.87±0.09	1.7±0.05	Orbitrap MS	(O'brien et al., 2014)
		morning		0.93±0.1	1.8±0.1		
		afternoon		0.82±0.09	1.8±0.05		
		before midnight		0.88±0.05	1.8±0.0		
TSP	Virginia		Water	0.47±0.23	1.46±0.35	FT-ICR MS	(Willoughby et al., 2014)
			Pyridine	0.49±0.31	1.54±0.38		
			Acetonitrile	0.49±0.32	1.42±0.36		
$PM_{2.5}$	Beijing	Hazy	DCM	0.49±0.26	1.55±0.41	FT-ICR MS	(Jiang et al., 2016)
		Clear		0.62±0.34	1.74±0.34		
		Hazy	Water	0.65±0.28	1.64±0.37		
		Clear		0.75±0.3	1.82±0.2		

				7	6		
$PM_{2.5}$	Wuhan	Winter	Methanol	0.37±0.25	1.68±0.44	Orbitrap MS	(Wang et al., 2016)
		Summer		0.39±0.23	1.75±0.36		
	Nanjing	Summer		0.43±0.32	1.68±0.41		
	Shanghai	Winter		0.40±0.29	1.68±0.46		
		Summer		0.47±0.31	1.68±0.42		
$PM_{2.5}$	Shanghai	Spring	Acetonitrile	0.2	1	Orbitrap MS	(Wang et al., 2017a)
		Summer		0.6	1.1		
		Fall		0.4	1.2		
		Winter		0.2	1.3		
$PM_{2.5}$	Mainz	low-pollution	Acetonitrile-water	0.78	1.66	Orbitrap MS	(Wang et al., 2018a)
	Beijing	low-pollution		0.63	1.81		
		high-pollution		0.51	1.74		
Cloud	France		Water	0.3	1.52	FT-ICR MS	(Bianco et al., 2018)
$PM_{2.5}$	Changchun		Acetonitrile water	1.17±0.13	1.56±0.11	Orbitrap MS	(Wang et al., 2021b)
	Shanghai			1.41±0.19	1.85±0.04		
	Guangzhou			1.48±0.05	1.85±0.02		

Table S4. Comparison of O/C and H/C ratios of CHONS compounds in this study and other studies.

Sample/type	Site/type		Extraction solution	O/C	H/C	Instrument	Ref.
$PM_{2.5}$	CHONS/Guangzhou		Methanol	0.72±0.06	1.72±0.03	FT-ICR MS	This study
rainwater	Northeastern United States		Water	1.7 ±0.9	1.8 ±0.6	FT-ICR MS	(Altieri et al., 2009)
$PM_{2.5}$	Pearl River Delta		Water	0.81 ± 0.22	1.73 ± 0.29	Orbitrap MS	(Lin et al., 2012a)
$PM_{2.5}$	Cambridge	winter	Water and acetonitrile	0.73	1.99	Orbitrap MS	(Rincón et al., 2012)
		summer		0.80	1.65		
Cloud	Colorado		Water	0.44±0.04	1.17±0.10	FT-ICR MS	(Zhao et al., 2013)
				0.43±0.04	1.19±0.11		
PM (0.18-1.8 μm)	California	after midnight		0.99±0.02	1.7±0.0	Orbitrap MS	(O'brien et al., 2014)
		morning		1.0±0.005	1.7±0.0		
		afternoon		0.92±0.03	1.7±0.05		
		before midnight		0.89±0.09	1.7±0.05		
TSP	Virginia		Water	0.71±0.21	1.65±0.20	FT-ICR MS	(Willoughby et al., 2014)
			Pyridine	0.64±0.23	1.52±0.28		
			Acetonitrile	0.45±0.25	1.27±0.29		
$PM_{2.5}$	Beijing	Hazy	DCM	0.69±0.31	1.57±0.37	FT-ICR MS	(Jiang et al., 2016)
		Clear		0.76±0.27	1.75±0.31		
		Hazy	Water	0.70±0.3	1.51±0.3		

		Clear		2	7		
$PM_{2.5}$	Wuhan	Winter	Methanol	0.35±0.13	1.58±0.46	Orbitrap MS	(Wang et al., 2016)
		Summer		0.40±0.17	1.69±0.34		
	Nanjing	Summer		0.44±0.21	1.69±0.35		
	Shanghai	Winter		0.42±0.27	1.64±0.52		
		Summer		0.53±0.38	1.64±0.47		
$PM_{2.5}$	Shanghai	Spring	Acetonitrile	0.2	1.5	Orbitrap MS	(Wang et al., 2017a)
		Summer		0.4	1.5		
		Fall		0.3	1.6		
		Winter		0.4	1.5		
$PM_{2.5}$	Mainz	low-pollution	Acetonitrile-water	0.91	1.54	Orbitrap MS	(Wang et al., 2018a)
	Beijing	low-pollution		0.81	1.57		
		high-pollution		0.59	1.56		
Cloud	France		Water	0.23	1.47	FT-ICR MS	(Bianco et al., 2018)
$PM_{2.5}$	Changchun		Acetonitrile-water	1.07±0.11	1.35±0.02	Orbitrap MS	(Wang et al., 2021b)
	Shanghai			1.00±0.13	1.56±0.03		
	Guangzhou			0.82±0.03	1.56±0.04		

Table S5. Summary of the calculated molecular characteristics of organosulfur compounds groups detected in source samples, as the FT-ICR MS data are obtained from Cui et al. (2019) and Tang et al. (2020)

		Formula number	MW	H/C	O/C	O/S	DBE	% of (DBE-N) ≥4	% of Xc≥2.5	% of *o*/(4*s*+3*n*) ≥ 1
BBOA1(Musa)	CHOS	444	360	1.52	0.47	6.21	4.76	57	43	88
	CHONS	371	379	1.55	0.50	7.21	4.98	58	64	64
	Avg/total	815	367	1.53	0.48	6.59	4.85	57	53	77
BBOA2(Hevea)	CHOS	174	396	1.35	0.40	5.97	7.68	69	59	86
	CHONS	65	411	1.56	0.50	7.51	4.79	62	69	63
	Avg/total	239	400	1.40	0.42	6.34	6.98	67	62	80
CCOA1(Anthracite)	CHOS	549	323	1.01	0.40	5.40	8.55	85	82	95
	CHONS	767	340	0.98	0.52	6.49	8.99	94	97	47
	Avg/total	1316	332	0.99	0.47	6.03	8.80	90	91	67
CCOA2(Bituminous coal)	CHOS	463	340	0.99	0.31	4.64	9.90	96	94	85
	CHONS	293	308	0.97	0.49	5.82	8.04	92	93	29
	Avg/total	756	328	0.98	0.38	5.10	9.18	94	93	63
Vehicle emissions	CHOS	112	441	1.31	0.25	4.47	9.54	71	71	75
	CHONS	17	400	1.17	0.72	8.59	6.92	59	59	47
	Avg/total	129	432	1.28	0.35	5.36	8.97	69	69	71
Tunnel aerosols	CHOS	635	325	1.74	0.59	6.79	2.75	46	23	96
	CHONS	410	340	1.81	0.90	8.73	2.78	28	29	91
	Avg/total	1045	331	1.76	0.71	7.53	2.76	39	25	94
Excavator-idling(diesel)	CHOS	1004	353	1.61	0.38	5.81	4.18	68	58	96
	CHONS	310	325	1.47	0. 41	5.59	5.18	56	65	42
	Avg/total	1314	347	1.59	0.38	5.77	4.38	65	60	83

	CHOS	334	326	1.51	0.46	5.20	3.58	54	49	98
Excavator-moving(diesel)	CHONS	117	298	1.62	0.48	5.17	5.55	59	64	9
	Avg/total	451	314	1.35	0.42	5.19	4.38	56	53	75
	CHOS	631	342	1.63	0.36	5.44	4.00	62	55	93
Excavator-working(diesel)	CHONS	260	323	1.47	0.40	5.41	5.26	62	69	27
	Avg/total	891	337	1.58	0.37	5.19	4.35	62	59	74
	CHOS	334	306	1.66	0.40	5.14	3.47	55	50	95
Diesel-vessels	CHONS	13	461	1.50	0.36	6.74	9.38	38	38	46
	Avg/total	347	310	1.66	0.40	5.17	3.60	54	49	93
	CHOS	1110	311	1.48	0.36	4.77	4.85	76	71	83
Heavy-fuel-oil-vessels	CHONS	398	343	1.35	0.39	5.68	6.35	80	86	28
	Avg/total	1508	314	1.47	0.36	4.86	5.00	77	75	68

Table S6. Detailed intensity percentages~~relative abundance~~ of isoprene-derived OSs detected at Guangzhou. Noted the formulas in the Table S6-S10 were from the summarization of recent studies and the reference in (Bruggemann et al., 2020; Ye et al., 2020; Zhu et al., 2019; Wang et al., 2019).

Formula [M-H]$^-$	MW (Da)	DBE	Average RI (‰)
$C_4H_5O_5S^-$	164.9863	2	0.019
$C_4H_7O_5S^-$	167.0020	1	0.067
$C_3H_5O_6S^-$	168.9812	1	0.093
$C_3H_7O_6S^-$	170.9969	0	0.106
$C_4H_5O_6S^-$	180.9812	2	0.049
$C_5H_9O_5S^-$	181.0176	1	0.109
$C_4H_7O_6S^-$	182.9969	1	0.145
$C_3H_5O_7S^-$	184.9761	1	0.200
$C_5H_7O_6S^-$	194.9969	2	0.179
$C_5H_9O_6S^-$	197.0125	1	0.366
$C_3H_3O_8S^-$	198.9554	2	0.372
$C_4H_7O_7S^-$	198.9918	1	0.169
$C_5H_{11}O_6S^-$	199.0282	0	0.191
$C_3H_5O_8S^-$	200.9711	1	0.192
$C_5H_7O_7S^-$	210.9918	2	0.752
$C_5H_9O_7S^-$	213.0074	1	0.482
$C_4H_7O_8S^-$	214.9867	1	0.119
$C_5H_{11}O_7S^-$	215.0231	0	0.141
$C_3H_5O_9S^-$	216.9660	1	0.100
$C_7H_9O_6S^-$	221.0125	3	0.106
$C_8H_{13}O_5S^-$	221.0489	2	0.167
$C_5H_7O_8S^-$	226.9867	2	0.509
$C_5H_9O_8S^-$	229.0024	1	0.170
$C_4H_7O_9S^-$	230.9816	1	0.062
$C_5H_{11}O_8S^-$	231.0180	0	0.030
$C_8H_{11}O_6S^-$	235.0282	3	0.175
$C_7H_9O_7S^-$	237.0074	3	0.703
$C_8H_{13}O_6S^-$	237.0438	2	1.079

$C_8H_{11}O_7S^-$	251.0231	3	0.789
$C_8H_{13}O_7S^-$	253.0387	2	2.206
$C_9H_{15}O_7S^-$	267.0544	2	1.512
$C_8H_{13}O_8S^-$	269.0337	2	0.579
$C_5H_7O_{11}S^-$	274.9715	2	0.036
$C_{12}H_{19}O_6S^-$	291.0908	3	0.206
$C_8H_{13}O_{10}S^-$	301.0235	2	0.061
$C_{12}H_{17}O_8S^-$	321.0650	4	0.139
$C_{10}H_{19}O_{10}S^-$	331.0704	1	0.028
$C_{10}H_{21}O_{10}S^-$	333.0861	0	0.070
$C_{15}H_{31}O_{13}S^-$	451.1491	0	0.035
$C_5H_{10}NO_8S^-$	244.0133	1	0.172
$C_5H_{10}NO_9S^-$	260.0082	1	0.230
$C_5H_8NO_{10}S^-$	273.9874	2	0.099
$C_5H_9N_2O_{11}S^-$	304.9933	2	0.108
$C_8H_{12}NO_{12}S^-$	346.0086	3	0.039

Table S7. Detailed intensity percentages~~relative abundance~~ of terpene-derived OSs (including limonene) detected at Guangzhou.

Formula $[M\text{-}H]^-$	MW (Da)	DBE	Average RI (‰)
$C_6H_{11}O_4S^-$	179.0384	1	0.055
$C_5H_{11}O_6S^-$	199.0282	0	0.166
$C_3H_5O_8S^-$	200.9711	1	0.167
$C_6H_{11}O_6S^-$	211.0282	1	0.348
$C_5H_{11}O_7S^-$	215.0231	0	0.431
$C_9H_{15}O_4S^-$	219.0697	2	0.169
$C_9H_{17}O_4S^-$	221.0853	1	0.189
$C_7H_{11}O_6S^-$	223.0282	2	0.291
$C_9H_{19}O_4S^-$	223.1010	0	0.391
$C_7H_{13}O_6S^-$	225.0438	1	0.462
$C_5H_7O_8S^-$	226.9867	2	0.503
$C_5H_9O_8S^-$	229.0024	1	0.469

$C_9H_9O_5S^-$	229.0176	5	0.471
$C_{10}H_{13}O_4S^-$	229.0540	4	0.478
$C_{10}H_{15}O_4S^-$	231.0697	3	0.453
$C_9H_{15}O_5S^-$	235.0646	2	0.252
$C_8H_{13}O_6S^-$	237.0438	2	0.403
$C_{10}H_{21}O_4S^-$	237.1166	0	0.478
$C_{10}H_9O_5S^-$	241.0176	6	0.630
$C_8H_{17}O_6S^-$	241.0751	0	0.669
$C_6H_{11}O_8S^-$	243.0180	1	0.656
$C_9H_9O_6S^-$	245.0125	5	0.279
$C_{10}H_{15}O_5S^-$	247.0646	3	0.129
$C_9H_{13}O_6S^-$	249.0438	3	0.140
$C_{10}H_{17}O_5S^-$	249.0802	2	0.217
$C_7H_7O_8S^-$	250.9867	4	0.236
$C_8H_{11}O_7S^-$	251.0231	3	0.326
$C_9H_{15}O_6S^-$	251.0595	2	0.507
$C_{10}H_{19}O_5S^-$	251.0959	1	0.771
$C_7H_9O_8S^-$	253.0024	3	0.793
$C_8H_{13}O_7S^-$	253.0387	2	0.912
$C_9H_{17}O_6S^-$	253.0751	1	1.038
$C_{10}H_{21}O_5S^-$	253.1115	0	1.056
$C_9H_7O_7S^-$	258.9918	6	0.416
$C_{10}H_{11}O_6S^-$	259.0282	5	0.290
$C_{10}H_{13}O_6S^-$	261.0438	4	0.062
$C_9H_{11}O_7S^-$	263.0231	4	0.080
$C_{10}H_{15}O_6S^-$	263.0595	3	0.153
$C_8H_9O_8S^-$	265.0024	4	0.189
$C_9H_{13}O_7S^-$	265.0387	3	0.352
$C_{10}H_{17}O_6S^-$	265.0751	2	0.480
$C_8H_{11}O_8S^-$	267.0180	3	0.613
$C_9H_{15}O_7S^-$	267.0544	2	0.799
$C_{10}H_{19}O_6S^-$	267.0908	1	0.910

$C_9H_{17}O_7S^-$	269.0700	1	0.899
$C_7H_{11}O_9S^-$	271.0129	2	0.751
$C_{10}H_9O_7S^-$	273.0074	6	0.313
$C_8H_{17}O_8S^-$	273.0650	0	0.186
$C_{10}H_{15}O_7S^-$	279.0544	3	0.443
$C_9H_{13}O_8S^-$	281.0337	3	0.768
$C_{10}H_{17}O_7S^-$	281.0700	2	0.986
$C_{12}H_{11}O_6S^-$	283.0282	7	1.001
$C_9H_{15}O_8S^-$	283.0493	2	1.067
$C_{10}H_{19}O_7S^-$	283.0857	1	1.150
$C_8H_{13}O_9S^-$	285.0286	2	0.826
$C_{11}H_{15}O_7S^-$	291.0544	4	0.089
$C_9H_{11}O_9S^-$	295.0129	4	0.475
$C_{10}H_{15}O_8S^-$	295.0493	3	0.595
$C_9H_{13}O_9S^-$	297.0286	3	0.737
$C_{10}H_{17}O_8S^-$	297.0650	2	0.834
$C_9H_{15}O_9S^-$	299.0442	2	0.580
$C_{14}H_{23}O_5S^-$	303.1272	3	0.137
$C_{11}H_{17}O_8S^-$	309.0650	3	0.477
$C_{10}H_{15}O_9S^-$	311.0442	3	0.642
$C_{10}H_{17}O_9S^-$	313.0599	2	0.478
$C_{15}H_{25}O_5S^-$	317.1428	3	0.106
$C_{14}H_{23}O_6S^-$	319.1221	3	0.152
$C_{10}H_{15}O_{10}S^-$	327.0391	3	0.358
$C_{14}H_{21}O_7S^-$	333.1013	4	0.129
$C_{15}H_{25}O_6S^-$	333.1377	3	0.164
$C_{10}H_{13}O_{11}S^-$	341.0184	4	0.411
$C_{15}H_{23}O_7S^-$	347.1170	4	0.136
$C_{14}H_{21}O_8S^-$	349.0963	4	0.206
$C_{14}H_{23}O_8S^-$	351.1119	3	0.305
$C_{15}H_{23}O_8S^-$	363.1119	4	0.188
$C_{16}H_{27}O_7S^-$	363.1483	3	0.235

$C_{16}H_{27}O_8S^-$	379.1432	3	0.321
$C_{20}H_{31}O_5S^-$	383.1898	5	0.240
$C_{20}H_{33}O_5S^-$	385.2054	4	0.074
$C_{20}H_{33}O_9S_2^-$	481.1571	4	0.061
$C_{10}H_{16}NO_7S^-$	294.0653	3	1.416
$C_9H_{14}NO_8S^-$	296.0446	3	1.483
$C_{10}H_{16}NO_8S^-$	310.0602	3	0.130
$C_9H_{14}NO_9S^-$	312.0395	3	0.178
$C_{10}H_{16}NO_9S^-$	326.0551	3	0.164
$C_{10}H_{18}NO_9S^-$	328.0708	2	0.274
$C_9H_{16}NO_{10}S^-$	330.0500	2	0.295
$C_{10}H_{16}NO_{10}S^-$	342.0500	3	0.212
$C_{10}H_{15}N_2O_{10}S^-$	355.0453	4	0.153
$C_{15}H_{24}NO_7S^-$	362.1279	4	0.097
$C_{10}H_{17}N_2O_{11}S^-$	373.0559	3	0.201
$C_{14}H_{24}NO_9S^-$	382.1177	3	0.131
$C_{10}H_{17}N_2O_{12}S^-$	389.0508	3	0.066

Table S8. Detailed intensity percentages~~relative abundance~~ of other biogenic VOCs-derived OSs (2-Methyl-3-Buten-2-ol; 2-E-pentenal, 2-E-hexenal, 3-Z-hexenal, and cis-3-hexen-1-ol, β-caryophyllene) detected at Guangzhou.

Formula $[M-H]^-$	MW (Da)	DBE	Average RI (‰)
$C_3H_5O_6S^-$	168.9812	1	0.060
$C_4H_9O_5S^-$	169.0176	0	0.069
$C_3H_5O_7S^-$	184.9761	1	0.142
$C_5H_{11}O_6S^-$	199.0282	0	0.264
$C_6H_9O_6S^-$	209.0125	2	0.219
$C_6H_{11}O_6S^-$	211.0282	1	0.607
$C_5H_9O_7S^-$	213.0074	1	0.630
$C_5H_9O_8S^-$	229.0024	1	0.387
$C_9H_{15}O_6S^-$	251.0595	2	0.790
$C_9H_{17}O_7S^-$	269.0700	1	0.910
$C_{14}H_{23}O_5S^-$	303.1272	3	0.140

$C_{15}H_{25}O_5S^-$	317.1428	3	0.110
$C_{14}H_{23}O_6S^-$	319.1221	3	0.199
$C_{14}H_{21}O_7S^-$	333.1013	4	0.191
$C_{15}H_{25}O_6S^-$	333.1377	3	0.201
$C_{15}H_{23}O_7S^-$	347.1170	4	0.190
$C_{14}H_{21}O_8S^-$	349.0963	4	0.135
$C_{14}H_{23}O_8S^-$	351.1119	3	0.336
$C_{15}H_{23}O_8S^-$	363.1119	4	0.237
$C_{16}H_{27}O_7S^-$	363.1483	3	0.289
$C_{16}H_{27}O_8S^-$	379.1432	3	0.419
$C_{15}H_{24}NO_7S^-$	362.1279	4	0.162
$C_{14}H_{24}NO_9S^-$	382.1177	3	0.151

Table S9. Detailed intensity percentages~~relative abundance~~ of anthropogenic VOCs-derived OSs detected at Guangzhou.

Formula $[M-H]^-$	MW (Da)	DBE	Average RI (‰)
$C_6H_5O_4S^-$	172.9914	4	0.060
$C_7H_5O_4S^-$	184.9914	5	0.109
$C_7H_7O_4S^-$	187.0071	4	0.120
$C_5H_7O_6S^-$	194.9969	2	0.108
$C_8H_7O_4S^-$	199.0071	5	0.213
$C_7H_5O_5S^-$	200.9863	5	0.216
$C_8H_9O_4S^-$	201.0227	4	0.214
$C_6H_9O_6S^-$	209.0125	2	0.169
$C_7H_{13}O_5S^-$	209.0489	1	0.243
$C_8H_7O_5S^-$	215.0020	5	0.506
$C_9H_{11}O_4S^-$	215.0384	4	0.358
$C_8H_5O_6S^-$	228.9812	6	0.597
$C_9H_9O_5S^-$	229.0176	5	0.574
$C_9H_{11}O_5S^-$	231.0333	4	0.164
$C_9H_{17}O_5S^-$	237.0802	1	0.624
$C_{10}H_{19}O_5S^-$	251.0959	1	1.026
$C_{10}H_{17}O_6S^-$	265.0751	2	0.623

$C_9H_{15}O_7S^-$	267.0544	2	1.043
$C_9H_{17}O_7S^-$	269.0700	1	0.986
$C_{10}H_9O_7S^-$	273.0074	6	0.234
$C_{10}H_{11}O_7S^-$	275.0231	5	0.049
$C_{12}H_{23}O_5S^-$	279.1272	1	0.830
$C_{10}H_{17}O_7S^-$	281.0700	2	1.192
$C_9H_{17}O_8S^-$	285.0650	1	0.473
$C_{11}H_{11}O_7S^-$	287.0231	6	0.312
$C_{11}H_{13}O_7S^-$	289.0387	5	0.062
$C_{10}H_{15}O_8S^-$	295.0493	3	0.651
$C_{10}H_{17}O_8S^-$	297.0650	2	0.669
$C_6H_4NO_6S^-$	217.9765	5	0.061
$C_{10}H_{10}NO_9S^-$	320.0082	6	0.040
$C_{10}H_{16}NO_9S^-$	326.0551	3	0.196

Table S10. Detailed intensity percentages ~~relative abundance~~ of OSs derived from precursors of multiple sources detected at Guangzhou, including Methyl Vinyl, Methacrolein, glyoxal, methylglyoxal, Oleic acid, and other unsaturated acids, such as Palmitoleic acid, Linoleic acid, Conjugated linoleic acid, 10-Undecenoic acid, as well as some alkanes such as 1-Dodecene.

Formula $[M-H]^-$	MW (Da)	DBE	Average RI (‰)
$C_3H_7O_5S^-$	155.0020	0	0.087
$C_4H_5O_5S^-$	164.9863	2	0.076
$C_4H_7O_5S^-$	167.0020	1	0.588
$C_3H_5O_6S^-$	168.9812	1	0.127
$C_5H_7O_5S^-$	179.0020	2	0.144
$C_5H_9O_5S^-$	181.0176	1	0.719
$C_4H_7O_6S^-$	182.9969	1	0.683
$C_5H_7O_6S^-$	194.9969	2	0.907
$C_6H_{11}O_5S^-$	195.0333	1	1.546
$C_5H_9O_6S^-$	197.0125	1	1.113
$C_3H_3O_8S^-$	198.9554	2	0.004
$C_3H_5O_8S^-$	200.9711	1	0.015
$C_6H_7O_6S^-$	206.9969	3	0.312

$C_7H_{11}O_5S^-$	207.0333	2	0.487
$C_8H_{15}O_4S^-$	207.0697	1	0.392
$C_6H_9O_6S^-$	209.0125	2	2.961
$C_7H_{13}O_5S^-$	209.0489	1	2.110
$C_8H_{17}O_4S^-$	209.0853	0	2.239
$C_5H_7O_7S^-$	210.9918	2	1.181
$C_6H_{11}O_6S^-$	211.0282	1	2.907
$C_7H_{15}O_5S^-$	211.0646	0	0.858
$C_5H_9O_7S^-$	213.0074	1	0.565
$C_4H_7O_8S^-$	214.9867	1	0.002
$C_3H_5O_9S^-$	216.9660	1	0.017
$C_8H_{13}O_5S^-$	221.0489	2	0.742
$C_9H_{17}O_4S^-$	221.0853	1	0.344
$C_8H_{15}O_5S^-$	223.0646	1	3.136
$C_9H_{19}O_4S^-$	223.1010	0	0.657
$C_5H_9O_8S^-$	229.0024	1	0.084
$C_4H_7O_9S^-$	230.9816	1	0.007
$C_9H_{15}O_5S^-$	235.0646	2	5.496
$C_{10}H_{19}O_4S^-$	235.1010	1	0.431
$C_7H_9O_7S^-$	237.0074	3	1.350
$C_8H_{13}O_6S^-$	237.0438	2	4.505
$C_9H_{17}O_5S^-$	237.0802	1	2.513
$C_8H_{15}O_6S^-$	239.0595	1	4.788
$C_5H_9O_9S^-$	244.9973	1	0.006
$C_{10}H_{17}O_5S^-$	249.0802	2	2.914
$C_{11}H_{21}O_4S^-$	249.1166	1	0.448
$C_9H_{15}O_6S^-$	251.0595	2	6.871
$C_{10}H_{19}O_5S^-$	251.0959	1	10.186
$C_9H_{17}O_6S^-$	253.0751	1	4.825
$C_8H_{15}O_7S^-$	255.0544	1	1.826
$C_9H_{19}O_6S^-$	255.0908	0	0.549
$C_{10}H_{17}O_6S^-$	265.0751	2	4.866

$C_{11}H_{21}O_5S^-$	265.1115	1	3.640
$C_8H_{11}O_8S^-$	267.0180	3	2.195
$C_9H_{15}O_7S^-$	267.0544	2	7.408
$C_{10}H_{19}O_6S^-$	267.0908	1	4.505
$C_9H_{17}O_7S^-$	269.0700	1	2.203
$C_8H_{15}O_8S^-$	271.0493	1	0.394
$C_5H_7O_{11}S^-$	274.9715	2	0.006
$C_{13}H_{25}O_4S^-$	277.1479	1	0.545
$C_{10}H_{15}O_7S^-$	279.0544	3	9.100
$C_{11}H_{19}O_6S^-$	279.0908	2	3.420
$C_{12}H_{23}O_5S^-$	279.1272	1	4.561
$C_{11}H_{21}O_6S^-$	281.1064	1	3.002
$C_{10}H_{19}O_7S^-$	283.0857	1	2.828
$C_9H_{17}O_8S^-$	285.0650	1	0.564
$C_{12}H_{19}O_6S^-$	291.0908	3	1.309
$C_{12}H_{21}O_6S^-$	293.1064	2	2.970
$C_{13}H_{25}O_5S^-$	293.1428	1	5.245
$C_{10}H_{15}O_8S^-$	295.0493	3	4.782
$C_{10}H_{17}O_8S^-$	297.0650	2	3.585
$C_{11}H_{21}O_7S^-$	297.1013	1	1.343
$C_{10}H_{19}O_8S^-$	299.0806	1	1.084
$C_9H_{17}O_9S^-$	301.0599	1	0.076
$C_{14}H_{23}O_5S^-$	303.1272	3	0.671
$C_{14}H_{25}O_5S^-$	305.1428	2	1.476
$C_{15}H_{29}O_4S^-$	305.1792	1	0.614
$C_{14}H_{27}O_5S^-$	307.1585	1	6.946
$C_{15}H_{31}O_4S^-$	307.1949	0	1.458
$C_{13}H_{25}O_6S^-$	309.1377	1	2.465
$C_{15}H_{25}O_5S^-$	317.1428	3	0.720
$C_{14}H_{23}O_6S^-$	319.1221	3	1.328
$C_{15}H_{27}O_5S^-$	319.1585	2	1.399
$C_{14}H_{25}O_6S^-$	321.1377	2	2.457

$C_{15}H_{29}O_5S^-$	321.1741	1	7.015
$C_{14}H_{27}O_6S^-$	323.1534	1	2.529
$C_{15}H_{31}O_5S^-$	323.1898	0	0.906
$C_{13}H_{25}O_7S^-$	325.1326	1	1.016
$C_{14}H_{21}O_7S^-$	333.1013	4	1.254
$C_{15}H_{25}O_6S^-$	333.1377	3	1.362
$C_{16}H_{29}O_5S^-$	333.1741	2	1.408
$C_{15}H_{27}O_6S^-$	335.1534	2	2.050
$C_{16}H_{31}O_5S^-$	335.1898	1	6.059
$C_{14}H_{25}O_7S^-$	337.1326	2	2.532
$C_{15}H_{29}O_6S^-$	337.1690	1	2.283
$C_{16}H_{33}O_5S^-$	337.2054	0	1.863
$C_{15}H_{23}O_7S^-$	347.1170	4	1.842
$C_{17}H_{31}O_5S^-$	347.1898	2	1.309
$C_{14}H_{21}O_8S^-$	349.0963	4	1.610
$C_{15}H_{25}O_7S^-$	349.1326	3	2.194
$C_{16}H_{29}O_6S^-$	349.1690	2	2.253
$C_{14}H_{23}O_8S^-$	351.1119	3	2.031
$C_{15}H_{27}O_7S^-$	351.1483	2	2.370
$C_{16}H_{31}O_6S^-$	351.1847	1	5.103
$C_{14}H_{25}O_8S^-$	353.1276	2	1.433
$C_{15}H_{29}O_7S^-$	353.1639	1	1.019
$C_{18}H_{31}O_5S^-$	359.1898	3	0.433
$C_{18}H_{33}O_5S^-$	361.2054	2	1.181
$C_{15}H_{23}O_8S^-$	363.1119	4	1.893
$C_{16}H_{27}O_7S^-$	363.1483	3	1.767
$C_{17}H_{31}O_6S^-$	363.1847	2	1.538
$C_{18}H_{35}O_5S^-$	363.2211	1	3.739
$C_{16}H_{29}O_7S^-$	365.1639	2	3.434
$C_{17}H_{33}O_6S^-$	365.2003	1	3.154
$C_{15}H_{27}O_8S^-$	367.1432	2	1.283
$C_{18}H_{31}O_6S^-$	375.1847	3	0.767

$C_{18}H_{33}O_6S^-$	377.2003	2	1.728
$C_{19}H_{37}O_5S^-$	377.2367	1	2.472
$C_{16}H_{27}O_8S^-$	379.1432	3	1.754
$C_{18}H_{35}O_6S^-$	379.2160	1	2.906
$C_{16}H_{29}O_8S^-$	381.1589	2	1.390
$C_{15}H_{15}O_{10}S^-$	387.0391	8	0.037
$C_{20}H_{37}O_5S^-$	389.2367	2	0.666
$C_{18}H_{31}O_7S^-$	391.1796	3	1.175
$C_{19}H_{35}O_6S^-$	391.2160	2	1.002
$C_{20}H_{39}O_5S^-$	391.2524	1	1.834
$C_{18}H_{33}O_7S^-$	393.1952	2	2.059
$C_{17}H_{31}O_8S^-$	395.1745	2	1.121
$C_{18}H_{35}O_7S^-$	395.2109	1	2.020
$C_{20}H_{37}O_6S^-$	405.2316	2	0.823
$C_{21}H_{41}O_5S^-$	405.2680	1	1.159
$C_{18}H_{31}O_8S^-$	407.1745	3	1.129
$C_{18}H_{33}O_8S^-$	409.1902	2	1.211
$C_{22}H_{41}O_5S^-$	417.2680	2	0.406
$C_{22}H_{43}O_5S^-$	419.2837	1	0.879
$C_{22}H_{41}O_6S^-$	433.2629	2	0.466
$C_{23}H_{45}O_5S^-$	433.2993	1	0.859
$C_{24}H_{45}O_6S^-$	461.2942	2	0.342
$C_{24}H_{47}O_6S^-$	463.3099	1	0.925
$C_{24}H_{45}O_7S^-$	477.2891	2	0.426
$C_5H_8NO_8S^-$	241.9976	2	0.591
$C_6H_{12}NO_8S^-$	258.0289	1	1.249
$C_{10}H_{16}NO_9S^-$	326.0551	3	3.361
$C_9H_{16}NO_{10}S^-$	330.0500	2	0.461
$C_{15}H_{24}NO_7S^-$	362.1279	4	2.253
$C_{14}H_{24}NO_9S^-$	382.1177	3	0.923

Table S11. Number and percentage occurrences of the plausible reactant− product pairs

Type		CHOS − SO_3 → CHO (1)	CHONS − SO_3 → CHON (2)	Total
Number	Median	708	480	1158
	Range	87-1249	48-971	135-2165
	Average±STD	699±324	508±261	1207±578
Percentage(%)	Median	28	20	48
	Range	11-37	5-27	18-62
	Average±STD	27±7	19±6	46±12
Intensity percentages (%)	Median	30	17	49
	Range	10-40	4-29	15-61
	Average±STD	28±7	17±6	46±12

Table S12. Selected meteorological parameters and chemical variables that probably have influences on the formation of NOCs. This table has been revised from our previous study and the references therein (Jiang et al., 2021b).

Abbreviation	Full name	Major Sources/influences
SO_2	Sulfur dioxide	
NO	Nitric oxide	
NO_2	Nitrogen dioxide	Combustion sources
NO_x	Nitrogen oxides	
CO	Carbon monoxide	
O_3	Ozone	Photo-oxidization
NO_x+ O_3	Oxidants	
NH_4^+	Ammonium	Secondary nitrate formation process
NO_3^-	Nitrates	
SO_4^{2-}/nss-SO_4^{2-}	Sulfates/ non-sea-salt sulfates	Secondary sulfate formation process
Cl^-	Chloridion	Sea salt/coal conbustion
K^+/nss-K^+	Potassium/non-sea-salt potassium	Biomass burning (also from coal combustion and other sources)
Levo	levoglucosan	Biomass burning
MTLs	sum of 2-methylthreitol and 2-methylerythritol	Isoprene derived SOA
MSOA	monoterpene-derived secondary organic aerosols	α-/β-pinene derived SOA
FA	Fatty acids	Vehicle emission, coal combustion, cooking, high-level plans
PAHs	Polycyclic aromatic hydrocarbons	Combustion sources
Alkane	Long-chain alkanes with C number from 20 to 36	Combustion sources and high-level plans
ΣSH	steranes and hopanes	Fossil fuels combustion sources
LWC	Liquid water content	Influence the aqueous phase reaction
Tem	Temperature	Influence the gas-to-particle partitioning
RH	Relative humidity	Influence the aqueous phase reaction
OH	Hydroxyl radical	Influence the oxidation state of precursor/ photo-decomposed

设置了格式：下标

设置了格式：下标

pH	potential of hydrogen	Influence the aqueous phase reaction (range: -0.08-4.90)
$\Delta^{14}C$	Radiocarbon isotope	Indicator of fossil or non-fossil sources

Table S13. Number and percentage of compounds classes with significant correlations to the environmental variables.

Type	*p*-value original				*p*-value (FDR-adjusted)			
	CHOS		CHONS		CHOS		CHONS	
Parameters	Positive	Negative	Positive	Negative	Positive	Negative	Positive	Negative
RH	591 (77%)	172 (72%)	180 (23%)	66 (28%)	322 (83%)	20 (74%)	65 (17%)	7 (26%)
Tem	260 (83%)	697 (58%)	54 (17%)	514 (42%)	170 (89%)	352 (57%)	22 (11%)	261 (43%)
MSOA	478 (53%)	465 (88%)	416 (47%)	62 (12%)	375 (58%)	260 (92%)	277 (42%)	22 (8%)
MTLs	336 (73%)	696 (72%)	124 (27%)	274 (28%)	253 (81%)	451 (79%)	60 (19%)	123 (21%)
$\Delta^{14}C$	199 (70%)	440 (69%)	87 (30%)	200 (31%)	37 (71%)	225 (71%)	15 (29%)	92 (29%)
NH_4^+	230 (43%)	244 (85%)	306 (57%)	42 (15%)	21 (26%)	56 (89%)	59 (74%)	7 (11%)
NO_3^-	283 (44%)	159 (79%)	359 (56%)	42 (21%)	46 (36%)	40 (75%)	83 (64%)	13 (25%)
LWC	330 (46%)	22 (72%)	392 (54%)	8 (28%)	17 (100%)	0	43 (100%)	0
pH	65 (56%)	11 (48%)	51 (44%)	12 (52%)	0	0	0	0
H^+	11 (48%)	65 (56%)	12 (52%)	51 (44%)	0	0	0	0
SO_4^{2-}	247 (72%)	131 (63%)	95 (28%)	76 (37%)	0	0	0	0

References

Altieri, K. E., Turpin, B. J., and and Seitzinger, S. P.: Oligomers, organosulfates, and nitrooxy organosulfates in rainwater identified by ultra-high resolution electrospray ionization FT-ICR mass spectrometry, Atmos. Chem. Phys., 2533-2542, doi:10.5194/acp-9-2533-2009, 2009.

Aoki, E., Sarrimanolis, J. N., Lyon, S. A., and Elrod, M. J.: Determining the Relative Reactivity of Sulfate, Bisulfate, and Organosulfates with Epoxides on Secondary Organic Aerosol, ACS Earth and Space Chemistry, 4, 1793-1801, doi:10.1021/acsearthspacechem.0c00178, 2020.

Bateman, A. P., Laskin, J., Laskin, A., and Nizkorodov, S. A.: Applications of high-resolution electrospray ionization mass spectrometry to measurements of average oxygen to carbon ratios in secondary organic aerosols, Environ. Sci. Technol., 46, 8315-8324, doi:10.1021/es3017254, 2012.

Bates, J. T., Fang, T., Verma, V., Zeng, L., Weber, R. J., Tolbert, P. E., Abrams, J. Y., Sarnat, S. E., Klein, M., Mulholland, J. A., and Russell, A. G.: Review of Acellular Assays of Ambient Particulate Matter Oxidative Potential: Methods and Relationships with Composition, Sources, and Health Effects, Environ. Sci. Technol., 53, 4003-4019, doi:10.1021/acs.est.8b03430, 2019.

Bianco, A., Deguillaume, L., Vaitilingom, M., Nicol, E., Baray, J. L., Chaumerliac, N., and Bridoux, M.: Molecular Characterization of Cloud Water Samples Collected at the Puy de Dome (France) by Fourier Transform Ion Cyclotron Resonance Mass Spectrometry, Environ. Sci. Technol., 52, 10275-10285, doi:10.1021/acs.est.8b01964, 2018.

Blair, S. L., MacMillan, A. C., Drozd, G. T., Goldstein, A. H., Chu, R. K., Pasa-Tolic, L., Shaw, J. B., Tolic, N., Lin, P., Laskin, J., Laskin, A., and Nizkorodov, S. A.: Molecular Characterization of Organosulfur Compounds in Biodiesel and Diesel Fuel Secondary Organic Aerosol, Environ. Sci. Technol., 51, 119-127, doi:10.1021/acs.est.6b03304, 2017.

Bruggemann, M., Xu, R., Tilgner, A., Kwong, K. C., Mutzel, A., Poon, H. Y., Otto, T., Schaefer, T., Poulain, L., Chan, M. N., and Herrmann, H.: Organosulfates in Ambient Aerosol: State of Knowledge and Future Research Directions on Formation, Abundance, Fate, and Importance, Environ. Sci. Technol., 54, 3767-3782, doi:10.1021/acs.est.9b06751, 2020.

Bryant, D. J., Elzein, A., Newland, M., White, E., Swift, S., Watkins, A., Deng, W., Song, W., Wang, S., Zhang, Y., Wang, X., Rickard, A. R., and Hamilton, J. F.: Importance of Oxidants and Temperature in the Formation of Biogenic Organosulfates and Nitrooxy Organosulfates, ACS Earth Space Chem., 5, 2291-2306, doi:10.1021/acsearthspacechem.1c00204, 2021.

Chen, Y. and Bond, T. C.: Light absorption by organic carbon from wood combustion, Atmospheric Chemistry and Physics, 10, 1773-1787, 2010.

Chen, Y., Dombek, T., Hand, J., Zhang, Z., Gold, A., Ault, A. P., Levine, K. E., and Surratt, J. D.: Seasonal Contribution of Isoprene-Derived Organosulfates to Total Water-Soluble Fine Particulate Organic Sulfur in the United States, ACS Earth Space Chem., 5, 2419-2432, doi:10.1021/acsearthspacechem.1c00102, 2021.

Chen, Y., Zhang, Y., Lambe, A. T., Xu, R., Lei, Z., Olson, N. E., Zhang, Z., Szalkowski, T., Cui, T., Vizuete, W., Gold, A., Turpin, B. J., Ault, A. P., Chan, M. N., and Surratt, J. D.: Heterogeneous Hydroxyl Radical Oxidation of Isoprene-Epoxydiol-Derived Methyltetrol Sulfates: Plausible Formation Mechanisms of Previously Unexplained Organosulfates in Ambient Fine Aerosols, Environ. Sci. Technol. Lett., doi:10.1021/acs.estlett.0c00276, 2020.

Cheng, Y., He, K. B., Engling, G., Weber, R., Liu, J. M., Du, Z. Y., and Dong, S. P.: Brown and black carbon in Beijing aerosol: Implications for the effects of brown coating on light absorption by black carbon, Science of the Total Environment, 599-600, 1047-1055, doi:10.1016/j.scitotenv.2017.05.061, 2017.

Cui, M., Li, C., Chen, Y., Zhang, F., Li, J., Jiang, B., Mo, Y., Li, J., Yan, C., Zheng, M., Xie, Z., Zhang, G., and Zheng, J.: Molecular characterization of polar organic aerosol constituents in off-road engine emissions using Fourier transform ion cyclotron resonance mass spectrometry (FT-ICR MS): implications for source apportionment, Atmos. Chem. Phys., 19, 13945-13956, doi:10.5194/acp-19-13945-2019, 2019.

Daellenbach, K. R., Kourtchev, I., Vogel, A. L., Bruns, E. A., Jiang, J., Petäjä, T., Jaffrezo, J.-L., Aksoyoglu, S., Kalberer, M., Baltensperger, U., El Haddad, I., and Prévôt, A. S. H.: Impact of anthropogenic and biogenic sources on the seasonal variation in the molecular composition of urban organic aerosols: a field and laboratory study using ultra-high-resolution mass spectrometry, Atmos. Chem. Phys., 19, 5973-5991, doi:10.5194/acp-19-5973-2019, 2019.

Daellenbach, K. R., Uzu, G., Jiang, J., Cassagnes, L. E., Leni, Z., Vlachou, A., Stefenelli, G., Canonaco, F., Weber, S., Segers, A., Kuenen, J. J. P., Schaap, M., Favez, O., Albinet, A., Aksoyoglu, S., Dommen, J., Baltensperger, U., Geiser, M., El Haddad, I., Jaffrezo, J. L., and Prevot, A. S. H.: Sources of particulate-matter air pollution and its oxidative potential in Europe, Nature, 587, 414-419, doi:10.1038/s41586-020-2902-8, 2020.

Dai, S., Bi, X., Chan, L. Y., He, J., Wang, B., Wang, X., Peng, P., Sheng, G., and Fu, J.: Chemical and stable carbon isotopic composition of PM2.5 from on-road vehicle emissions in the PRD region and implications for vehicle emission control policy, Atmos. Chem. Phys., 15, 3097-3108, doi:10.5194/acp-15-3097-2015, 2015.

Dombek, T., Poitras, E., Hand, J., Schichtel, B., Harrington, J. M., and Levine, K. E.: Total sulfur analysis of fine particulate mass on nylon filters by ICP–OES, Journal of Environmental Quality, 49, 762-768, doi:https://doi.org/10.1002/jeq2.20066, 2020.

Duporte, G., Flaud, P. M., Kammer, J., Geneste, E., Augagneur, S., Pangui, E., Lamkaddam, H., Gratien, A., Doussin, J. F., Budzinski, H., Villenave, E., and Perraudin, E.: Experimental Study of the Formation of Organosulfates from alpha-Pinene Oxidation. 2. Time Evolution and Effect of Particle Acidity, J. Phys. Chem. A, 124, 409-421, doi:10.1021/acs.jpca.9b07156, 2020.

Eddingsaas, N. C., VanderVelde, D. G., and Wennberg, P. O.: Kinetics and Products of the Acid-Catalyzed Ring-Opening of Atmospherically Relevant Butyl Epoxy Alcohols, J. Phys. Chem. A, 114, 8106–8113, doi:10.1021/jp103907c, 2010.

Fleming, L. T., Ali, N. N., Blair, S. L., Roveretto, M., George, C., and Nizkorodov, S. A.: Formation of Light-Absorbing Organosulfates during Evaporation of Secondary Organic Material Extracts in the Presence of Sulfuric Acid, ACS Earth Space Chem., 3, 947-957, doi:10.1021/acsearthspacechem.9b00036, 2019.

Frossard, A. A., Shaw, P. M., Russell, L. M., Kroll, J. H., Canagaratna, M. R., Worsnop, D. R., Quinn, P. K., and Bates, T. S.: Springtime Arctic haze contributions of submicron organic particles from European and Asian combustion sources, Journal of Geophysical Research, 116, doi:10.1029/2010jd015178, 2011.

Gao, K. and Zhu, T.: Analytical methods for organosulfate detection in aerosol particles: Current status and future perspectives, Sci. Total Environ., 784, 147244, doi:10.1016/j.scitotenv.2021.147244, 2021.

Guo, H., Sullivan, A. P., Campuzano-Jost, P., Schroder, J. C., Lopez-Hilfiker, F. D., Dibb, J. E., Jimenez, J. L., Thornton, J. A., Brown, S. S., Nenes, A., and Weber, R. J.: Fine particle pH and the partitioning of nitric acid during winter in the northeastern United States, J. Geophys. Res. Atmos., 121, doi:10.1002/2016jd025311, 2016.

Guo, J., Zhou, S., Cai, M., Zhao, J., Song, W., Zhao, W., Hu, W., Sun, Y., He, Y., Yang, C., Xu, X., Zhang, Z., Cheng, P., Fan, Q., Hang, J., Fan, S., Wang, X., and Wang, X.: Characterization of submicron particles by time-of-flight aerosol chemical speciation monitor (ToF-ACSM) during wintertime: aerosol composition, sources, and chemical processes in Guangzhou, China, Atmos. Chem. Phys., 20, 7595-7615, doi:10.5194/acp-20-7595-2020, 2020.

Hawkins, L. N., Russell, L. M., Covert, D. S., Quinn, P. K., and Bates, T. S.: Carboxylic acids, sulfates, and organosulfates in processed continental organic aerosol over the southeast Pacific Ocean during VOCALS-REx 2008, Journal of Geophysical Research, 115, doi:10.1029/2009jd013276, 2010.

He, Q.-F., Ding, X., Tang, M.-J., Wang, X.-M., Fu, X.-X., Zhang, Y.-Q., Wang, J.-Q., Liu, Y.-X., and Rudich, Y.: Secondary Organic Aerosol Formation From Isoprene Epoxides in the Pearl River Delta, South China: IEPOX- and HMML-Derived Tracers, J. Geophys. Res. Atmos., 123, 6999–7012, doi:10.1029/2017JD028242, 2018.

He, Q. F., Ding, X., Wang, X. M., Yu, J. Z., Fu, X. X., Liu, T. Y., Zhang, Z., Xue, J., Chen, D. H., Zhong, L. J., and Donahue, N. M.: Organosulfates from pinene and isoprene over the Pearl River Delta, South China: seasonal variation and implication in formation mechanisms, Environ. Sci. Technol., 48, 9236-9245, doi:10.1021/es501299v, 2014.

Hettiyadura, A. P. S., Al-Naiema, I. M., Hughes, D. D., Fang, T., and Stone, E. A.: Organosulfates in Atlanta, Georgia: anthropogenic influences on biogenic secondary organic aerosol formation, Atmos. Chem. Phys., 19, 3191-3206, doi:10.5194/acp-19-3191-2019, 2019.

Hettiyadura, A. P. S., Stone, E. A., Kundu, S., Baker, Z., Geddes, E., Richards, K., and Humphry, T.: Determination of atmospheric organosulfates using HILIC chromatography with MS detection, Atmos. Meas. Tech., 8, 2347-2358, doi:10.5194/amt-8-2347-2015, 2015.

Hettiyadura, A. P. S., Jayarathne, T., Baumann, K., Goldstein, A. H., de Gouw, J. A., Koss, A., Keutsch, F. N., Skog, K., and Stone, E. A.: Qualitative and quantitative analysis of atmospheric organosulfates in Centreville, Alabama, Atmos. Chem. Phys., 17, 1343-1359, doi:10.5194/acp-17-1343-2017, 2017.

Huang, D. D., Li, Y. J., Lee, B. P., and Chan, C. K.: Analysis of organic sulfur compounds in atmospheric aerosols at the HKUST supersite in Hong Kong using HR-ToF-AMS, Environ Sci Technol, 49, 3672-3679, doi:10.1021/es5056269, 2015.

Huang, L., Coddens, E. M., and Grassian, V. H.: Formation of Organosulfur Compounds from Aqueous Phase Reactions of S(IV) with Methacrolein and Methyl Vinyl Ketone in the Presence of Transition Metal Ions, ACS Earth Space Chem., 3, 1749-1755, doi:10.1021/acsearthspacechem.9b00173, 2019.

Huang, L., Liu, T., and Grassian, V. H.: Radical-Initiated Formation of Aromatic Organosulfates and Sulfonates in the Aqueous Phase, Environ. Sci. Technol., 54, 11857-11864, doi:10.1021/acs.est.0c05644, 2020.

Huang, R.-J., Cao, J., Chen, Y., Yang, L., Shen, J., You, Q., Wang, K., Lin, C., Xu, W., Gao, B., Li, Y., Chen, Q., Hoffmann, T., amp, apos, Dowd, C. D., Bilde, M., and Glasius, M.: Organosulfates in atmospheric aerosol: synthesis and quantitative analysis of PM2.5 from Xi'an, northwestern China, Atmos. Meas. Tech., 11, 3447-3456, doi:10.5194/amt-11-3447-2018, 2018a.

Huang, R. J., Yang, L., Cao, J. J., Chen, Y., Chen, Q., Li, Y., Duan, J., Zhu, C., Dai, W., Wang, K., Lin, C., Ni, H., Corbin, J. C., Wu, Y., Zhang, R., Tie, X., Hoffmann, T., O'Dowd, C., and Dusek, U.: Brown Carbon Aerosol in Urban Xi'an, Northwest China: The Composition and Light Absorption Properties, Environmental Science & Technology, 52, 6825-6833, doi:10.1021/acs.est.8b02386, 2018b.

Iinuma, Y., Müller, C., Böge, O., Gnauk, T., and Herrmann, H.: The formation of organic sulfate esters in the limonene ozonolysis secondary organic aerosol (SOA) under acidic conditions, Atmos. Environ., 41, 5571-5583, doi:10.1016/j.atmosenv.2007.03.007, 2007a.

Iinuma, Y., Mu¨ Ller, C., Berndt, T., Bo¨ Ge, O., Claeys, M., and Herrmann, H.: Evidence for the Existence of Organosulfates from β-Pinene Ozonolysis in Ambient Secondary Organic Aerosol, Environ. Sci. Technol., 6678-6683, doi:10.1021/es070938t, 2007b.

Jiang, B., Kuang, B. Y., Liang, Y., Zhang, J., Huang, X. H. H., Xu, C., Yu, J. Z., and Shi, Q.: Molecular composition of urban organic aerosols on clear and hazy days in Beijing: a comparative study using FT-ICR MS, Environ. Chem., 13, 888-901, doi:10.1071/en15230, 2016.

Jiang, H., Li, J., Sun, R., Tian, C., Tang, J., Jiang, B., Liao, Y., Chen, C. E., and Zhang, G.: Molecular Dynamics and Light Absorption Properties of Atmospheric Dissolved Organic Matter, Environ. Sci. Technol., 55, 10268-10279, doi:10.1021/acs.est.1c01770, 2021a.
Jiang, H., Li, J., Chen, D., Tang, J., Cheng, Z., Mo, Y., Su, T., Tian, C., Jiang, B., Liao, Y., and Zhang, G.: Biomass burning organic aerosols significantly influence the light absorption properties of polarity-dependent organic compounds in the Pearl River Delta Region, China, Environ. Int., 144, 106079, doi:10.1016/j.envint.2020.106079, 2020.
Jiang, H., Li, J., Sun, R., Liu, G., Tian, C., Tang, J., Cheng, Z., Zhu, S., Zhong, G., Ding, X., and Zhang, G.: Determining the Sources and Transport of Brown Carbon Using Radionuclide Tracers and Modeling, J. Geophys. Res. Atmos., 126, e2021JD034616, doi:10.1029/2021jd034616, 2021b.
Jimenez, J. L., Canagaratna, M. R., Donahue, N. M., Prevot, A. S. H., Zhang, Q., Kroll, J. H., DeCarlo, P. F., Allan, J. D., Coe, H., Ng, N. L., Aiken, A. C., Docherty, K. S., Ulbrich, I. M., Grieshop, A. P., Robinson, A. L., Duplissy, J., Smith, J. D., Wilson, K. R., Lanz, V. A., Hueglin, C., Sun, Y. L., Tian, J., Laaksonen, A., Raatikainen, T., Rautiainen, J., Vaattovaara, P., Ehn, M., Kulmala, M., Tomlinson, J. M., Collins, D. R., Cubison, M. J., Dunlea, J., Huffman, J. A., Onasch, T. B., Alfarra, M. R., Williams, P. I., Bower, K., Kondo, Y., Schneider, J., Drewnick, F., Borrmann, S., Weimer, S., Demerjian, K., Salcedo, D., Cottrell, L., Griffin, R., Takami, A., Miyoshi, T., Hatakeyama, S., Shimono, A., Sun, J. Y., Zhang, Y. M., Dzepina, K., Kimmel, J. R., Sueper, D., Jayne, J. T., Herndon, S. C., Trimborn, A. M., Williams, L. R., Wood, E. C., Middlebrook, A. M., Kolb, C. E., Baltensperger, U., and Worsnop, D. R.: Evolution of Organic Aerosols in the Atmosphere, Science, 326, 1525, doi:10.1126/science.1180353, 2009.
Kellerman, A. M., Dittmar, T., Kothawala, D. N., and Tranvik, L. J.: Chemodiversity of dissolved organic matter in lakes driven by climate and hydrology, Nat. Commun., 5, 3804, doi:10.1038/ncomms4804, 2014.
Kourtchev, I., Giorio, C., Manninen, A., Wilson, E., Mahon, B., Aalto, J., Kajos, M., Venables, D., Ruuskanen, T., Levula, J., Loponen, M., Connors, S., Harris, N., Zhao, D., Kiendler-Scharr, A., Mentel, T., Rudich, Y., Hallquist, M., Doussin, J. F., Maenhaut, W., Back, J., Petaja, T., Wenger, J., Kulmala, M., and Kalberer, M.: Enhanced Volatile Organic Compounds emissions and organic aerosol mass increase the oligomer content of atmospheric aerosols, Sci Rep, 6, 35038, doi:10.1038/srep35038, 2016.
Kristensen, K., Bilde, M., Aalto, P. P., Petäjä, T., and Glasius, M.: Denuder/filter sampling of organic acids and organosulfates at urban and boreal forest sites: Gas/particle distribution and possible sampling artifacts, Atmos. Environ., 130, 36-53, doi:10.1016/j.atmosenv.2015.10.046, 2016.
Kuang, B. Y., Lin, P., Hu, M., and Yu, J. Z.: Aerosol size distribution characteristics of organosulfates in the Pearl River Delta region, China, Atmos. Environ., 130, 23-35, doi:10.1016/j.atmosenv.2015.09.024, 2016.
Lam, H. K., Kwong, K. C., Poon, H. Y., Davies, J. F., Zhang, Z., Gold, A., Surratt, J. D., and Chan, M. N.: Heterogeneous OH oxidation of isoprene-epoxydiol-derived organosulfates: kinetics, chemistry and formation of inorganic sulfate, Atmos. Chem. Phys., 19, 2433-2440, doi:10.5194/acp-19-2433-2019, 2019.
Le Breton, M., Wang, Y., Hallquist, Å. M., Pathak, R. K., Zheng, J., Yang, Y., Shang, D., Glasius, M., Bannan, T. J., Liu, Q., Chan, C. K., Percival, C. J., Zhu, W., Lou, S., Topping, D., Wang, Y., Yu, J., Lu, K., Guo, S., Hu, M., and Hallquist, M.: Online gas- and particle-phase measurements of organosulfates, organosulfonates and nitrooxy organosulfates in Beijing utilizing a FIGAERO ToF-CIMS, Atmos. Chem. Phys., 18, 10355-10371, doi:10.5194/acp-18-10355-2018, 2018.
Li, J. J., Wang, G. H., Cao, J. J., Wang, X. M., and Zhang, R. J.: Observation of biogenic secondary organic aerosols in the atmosphere of a mountain site in central China: temperature and relative humidity effects, Atmospheric Chemistry and Physics, 13, 11535-11549, doi:10.5194/acp-13-11535-2013, 2013.
Lin, P., Rincon, A. G., Kalberer, M., and Yu, J. Z.: Elemental Composition of HULIS in the Pearl River Delta Region, China: Results Inferred from Positive and Negative Electrospray High Resolution Mass Spectrometric Data, Environmental Science & Technology, 46, 7454-7462, doi:10.1021/es300285d, 2012a.
Lin, P., Yu, J. Z., Engling, G., and Kalberer, M.: Organosulfates in Humic-like Substance Fraction Isolated from Aerosols at Seven Locations in East Asia: A Study by Ultra-High-Resolution Mass Spectrometry, Environ. Sci. Technol., 46, 13118-13127, doi:10.1021/es303570v, 2012b.
Lin, Y.-H., Knipping, E. M., Edgerton, E. S., Shaw, S. L., and Surratt, J. D.: Investigating the influences of SO2 and NH3 levels on isoprene-derived secondary organic aerosol formation using conditional sampling approaches, Atmos. Chem. Phys., 13, 8457–8470, doi:10.5194/acp-13-8457-2013, 2013.
Lin, Y.-H., Arashiro, M., Martin, E., Chen, Y., Zhang, Z., Sexton, K. G., Gold, A., Jaspers, I., Fry, R. C., and Surratt, J. D.: Isoprene-Derived Secondary Organic Aerosol Induces the Expression of Oxidative Stress Response Genes in Human Lung Cells, Environ. Sci. Technol. Lett., 3, 250-254, doi:10.1021/acs.estlett.6b00151, 2016.
Lind, J. A., Lazrus, A. L., and Kok, G. L.: Aqueous phase oxidation of sulfur(IV) by hydrogen peroxide, methylhydroperoxide, and peroxyacetic acid, Journal of Geophysical Research: Atmospheres, 92, 4171-4177, doi:https://doi.org/10.1029/JD092iD04p04171, 1987.
Liu, J., Li, J., Zhang, Y., Liu, D., Ding, P., Shen, C., Shen, K., He, Q., Ding, X., Wang, X., Chen, D., Szidat, S., and Zhang, G.: Source apportionment using radiocarbon and organic tracers for PM2.5 carbonaceous aerosols in Guangzhou, South China: contrasting local- and regional-scale haze events, Environ. Sci. Technol., 48, 12002-12011, doi:10.1021/es503102w, 2014.
Liu, M., Song, Y., Zhou, T., Xu, Z., Yan, C., Zheng, M., Wu, Z., Hu, M., Wu, Y., and Zhu, T.: Fine particle pH during severe haze episodes in northern China, Geophys. Res. Lett., 44, 5213-5221, doi:10.1002/2017gl073210, 2017.

Luk´acs, H., Gelencs´er, A., Hoffer, A., Kiss, G., Horv´ath, K., and Harty´ani, Z.: Quantitative assessment of organosulfates in size-segregated rural fine aerosol, Atmos. Chem. Phys., 9, 231–238, doi:10.5194/acp-9-231-2009, 2009.

Mazzoleni, L. R., Ehrmann, B. M., Shen, X., Marshall, A. G., and Collett, J. L.: Water-Soluble Atmospheric Organic Matter in Fog: Exact Masses and Chemical Formula Identification by Ultrahigh-Resolution Fourier Transform Ion Cyclotron Resonance Mass Spectrometry, Environ. Sci. Technol., 44, 3690-3697, doi:10.1021/es903409k, 2010.

Meade, L. E., Riva, M., Blomberg, M. Z., Brock, A. K., Qualters, E. M., Siejack, R. A., Ramakrishnan, K., Surratt, J. D., and Kautzman, K. E.: Seasonal variations of fine particulate organosulfates derived from biogenic and anthropogenic hydrocarbons in the mid-Atlantic United States, Atmos. Environ., 145, 405-414, doi:10.1016/j.atmosenv.2016.09.028, 2016.

Nguyen, T. B., Lee, P. B., Updyke, K. M., Bones, D. L., Laskin, J., Laskin, A., and Nizkorodov, S. A.: Formation of nitrogen- and sulfur-containing light-absorbing compounds accelerated by evaporation of water from secondary organic aerosols, J. Geophys. Res. Atmos., 117, D01207, doi:10.1029/2011jd016944, 2012.

Noziere, B., Kalberer, M., Claeys, M., Allan, J., D'Anna, B., Decesari, S., Finessi, E., Glasius, M., Grgic, I., Hamilton, J. F., Hoffmann, T., Iinuma, Y., Jaoui, M., Kahnt, A., Kampf, C. J., Kourtchev, I., Maenhaut, W., Marsden, N., Saarikoski, S., Schnelle-Kreis, J., Surratt, J. D., Szidat, S., Szmigielski, R., and Wisthaler, A.: The molecular identification of organic compounds in the atmosphere: state of the art and challenges, Chem. Rev., 115, 3919-3983, doi:10.1021/cr5003485, 2015.

Nozière, B., Ekström, S., Alsberg, T., and Holmström, S.: Radical-initiated formation of organosulfates and surfactants in atmospheric aerosols, Geophys. Res. Lett., 37, n/a-n/a, doi:10.1029/2009gl041683, 2010.

O'Brien, R. E., Laskin, A., Laskin, J., Rubitschun, C. L., Surratt, J. D., and Goldstein, A. H.: Molecular characterization of S- and N-containing organic constituents in ambient aerosols by negative ion mode high-resolution Nanospray Desorption Electrospray Ionization Mass Spectrometry: CalNex 2010 field study, J. Geophys. Res. Atmos., 119, 12706-12720, doi:10.1002/2014jd021955, 2014.

Olson, C. N., Galloway, M. M., Yu, G., Hedman, C. J., Lockett, M. R., Yoon, T., Stone, E. A., Smith, L. M., and Keutsch, F. N.: Hydroxycarboxylic acid-derived organosulfates: synthesis, stability, and quantification in ambient aerosol, Environ. Sci. Technol., 45, 6468-6474, doi:10.1021/es201039p, 2011.

Passananti, M., Kong, L., Shang, J., Dupart, Y., Perrier, S., Chen, J., Donaldson, D. J., and George, C.: Organosulfate Formation through the Heterogeneous Reaction of Sulfur Dioxide with Unsaturated Fatty Acids and Long-Chain Alkenes, Angew. Chem. Int. Ed., 55, 10336-10339, doi:10.1002/anie.201605266, 2016.

Peng, C., Razafindrambinina, P. N., Malek, K. A., Chen, L., Wang, W., Huang, R.-J., Zhang, Y., Ding, X., Ge, M., Wang, X., Asa-Awuku, A. A., and Tang, M.: Interactions of organosulfates with water vapor under sub- and supersaturated conditions, Atmos. Chem. Phys., 21, 7135-7148, doi:10.5194/acp-21-7135-2021, 2021.

Rincón, A. G., Calvo, A. I., Dietzel, M., and and Kalberer, M.: Seasonal differences of urban organic aerosol composition – an ultra-high resolution mass spectrometry study, Environmental Chemistry, 9, 298-319, doi:10.1071/EN12016_AC, 2012.

Riva, M., Barbosa, T. D. S., Lin, Y.-H., Stone, E. A., Gold, A., and Surratt, J. D.: Chemical characterization of organosulfates in secondary organic aerosol derived from the photooxidation of alkanes, Atmos. Chem. Phys., 16, , 2016, 16, 11001-11018, doi:10.5194/acp-16-11001-2016, 2016a.

Riva, M., Da Silva Barbosa, T., Lin, Y.-H., Stone, E. A., Gold, A., and Surratt, J. D.: Chemical characterization of organosulfates in secondary organic aerosol
derived from the photooxidation of alkanes, Atmos. Chem. Phys., 16, 11001-11018, doi:10.5194/acp-16-11001-2016, 2016b.

Riva, M., Tomaz, S., Cui, T., Lin, Y. H., Perraudin, E., Gold, A., Stone, E. A., Villenave, E., and Surratt, J. D.: Evidence for an unrecognized secondary anthropogenic source of organosulfates and sulfonates: gas-phase oxidation of polycyclic aromatic hydrocarbons in the presence of sulfate aerosol, Environ. Sci. Technol., 49, 6654-6664, doi:10.1021/acs.est.5b00836, 2015.

Riva, M., Budisulistiorini, S. H., Chen, Y., Zhang, Z., D'Ambro, E. L., Zhang, X., Gold, A., Turpin, B. J., Thornton, J. A., Canagaratna, M. R., and Surratt, J. D.: Chemical Characterization of Secondary Organic Aerosol from Oxidation of Isoprene Hydroxyhydroperoxides, Environ Sci Technol, 50, 9889-9899, doi:10.1021/acs.est.6b02511, 2016c.

Rudzi´nski, K. J., Gmachowski, L., and Kuznietsova, I.: Reactions of isoprene and sulphoxy radical-anions – a possible source of atmospheric organosulphites and organosulphates, Atmospheric Chemistry and Physics, 9, 2129–2140, 2009.

Schwartz, R. E., Russell, L. M., Sjostedt, S. J., Vlasenko, A., Slowik, J. G., Abbatt, J. P. D., Macdonald, A. M., Li, S. M., Liggio, J., Toom-Sauntry, D., and Leaitch, W. R.: Biogenic oxidized organic functional groups in aerosol particles from a mountain forest site and their similarities to laboratory chamber products, Atmospheric Chemistry and Physics, 10, 5075-5088, doi:10.5194/acp-10-5075-2010, 2010.

Shakya, K. M. and Peltier, R. E.: Investigating missing sources of sulfur at Fairbanks, Alaska, Environ. Sci. Technol., 47, 9332-9338, doi:10.1021/es402020b, 2013.

Shakya, K. M. and Peltier, R. E.: Non-sulfate sulfur in fine aerosols across the United States: Insight for organosulfate prevalence, Atmos. Environ., 100, 159-166, doi:10.1016/j.atmosenv.2014.10.058, 2015.

Shang, J., Passananti, M., Dupart, Y., Ciuraru, R., Tinel, L., Rossignol, S., Perrier, S., Zhu, T., and George, C.: SO2 Uptake on Oleic Acid: A New Formation Pathway of Organosulfur Compounds in the Atmosphere, Environ. Sci. Technol. Lett., 3, 67-72, doi:10.1021/acs.estlett.6b00006, 2016.

Song, J., Li, M., Jiang, B., Wei, S., Fan, X., and Peng, P. a.: Molecular Characterization of Water-Soluble Humic like Substances in Smoke Particles Emitted from Combustion of Biomass Materials and Coal Using Ultrahigh-Resolution Electrospray Ionization Fourier Transform Ion Cyclotron Resonance Mass Spectrometry, Environ. Sci. Technol., 52, 2575-2585, doi:10.1021/acs.est.7b06126, 2018.
Stone, E. A., Yang, L., Yu, L. E., and Rupakheti, M.: Characterization of organosulfates in atmospheric aerosols at Four Asian locations, Atmos. Environ., 47, 323-329, doi:10.1016/j.atmosenv.2011.10.058, 2012.
Surratt, J. D., Chan, A. W., Eddingsaas, N. C., Chan, M., Loza, C. L., Kwan, A. J., Hersey, S. P., Flagan, R. C., Wennberg, P. O., and Seinfeld, J. H.: Reactive intermediates revealed in secondary organic aerosol formation from isoprene, Proceedings of the National Academy of Sciences of the United States of America, 107, 6640-6645, doi:10.1073/pnas.0911114107, 2010.
Surratt, J. D., Kroll, J. H., Kleindienst, X. T. E., Edney, E. O., Claeys, M., Sorooshian, A., Ng, N. L., Offenberg, J. H., Lewandowski, M., Jaoui, M., Flagan, R. C., and Seinfeld, J. H.: Evidence for Organosulfates in Secondary Organic Aerosol, Environ. Sci. Technol., 41, 517-527, doi:10.1021/es062081q, 2007.
Surratt, J. D., Gómez-González, Y., Chan, A. W. H., Vermeylen, R., Shahgholi, M., Kleindienst, T. E., Edney, E. O., Offenberg, J. H., Lewandowski, M., Jaoui, M., Maenhaut, W., Claeys, M., Flagan, R. C., and Seinfeld, J. H.: Organosulfate Formation in Biogenic Secondary Organic Aerosol, J. Phys. Chem. A, 112, 8345-8378, doi:10.1021/jp802310p, 2008.
Tang, J., Li, J., Su, T., Han, Y., Mo, Y., Jiang, H., Cui, M., Jiang, B., Chen, Y., Tang, J., Song, J., Peng, P. a., and Zhang, G.: Molecular compositions and optical properties of dissolved brown carbon in biomass burning, coal combustion, and vehicle emission aerosols illuminated by excitation–emission matrix spectroscopy and Fourier transform ion cyclotron resonance mass spectrometry analysis, Atmos. Chem. Phys., 20, 2513-2532, doi:10.5194/acp-20-2513-2020, 2020.
Tao, S., Lu, X., Levac, N., Bateman, A. P., Nguyen, T. B., Bones, D. L., Nizkorodov, S. A., Laskin, J., Laskin, A., and Yang, X.: Molecular characterization of organosulfates in organic aerosols from Shanghai and Los Angeles urban areas by nanospray-desorption electrospray ionization high-resolution mass spectrometry, Environ. Sci. Technol., 48, 10993-11001, doi:10.1021/es5024674, 2014.
Tolocka, M. P. and Turpin, B.: Contribution of organosulfur compounds to organic aerosol mass, Environ. Sci. Technol., 46, 7978-7983, doi:10.1021/es300651v, 2012.
Vogel, A. L., Schneider, J., Muller-Tautges, C., Phillips, G. J., Pohlker, M. L., Rose, D., Zuth, C., Makkonen, U., Hakola, H., Crowley, J. N., Andreae, M. O., Poschl, U., and Hoffmann, T.: Aerosol Chemistry Resolved by Mass Spectrometry: Linking Field Measurements of Cloud Condensation Nuclei Activity to Organic Aerosol Composition, Environ Sci Technol, 50, 10823-10832, doi:10.1021/acs.est.6b01675, 2016.
Wach, P., Spolnik, G., Rudzinski, K. J., Skotak, K., Claeys, M., Danikiewicz, W., and Szmigielski, R.: Radical oxidation of methyl vinyl ketone and methacrolein in aqueous droplets: Characterization of organosulfates and atmospheric implications, Chemosphere, 214, 1-9, doi:10.1016/j.chemosphere.2018.09.026, 2019.
Wang, J., Ye, J., Zhang, Q., Zhao, J., Wu, Y., Li, J., Liu, D., Li, W., Zhang, Y., Wu, C., Xie, C., Qin, Y., Lei, Y., Huang, X., Guo, J., Liu, P., Fu, P., Li, Y., Lee, H. C., Choi, H., Zhang, J., Liao, H., Chen, M., Sun, Y., Ge, X., Martin, S. T., and Jacob, D. J.: Aqueous production of secondary organic aerosol from fossil-fuel emissions in winter Beijing haze, Proc. Natl. Acad. Sci. U. S. A., 118, doi:10.1073/pnas.2022179118, 2021a.
Wang, K., Zhang, Y., Huang, R.-J., Cao, J., and Hoffmann, T.: UHPLC-Orbitrap mass spectrometric characterization of organic aerosol from a central European city (Mainz, Germany) and a Chinese megacity (Beijing), Atmospheric Environment, 189, 22-29, doi:10.1016/j.atmosenv.2018.06.036, 2018a.
Wang, K., Zhang, Y., Huang, R. J., Wang, M., Ni, H., Kampf, C. J., Cheng, Y., Bilde, M., Glasius, M., and Hoffmann, T.: Molecular Characterization and Source Identification of Atmospheric Particulate Organosulfates Using Ultrahigh Resolution Mass Spectrometry, Environ. Sci. Technol., 53, 6192-6202, doi:10.1021/acs.est.9b02628, 2019.
Wang, K., Huang, R.-J., Brüggemann, M., Zhang, Y., Yang, L., Ni, H., Guo, J., Wang, M., Han, J., Bilde, M., Glasius, M., and Hoffmann, T.: Urban organic aerosol composition in eastern China differs from north to south: molecular insight from a liquid chromatography–mass spectrometry (Orbitrap) study, Atmos. Chem. Phys., 21, 9089-9104, doi:10.5194/acp-21-9089-2021, 2021b.
Wang, X., Hayeck, N., Brüggemann, M., Yao, L., Chen, H., Zhang, C., Emmelin, C., Chen, J., George, C., and Wang, L.: Chemical Characteristics of Organic Aerosols in Shanghai: A Study by Ultrahigh-Performance Liquid Chromatography Coupled With Orbitrap Mass Spectrometry, J. Geophys. Res. Atmos., 122, 11703-11722, doi:10.1002/2017jd026930, 2017a.
Wang, X. K., Rossignol, S., Ma, Y., Yao, L., Wang, M. Y., Chen, J. M., George, C., and Wang, L.: Molecular characterization of atmospheric particulate organosulfates in three megacities at the middle and lower reaches of the Yangtze River, Atmos. Chem. Phys., 16, 2285–2298, doi:10.5194/acp-16-2285-2016, 2016.
Wang, Y., Ren, J., Huang, X. H. H., Tong, R., and Yu, J. Z.: Synthesis of Four Monoterpene-Derived Organosulfates and Their Quantification in Atmospheric Aerosol Samples, Environ. Sci. Technol., 51, 6791-6801, doi:10.1021/acs.est.7b01179, 2017b.
Wang, Y., Hu, M., Wang, Y.-C., Li, X., Fang, X., Tang, R., Lu, S., Wu, Y., Guo, S., Wu, Z., Hallquist, M., and Yu, J. Z.: Comparative Study of Particulate Organosulfates in Contrasting Atmospheric Environments: Field Evidence for the Significant Influence of Anthropogenic Sulfate and NOx, Environ. Sci. Technol. Lett., 7, 787-794, doi:10.1021/acs.estlett.0c00550, 2020.
Wang, Y., Hu, M., Guo, S., Wang, Y., Zheng, J., Yang, Y., Zhu, W., Tang, R., Li, X., Liu, Y., Le Breton, M., Du, Z., Shang, D., Wu, Y., Wu, Z., Song, Y., Lou, S., Hallquist, M., and Yu, J.: The secondary formation of organosulfates under interactions between biogenic

emissions and anthropogenic pollutants in summer in Beijing, Atmos. Chem. Phys., 18, 10693-10713, doi:10.5194/acp-18-10693-2018, 2018b.
Willoughby, A. S., Wozniak, A. S., and Hatcher, P. G.: A molecular-level approach for characterizing water-insoluble components of ambient organic aerosol particulates using ultrahigh-resolution mass spectrometry, Atmos. Chem. Phys., 14, 10299-10314, doi:10.5194/acp-14-10299-2014, 2014.
Worton, D. R., Surratt, J. D., Lafranchi, B. W., Chan, A. W., Zhao, Y., Weber, R. J., Park, J. H., Gilman, J. B., de Gouw, J., Park, C., Schade, G., Beaver, M., Clair, J. M., Crounse, J., Wennberg, P., Wolfe, G. M., Harrold, S., Thornton, J. A., Farmer, D. K., Docherty, K. S., Cubison, M. J., Jimenez, J. L., Frossard, A. A., Russell, L. M., Kristensen, K., Glasius, M., Mao, J., Ren, X., Brune, W., Browne, E. C., Pusede, S. E., Cohen, R. C., Seinfeld, J. H., and Goldstein, A. H.: Observational insights into aerosol formation from isoprene, Environ. Sci. Technol., 47, 11403-11413, doi:10.1021/es4011064, 2013.
Xu, B., Zhang, G., Gustafsson, Ö., Kawamura, K., Li, J., Andersson, A., Bikkina, S., Kunwar, B., Pokhrel, A., Zhong, G., Zhao, S., Li, J., Huang, C., Cheng, Z., Zhu, S., Peng, P. a., and Sheng, G.: Large contribution of fossil anthropogenic source components to aqueous secondary organic aerosols, Submitted, doi:10.21203/rs.3.rs-1155038/v1, 2021a.
Xu, L., Yang, Z., Tsona, N. T., Wang, X., George, C., and Du, L.: Anthropogenic-Biogenic Interactions at Night: Enhanced Formation of Secondary Aerosols and Particulate Nitrogen- and Sulfur-Containing Organics from beta-Pinene Oxidation, Environ. Sci. Technol., 55, 7794-7807, doi:10.1021/acs.est.0c07879, 2021b.
Yassine, M. M., Harir, M., Dabek-Zlotorzynska, E., and Schmitt-Kopplin, P.: Structural characterization of organic aerosol using Fourier transform ion cyclotron resonance mass spectrometry: aromaticity equivalent approach, Rapid Commun. Mass Spectrom., 28, 2445-2454, doi:10.1002/rcm.7038, 2014.
Ye, J., Abbatt, J. P. D., and Chan, A. W. H.: Novel pathway of SO2 oxidation in the atmosphere: reactions with monoterpene ozonolysis intermediates and secondary organic aerosol, Atmos. Chem. Phys., 18, 5549-5565, doi:10.5194/acp-18-5549-2018, 2018.
Ye, Y., Zhan, H., Yu, X., Li, J., Wang, X., and Xie, Z.: Detection of organosulfates and nitrooxy-organosulfates in Arctic and Antarctic atmospheric aerosols, using ultra-high resolution FT-ICR mass spectrometry, Sci. Total Environ., 767, 144339, doi:10.1016/j.scitotenv.2020.144339, 2020.
Zhao, Y., Hallar, A. G., and Mazzoleni, L. R.: Atmospheric organic matter in clouds: exact masses and molecular formula identification using ultrahigh-resolution FT-ICR mass spectrometry, Atmos. Chem. Phys., 13, 12343-12362, doi:10.5194/acp-13-12343-2013, 2013.
Zhu, M., Jiang, B., Li, S., Yu, Q., Yu, X., Zhang, Y., Bi, X., Yu, J., George, C., Yu, Z., and Wang, X.: Organosulfur Compounds Formed from Heterogeneous Reaction between SO2 and Particulate-Bound Unsaturated Fatty Acids in Ambient Air, Environ. Sci. Technol. Lett., 6, 318-322, doi:10.1021/acs.estlett.9b00218, 2019.